



University of
Salford
MANCHESTER

Masters by Research

Nicole Hoyles

**Exploring potential inhibitors of the HGF-Met
signalling pathway as a prospective treatment for
paediatric medulloblastoma.**

School of Environment & Life Sciences

Volume 1, 2021

Table of Contents

List of tables and illustrations	5-7
Acknowledgements	8
Declaration	8
Abbreviation	9-12
Abstract	13-14
Introduction	
1.1 Cancer is a global health concern.....	15
1.2 Paediatric cancer	15-16
1.3 Medulloblastoma.....	16
1.4 Late effects of treatment in medulloblastoma patients	17
1.5 Genetics heterogeneity in medulloblastoma	18-20
1.5.1 WNT subgroup.....	21
1.5.2 SHH subgroup	22-23
1.5.3 Group 3 subgroup.....	23
1.5.4 Group 4 subgroup.....	24
1.6 Current treatments for medulloblastoma.....	24-25
1.7 The role of the HGF-Met signalling pathway	25
1.7.1 Hepatocyte growth factor and mesenchymal epithelial transition protein	26-27
1.7.2 The hepatocyte growth factor-Met kinase signalling pathway.....	28-29
1.7.3 Inhibitors of the HGF-Met signalling pathway	30-33
1.7.3.1 GAG mimetics and JD-Compounds.....	34
1.7.4 HGF-Met signalling pathway's role in wound healing.....	35
1.8 Model systems for medulloblastoma	36
1.9 Current work being performed at The University of Salford on c-Met inhibition and medulloblastoma.....	37
Aims and Objectives	38-39
Methods	

2.1 Media preparation.....	40
2.2 Cell thawing	40
2.3 Cell culture.....	40-41
2.4 Cell counting and using a haemocytometer.....	41-42
2.5 Plating a 96-well plate	42
2.6 JD compounds	43-44
2.7 Serial dilution.....	44
2.8 MTT assay	45-46
2.9 R2 database	46-47
2.10 Statistical analysis.....	48
Results	
3.1 Screening of potential c-Met inhibitors, in addition to known c-Met inhibitors, using MTT assays on different medulloblastoma cell lines	49
3.2 Known c-Met inhibitors reduced the viability of ONS76 cells, whereas the novel JD compounds had less impact on cell viability.....	50-51
3.3 Known c-Met inhibitors reduced the viability of UW228 cells, whereas the novel JD compounds had less impact on cell viability.....	52-53
3.4 Known c-Met inhibitors reduced the viability of Daoy cells, whereas the novel JD compounds had less impact on cell viability.....	54-55
3.5 Known c-Met inhibitors reduced the cell viability of HD-MB03	56
3.6 Tivantinib treatment had the most potent effect on cell viability in all cell lines (HD-MB03, Daoy, ONS76, UW228	57-58
3.7 The novel c-Met inhibitors displayed lower efficacy than the known c-Met inhibitors...	59
3.8 High <i>Met</i> expression correlated with increased survival probability in patients with SHH tumours and decreased survival probability in patients with group 3 tumours	60-61

3.9 Expression of <i>Met</i> is found to be highest in SHH medulloblastoma tumours	62-64
3.10 The average expression of <i>Met</i> was found to be highest in SHH medulloblastoma in both males and females	65-66
3.11 The age group 4-17 year olds express the highest average level of <i>Met</i> expression when compared with other age groups	67-68
3.12 Expression of <i>Met</i> is higher in desmoplastic medulloblastoma tumours than in classic and LCA tumours	69-70
3.13 Expression of <i>GSK3α</i> and <i>GSK3β</i> in medulloblastoma subtypes.....	71-73
3.14 Expression of genes of interest in group 3 and SHH medulloblastoma	74-76
Discussion	
4.1 Aims and Objectives of this project.....	77
4.2 The medulloblastoma cell lines utilised in this study (ONS76, UW228, Daoy and HD-MB03).....	77-78
4.3 Tivantinib, tepotinib, AMG337, JD-1 and JD-5 had cytotoxic effects on the SHH medulloblastoma cell line ONS76	78-80
4.4 Tivantinib was the most cytotoxic drug against the SHH α cell line UW228	80-81
4.5 The known c-Met inhibitors all had cytotoxic effects on SHH α cell line Daoy while the effects of the JD compound were not determined.....	82
4.6 Tivantinib, tepotinib and AMG337 all showed cytotoxicity toward the group 3 medulloblastoma cell line HD-MB03.....	83
4.7 Tivantinib was the most potent against all medulloblastoma cell lines followed by tepotinib, with AMG337 having the least cytotoxic effects.....	84-85
4.8 Tepotinib and tivantinib showed some level of cytotoxicity against all of the medulloblastoma cell lines (ONS76, UW228, Daoy and HD-MB03)	86
4.9 Patients with high <i>Met</i> expression in HD-MB03 had a worse survival prognosis whereas patients with high <i>Met</i> expression in SHH has a better survival prognosis	87

4.10 The levels of <i>Met</i> expression in each subgroup of medulloblastoma.....	88
4.11 Gender has no apparent effect on the <i>Met</i> expression in the subgroup of medulloblastoma.....	89
4.12 The highest average levels of <i>Met</i> expression were presented in 4 to 17 year olds when compared with other age groups	90
4.13 Desmoplastic tumours have the highest level of <i>Met</i> expression when compared with classic medulloblastoma and LCA medulloblastoma	91
4.14 <i>GSK3α</i> and <i>GSK3β</i> expression levels in SHH and group 3 medulloblastoma subtypes...	92
4.15 Genes of interest and their level of expression in SHH and group 3 medulloblastoma	93-95
Conclusion	96
Future testing	97-98
The Impact the Covid-19 pandemic on this thesis	98
Bibliography	99-111

Table of tables and Illustrations

Figure A1: Skeletal structures of JD1, JD2, tivantinib, Tepotinib and AMG337	13
Figure 1: The general prognosis of the four main groups of medulloblastoma	19
Figure 2: A graphical representation of the subtypes found in each of the four subgroups of medulloblastoma.....	20
Figure 3: A graphical summary of the demographics, clinical features, and molecular features of each subtype of the medulloblastoma subgroup SHH.....	22
Figure 4: Illustrative structures of HGF and c-Met RTK	26
Figure 5: The hepatocyte growth factor and mesenchymal epithelial transition receptor signalling pathway and its subsequent downstream signalling pathways	28
Figure 6: Diagram of the location that potential inhibitors will inactivate the HGF-Met signaling pathway	30
Table 1: List of clinically notable inhibitors of the HGF-Met signalling pathway.....	31
Figure 7: Images produced from a scratch assay performed taken at different times in the experiments to show the migration of the cells to close the wound created	35
Table 2: A list of the model systems of medulloblastoma cell lines utilized in this study...	36
Table 3: The skeletal structures of the series of organic JD compounds used in the experiments performed on different medulloblastoma cell lines	43-44
Table 4: The gene symbol, name, gene ID and other known names of the genes utilised in the R2 database experiments	47
Figure 8: MTT Assay results to show the cell viability of the cell line ONS76 when treated with different potential chemotherapeutic drugs	50
Figure 9: MTT Assay to show the cell viability of the cell line UW228 when treated with different potential chemotherapeutic drugs	52

Figure 10: MTT Assay to show the cell viability of the cell line Daoy when treated with different potential chemotherapeutic drugs	54
Figure 11: MTT Assay to showcase the cell viability of the cell line HD-MB03 when treated with different potential chemotherapeutic drugs.	56
Figure 12: MTT Assays to show the cell viability of each potential chemotherapeutic treatment in each medulloblastoma cell line.....	57
Table 5: Cytotoxicity of various treatment on four medulloblastoma cell lines (ONS76, UW228, DAOY and MB03) as determined by MTT assays.	59
Figure 13: Kaplan curve using Cavalli medulloblastoma dataset showing survival of patients with high and low <i>Met</i> gene expression c-Met RTK	60
Figure 14: Expression of <i>Met</i> in the four main subgroups and each subtype of medulloblastoma.	62
Table 6: P values created in correspondence with Fig. 14	63
Figure 15: Expression of <i>Met</i> in each subgroup and subtype of medulloblastoma.....	65
Table 7: P values created in correspondence with Fig. 15	66
Figure 16: Expression of <i>Met</i> in differing age groups of medulloblastoma patients.....	67
Table 8: P values created in correspondence with Fig. 16	67
Figure 17: <i>Met</i> expression in medulloblastoma tumours of different histology	69
Table 9: P values in correspondence with Fig. 17	69
Figure 18: The expression of <i>GSK3 alpha</i> and <i>GSK3 beta</i> in the different medulloblastoma sub types of the subgroups SHH and Group 3 medulloblastoma tumours	71
Table 10: P Value in correspondence with Fig. 18	72

Figure 19: Boxplot showing the expression levels of key genes that are important in the HGF-<i>Met</i> signalling pathway	74
Table 11: P values of the R2 database box plot graphs produced in Fig. 19	75
Table 12: Summary of Fig. 19 showcasing the medulloblastoma subgroup (SHH or Group 3) that had the highest average levels of gene expression	95

Acknowledgements

I would like to thank my supervisor Dr. Caroline Topham who has continuously provided help, guidance, and support throughout the duration of this research project.

I would also like to say thank you to Dr James Wilkinson, Sonia Morlando and all the other post graduate research members of the transitional medicine laboratory who have been extremely helpful in showing me around the laboratory, sharing and discussing their own research ideas and helping me develop ideas for my research project.

Finally, I would like to thank my family who have been extremely supportive throughout my entire university life and have encouraged me to always do my best in life.

Declaration

I have previously completed work on the HGF-Met signalling pathway in my undergraduate final year project report. Dr James Wilkinson was my supervisor during my final year report. This report was on the synthesis of a glycosaminoglycan mimic which could act as a potential inhibitor to the HGF-Met signalling pathway. The final year report focused on using organic chemistry to synthesise a compound that may potentially inhibit the HGF-Met signalling pathway. As such some relevant articles and figures that were used in the final year project report have also been referenced and reused as necessary in this thesis.

This thesis was not joint research however Sonia Morlando (PhD student) was extremely helpful in supervising me whilst in the lab. Her research was closely related to my research in that we were both working on treatment of medulloblastoma using potential c-Met inhibitors. However, her research involved targeting group 3 medulloblastoma specifically due to it's poor prognosis whereas my research was targeting the HGF-Met pathway to potentially provide a treatment for medulloblastoma.

Abbreviations

AKT	Protein kinase B (PKB)
AKT1	AKT serine/threonine kinase 1
ALK	Anaplastic lymphoma kinase
ATP	Adenosine triphosphate
CCNU	<i>N</i> -(2-chloroethyl)- <i>N'</i> -cyclo-hexyl- <i>N</i> -nitrosurea
CNS	Central nervous system
c-Met	Mesenchymal epithelial transition factor
CRC	Colorectal cancer
CYP2C19	Cytochrome P450 Family 2 Subfamily C Member 19
DOCK1	Dedicator of cytokinesis 1
DMSO	Dimethyl sulfoxide
EGL	External granular layer
ERK	Extracellular signal-regulated kinase
FAP	Familial adenomatous polyposis
FBS	Foetal bovine serum
FDA	Food and drug administration
FLT-3	FMS related receptor tyrosine kinase 3
FLT-4	FMS related receptor tyrosine kinase 4
GAB1	GRB2 associated binding protein 1
GAG	Glycosaminoglycan
GBM	Glioblastoma multiforme
GRB2	Growth factor receptor bound protein 2

GSK3	Glycogen synthase kinase 3
GSK3 α	Glycogen synthase kinase 3 alpha
GSK3 β	Glycogen synthase kinase 3 beta
HCC	Hepatocellular carcinoma
HNSCC	Head and neck squamous cell carcinoma
HGF	Hepatocyte growth factor
HGF-Met	Hepatocyte growth factor – mesenchymal epithelial transition factor
IC ₅₀	Half maximal inhibitory concentration
IPT	Immunoglobulin-like plexins transcription
KDR	Vascular endothelial growth factor receptor-2
KRAS	Kirsten ras oncogene homolog
LCA	Large cell/Anaplastic
mAb	Monoclonal antibody
MAPK1	Mitogen-activated protein kinase 1
MB	Medulloblastoma
MBEN	Medulloblastoma with extensive nodularity
MEK	Mitogen-activated protein kinase
Met	Mesenchymal epithelial transition
MTOR	Mechanistic target of rapamycin
MTT	Thiazolyl Blue tetrazolium bromide
MYC	Myelocytomatosis
NBCCS	Nevoid basal cell carcinoma syndrome
NSCLC	Non-small cell lung cancer

ORR	Overall response rate
P53	Tumour protein 53 (also known as TP53)
PBS	Phosphate buffered saline
PFS	Progression-free survival
PI3K	Phosphoinositide 3-kinase
PNETs	Primitive neuroectodermal tumours
pRCC	Papillary renal cell carcinoma
P/S	Penicillin / streptomycin
PSI	Plexin, Semaphorin and Integrin cysteine-rich
PTCH	Patched
PTPs	Protein tyrosine phosphatases
RAF	Rapidly accelerated fibrosarcoma
RAP1	Ras-related protein 1
RAP1A	Ras-related protein 1 gene
RAS	Rat sarcoma viral oncogene homolog
RCC	Renal cell carcinoma
RON	Receptor originated from Nantes
ROS1	ROS proto-oncogene 1 (ROS1)
RPMI 1640	Roswell Park Memorial Institute 1640 media
RTK	Receptor Tyrosine Kinase
SCCHN	Squamous cell cancer of the head and neck
SEMA	Semaphorin
SH2	Src homology-2

SHH	Sonic hedgehog
STAT3	Signal transducer and activator of transcription 3
Tie-2	Tyrosine-protein kinase receptor Tie-2
TKI	Tyrosine kinase inhibitors
TNBC	Triple-negative breast cancer
WNT	Wingless

Abstract

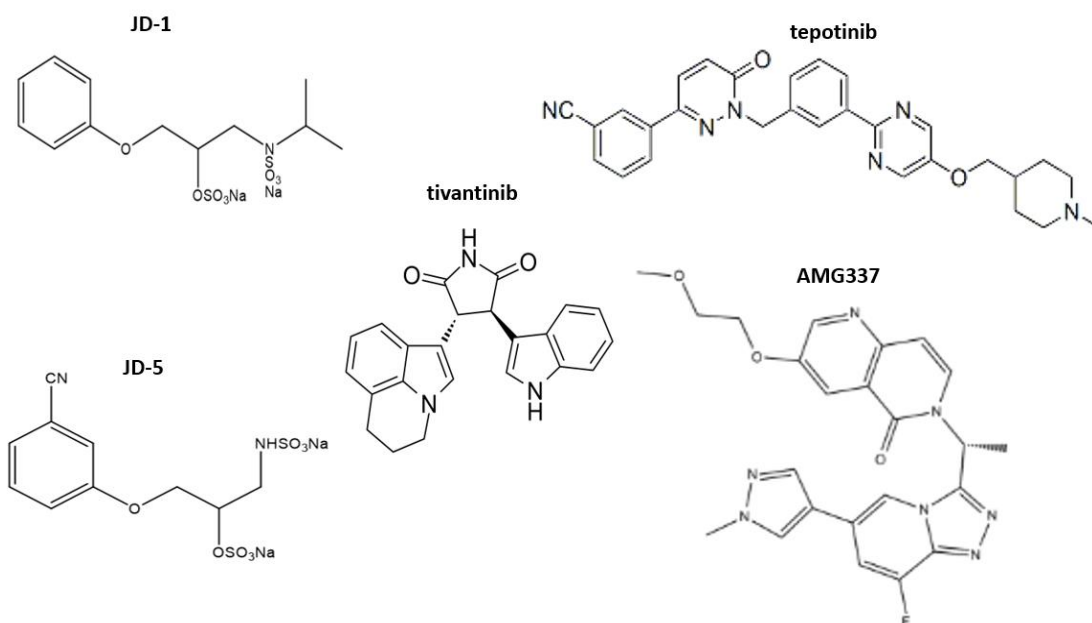


Figure A1: Skeletal structures of JD-1, JD-2, tivantinib, tepotinib and AMG337. These compounds each showed some level of cytotoxicity when treating the medulloblastoma cell lines (ONS76, UW228, Daoy and HD-MB03). (Adapted from data provided by Sonia Morlando of The University of Salford; Adooq Bioscience, 2021; Selleckchem, 2021)

Understanding the function of the HGF-Met signalling axis could present opportunities for new therapeutic treatments for cancer patients. The brain tumour Medulloblastoma is the leading cause of cancer-related death in children and infants meaning research into better treatment of this cancer is vital. Using cell culture model systems and bioinformatics resources, this project investigated the possible inhibition of c-Met as a potential strategy to improve the treatment options for the childhood cancer medulloblastoma and potentially reduce the impact of late effects on those affected by this form of brain tumour. A panel of known c-Met inhibitors (AMG337, tepotinib and tivantinib) were compared with a panel of novel c-Met inhibitors (JD-1, JD-2, JD-3, JD-4 and JD-5) designed at the University of Salford in order to determine the cytotoxic effect on four medulloblastoma cell lines (ONS76, UW288, Daoy and HD-MB03). However, the novel JD compounds were mostly found to have no cytotoxic effect with the exception of JD-1 and JD-5. In addition, the R2 genomics database

was interrogated in order to better understand c-Met as a therapeutic target in medulloblastoma. The Cavalli 2017 medulloblastoma expression dataset consisting of 763 patient biopsies was primarily used in order to identify patient characteristics and survival probability linked to high *Met* expression such as age, gender and sub-group of disease. The SHH medulloblastoma sub-group was found to express the highest average level of *Met* expression in patients of each medulloblastoma subgroup yet surprisingly these patients also displayed a higher survival probability when *Met* expression was high. In contrast, in the most aggressive medulloblastoma subgroup Group 3 the survival prognosis was shown to be worse when *Met* expression was high. The opposite effects that *Met* expression levels had on each of these sub-groups highlights the importance of patient stratification for the use of *Met* inhibition as a novel therapeutic strategy for the treatment of medulloblastoma.

1. Introduction

1.1 Cancer is a Global Health Concern

Cancer is extremely prevalent in modern society with around 1000 new cases of cancer diagnosed each day in the UK in 2016 (Macmillan Cancer Support, 2019). By the year 2035 incidence rates of cancer is projected to rise by approximately 2% (Cancer Research UK, 2018). The most common cancers are liver cancers, bowel cancers, stomach cancers and lung cancers (Cancer Research UK, 2018). In 2018 9.6 million deaths were recorded worldwide (World Health Organisation, 2018) 44% of which were females and 56% males (Cancer Research UK, 2018). This is equivalent to one-sixth of all deaths worldwide being a result of cancer (World Health Organisation, 2018). The cancer mortality rate in the United Kingdom is two-thirds larger than the cancer mortality rate in the rest of the world (Cancer Research UK, 2018).

1.2 Paediatric Cancer

Childhood cancers account for >1% of cancer cases in the UK in 2017 with the incidence rates being shown as similar worldwide (Cancer research UK, 2018). Children under the age of 5 present 46% of all cancer cases in children in the UK in 2014-2016 (Children with Cancer UK, 2019). The incidence rate of cancer in children has increased by 15% between 1993 to 1995 and 2015 to 2017 (Cancer research UK, 2018). Cancer is the primary cause of mortality in children worldwide with around 300,000 cases of cancer confirmed in young persons aged 0 to 19 years of age each year (World Health Organisation, 2018). There are approximately 240 deaths in the UK per year of children diagnosed with cancer in 2015-2017 (Cancer research UK, 2018). Survival of childhood cancers in 2006-2010 in the UK has increased to around 82% of children with cancer surviving the disease for 5 years or more (Children with Cancer UK, 2019). Childhood cancer survival is constantly improving and the survival of children with cancer has doubled in Great Britain in the last 40 years (Cancer research UK, 2018). The most common cancer diagnosed in children to date is leukaemia (Cancer research UK, 2018). Central nervous system (CNS) and brain tumours account for 25% of cancer cases making these tumours the second most common cancers in children (Tidy, 2015). Astrocytoma is the most frequent subgroup of all brain and CNS tumours

accounting for 43% with intracranial and intraspinal embryonal tumours being the second most common tumours accounting for approximately one fifth of this category of tumours (Cancer research UK, 2018). Most of the intracranial and intraspinal embryonal tumours are Primitive neuroectodermal tumours (PNETs) of which 73% being medulloblastomas (Tidy, 2015). PNETs commonly occur in young children and the incidence rate decreases with age (Cancer research UK, 2018).

1.3 Medulloblastoma

The embryonal brain tumour medulloblastoma is located in the cerebellum (Waszak et al., 2018). It is currently the most frequent malignant brain tumour to occur in children (Susanto et al., 2020). Approximately 35% of children diagnosed with medulloblastoma have a metastatic tumour (Carta et al., 2020). Around 5% of cases are associated with either Neurofibromatosis type 1 (NF1) or Familial adenomatous polyposis (FAP) (Cancer Research UK, 2020). These inherited cancer syndromes increase the risk of a child developing medulloblastoma (Cancer Research UK, 2020). The extent of metastasis of paediatric medulloblastoma tumours is inversely correlated to the patient's survival (Kahn et al., 2018). Considerable improvements have been made into the therapeutic treatments for childhood malignancies (National Cancer Institute, 2020). Exploring treatments targeted towards the molecular characteristics of tumours using chemotherapies such as stem-cell strategies, immunotherapies and target agents have allowed for a better survival prognosis in people affected by cancer (Luzzi et al., 2020). Survival rates of cancer patients have consistently increased in recent decades from 22% in 1950 to as high as 85% with current treatments available today (Bautista et al., 2017). The long-term survival of children who suffer from malignancies is expected to be more than 80% for children who have access to up to date chemotherapy (Cancer research UK, 2020). Current treatments available for childhood medulloblastomas consists of surgery, radiotherapy, and chemotherapy. Cisplatin, methotrexate, and vincristine are just a few of the chemotherapeutic drugs that may be used as a treatment for medulloblastoma (Cancer Research UK, 2020). Genetic heterogeneity plays a role in the unpredictability of the therapeutic efficacy of medulloblastoma treatments (Topham *et al.*, 2016).

1.4 Late Effects of Treatment in Medulloblastoma patients

Current medulloblastoma treatments have resulted in an improved overall 5-year survival rate for medulloblastoma patients, as high as 70% (Kuzan-Fischer, Juraschka & Taylor, 2018). However, the treatments and improved survival rate has been linked with late effects (Kuzan-Fischer, Juraschka & Taylor, 2018). Late effects are long-term side effects that may present themselves years after the initial treatment of a patient (National Cancer Institute, 2020). The number of cancer survivors that experience late effects after treatment is substantial (Bhakta et al., 2017). One or more chronic conditions emerge in 60%-90% of paediatric cancer survivors (National Cancer Institute, 2020). This statistic is more staggering when compared with the fact that up to 80% of survivors encounter life-threatening health problem in their adulthood as a result (National Cancer Institute, 2020). The increased risk of morbidity in childhood cancer patients and the detrimental impact late effects have on survivor's quality of life present a need for better treatments that present fewer late effects (National Cancer Institute, 2020). Some of the late effects that largely effect the survivors of medulloblastoma treatment include endocrine deficiencies, secondary tumours and neurocognitive impairment (Kuzan-Fischer, Juraschka & Taylor, 2018). Frič et al., 2020 conducted a study into the effects suffered by long term medulloblastoma cancer survivors (surviving >20 years after treatment). The conclusion of this study highlighted a concern of medulloblastoma survivors dying due to the recurrence of a tumour in the decades following treatment (Frič et al., 2020). However, the main cause for concern was the late mortality and morbidity caused by late effects related to the oncological treatment occurring in long-term medulloblastoma survivors (Frič et al., 2020). Complications suffered resulting from neuro-oncological treatment include: reduced neurocognitive capacity, loss of hearing, cavernous malformation, stroke, cardiovascular disease, posterior fossa syndrome, stunted growth, and hypopituitarism (Juraschka & Taylor, 2019). These secondary illnesses are becoming a larger problem as survival rates of paediatric medulloblastoma patients is increasing thus leaving a need for better treatment efficacy with as little late effects as possible (Kuzan-Fischer, Juraschka & Taylor, 2018).

1.5 Genetic Heterogeneity in Medulloblastoma

The recognition of utilising medulloblastoma tumour heterogeneity to predict a prognosis for individualised patients has made the heterogeneity of this disease a research focus to assist the personalised treatment of medulloblastoma patients (Danilenko, Clifford & Schwalbe, 2021). Medulloblastoma has been historically characterised into four histological variants, that are separated based on the morphology of the cells under a microscope (Taylor et al., 2011). These groups include: classic medulloblastoma, medulloblastoma with extensive nodularity (MBEN), large cell anaplastic (LCA) medulloblastoma and desmoplastic medulloblastoma (Danilenko, Clifford & Schwalbe, 2021). Currently classic medulloblastoma accounts for 68%-80%, desmoplastic has a more favourable prognosis and accounts for 7%, MBEN accounts for 3% and LCA accounts for 10-22% of medulloblastomas (Carta et al., 2020). More recently, medulloblastoma has been classified into molecular subgroups of the disease (Danilenko, Clifford & Schwalbe, 2021).

Subgroup		WNT	SHH	Group 3	Group 4
Clinical Characteristics	% of Cases	10	30	25	35
	Age at Diagnosis				
	Gender Ratio (M:F)	1:1	1:1	2:1	3:1
	Anatomic Location				
	Histology	Classic, Rarely LCA	Desmoplastic, Classic, LCA	Classic, LCA	Classic, LCA
	Metastasis at Diagnosis (%)	5-10	15-20	40-45	35-40
	Recurrence Pattern	Rare; Local or metastatic	Local	Metastatic	Metastatic
	Prognosis	Very good	Infants good, others intermediate	Poor	Intermediate
Molecular Characteristics	Proposed Cell of Origin	Progenitor cells in the lower rhombic lip	Granule precursors of the external granule layer	Neural stem cells	Unipolar brush cells
	Recurrent Gene Amplifications	-	<i>MYCN</i> <i>GLI1</i> or <i>GLI2</i>	<i>MYC</i> <i>MYCN</i> <i>OTX2</i>	<i>SNCAIP</i> <i>MYCN</i> <i>OTX2</i> <i>CDK6</i>
	Recurrent SNVs	<i>CTNNB1</i> <i>DDX3X</i> <i>SMARCA4</i> <i>TP53</i>	<i>PTCH1</i> <i>TERT</i> <i>SUFU</i> <i>SMO</i> <i>TP53</i>	<i>SMARCA4</i> <i>KBTD4</i> <i>CTDNBP1</i> <i>KMT2D</i>	<i>KDM6A</i> <i>ZMYM3</i> <i>KTM2C</i> <i>KBTD4</i>
	Cytogenetic Events ■ Gain ■ Loss	6	3q, 9p 9q, 10q, 17p	1q, 7, 18 8, 10q, 11, 16q i17q	7, 18q 8, 11p, X i17q
	Other Recurrent Genetic Events	-	-	<i>GF11</i> and <i>GF11B</i> enhancer hijacking	<i>PRDM6</i> , <i>GF11</i> , and <i>GF11B</i> enhancer hijacking

Age: Infant Child Adult

Fig. 1: The general prognosis of the four main subgroups of medulloblastoma (Wingless (WNT), Sonic hedgehog (SHH), Group 3 and Group 4) showing a breakdown of both clinical characteristics and molecular characteristics found in each of the subgroups. Prognosis for WNT is the most favourable whilst the prognosis for Group 3 medulloblastoma is poor. Group 4 medulloblastoma is the most common diagnosis. Group 3 medulloblastoma presents the highest level of metastasis of other medulloblastoma subgroups (Juraschka & Taylor, 2019).

In present times medulloblastoma has been categorised into four subgroups of medulloblastoma that further differentiate between the cells present in the tumour (Juraschka & Taylor, 2019). These subgroups include: Sonic hedgehog medulloblastoma (SHH), Wingless medulloblastoma (WNT), group 3 medulloblastoma and group 4

medulloblastoma (Fig. 1) (Danilenko, Clifford & Schwalbe, 2021). The identification of the subgroups is concluded through genetics and the overall prognosis (Juraschka & Taylor, 2019). These subgroups are further differentiated by clinical characteristics into medulloblastoma subtypes (Cavalli et al., 2017).

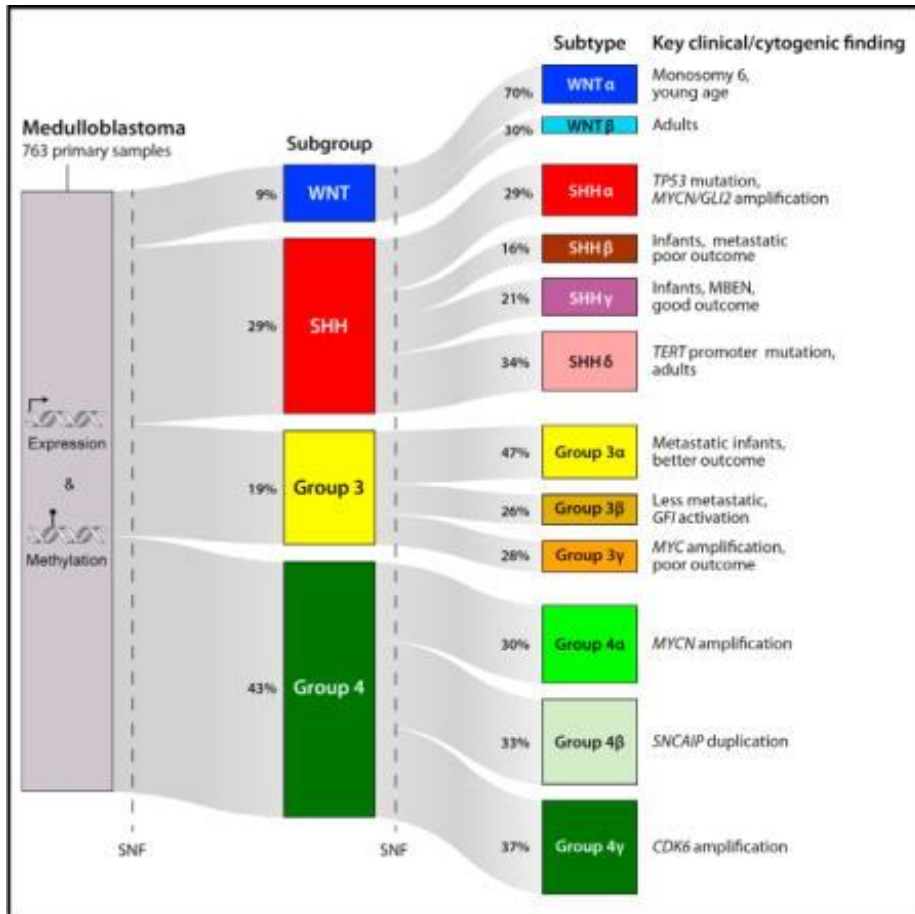


Fig. 2: A graphical representation of the subtypes found in each of the four subgroups of medulloblastoma (WNT, SHH, Group 3 and Group 4) and the key clinical characteristics of the subtypes. The medulloblastoma subtypes are comprised of: WNT α , WNT β , SHH α , SHH β , SHH γ , SHH δ , Group 3 α , Group 3 β , Group 3 γ , Group 4 α , Group 4 β and Group 4 γ (Cavalli et al., 2017).

Cavalli et al., 2017 identified 12 subtypes existing within the previously categorised subgroups: WNT α , WNT β , SHH α , SHH β , SHH γ , SHH δ , Group 3 α , Group 3 β , Group 3 γ , Group 4 α , Group 4 β and Group 4 γ (Fig. 2). Unexplained variations within subgroups can be explained by intra-subgroup heterogeneity (Cavalli et al., 2017).

1.5.1 WNT subgroup

WNT signalling is present in many cancers (Zhan, Rindtorff & Boutros, 2016). WNT medulloblastoma tumours are presented predominantly in children and adolescents (Fig.1). The origin of WNT tumours has been found to be in the progenitor cells in the lower rhombic lip of the brain (Kijima & Kanemura, 2016). WNT is the least common medulloblastoma subgroup that presents the lowest percentage of metastatic disease at diagnosis ~ 10% (Doussouki, Gajjar & Chamdine, 2019). A cytogenetic loss of chromosome 6 occurs in WNT medulloblastoma tumour cells (Fig. 1). WNT medulloblastoma tumours present upregulated expression of genes found downstream of the WNT signalling pathway such as: *WIF1*, *AXIN2*, *WNT11*, *WNT16*, *DKK1*, *DKK2*, *DKK4*, *FZ6* and *FZ10* (Northcott, Dubuc, Pfister & Taylor, 2012) A number of these genes are known inhibitors of the WNT signalling pathway and when overexpressed create a negative-feedback loop in abnormal WNT signalling (Northcott, Dubuc, Pfister & Taylor, 2012). WNT α and WNT β account for 70% and 30% of WNT medulloblastomas retrospectively (Fig.2). There is no significant difference in survival prognosis of the WNT subtypes despite WNT α mostly occurring in children with monosomy 6 while WNT β occurs mostly in adults with diploid chromosome 6 (Doussouki, Gajjar & Chamdine, 2019).

1.5.2 SHH subgroup

	Demographics		Clinical features		Molecular features	
β (SHH-1)	Frequency	15%	Histology	Desmoplastic > Classic	Cytogenetics	2+ 
	Age	 0-3	Metastasis	30-35%	Driver events	<i>PTEN</i> loss <i>KMT2D</i> , <i>PTCH1</i> , <i>SUFU</i> mutations
	Gender	♀ 50 ♂ 50	5-year survival (OS)	65-70%		
γ (SHH-2)	Frequency	35%	Histology	Desmoplastic > MBEN classic	Cytogenetics	Balanced 
	Age	 0-3	Metastasis	10%	Driver events	<i>PTCH1</i> mutations
	Gender	♀ 45 ♂ 55	5-year survival (OS)	85-90%		
α (SHH-3)	Frequency	30%	Histology	Classic > desmoplastic > LCA	Cytogenetics	9p+ 
	Age	 3-10 10-17	Metastasis	20%	Driver events	<i>MYCN</i> , <i>GLI2</i> , amplification <i>TP53</i> , <i>ELP1</i> , <i>PTCH1</i> , <i>U1 snRNA</i> mutations
	Gender	♀ 35 ♂ 65	5-year survival (OS)	70%		
δ (SHH-4)	Frequency	20%	Histology	Classic > desmoplastic >	Cytogenetics	
	Age	 10-17 17+	Metastasis	10%	Driver events	<i>DDX3X</i> , <i>SMO</i> , <i>TERT</i> , <i>PTCH1</i> , <i>U1 snRNA</i> mutations
	Gender	♀ 30 ♂ 70	5-year survival (OS)	90%		

Fig. 3: A graphical summary of the demographics, clinical features, and molecular features of each subtype of the medulloblastoma subgroup SHH (Garcia-Lopez, Kumar, Smith and Northcott, 2021).

The SHH signalling pathway was the namesake of the SHH medulloblastoma subgroup as this pathway is key in the regulation of this medulloblastoma subgroup (Doussouki, Gajjar & Chamdine, 2019). Normal SHH signalling is essential in cerebellar development (Garcia-Lopez, Kumar, Smith and Northcott, 2021). SHH medulloblastomas originate from the granule neuron progenitors located in the external granular layer (EGL) (Tao et al., 2019).

Genes in the SHH signalling pathway are upregulated in SHH medulloblastoma causing aberrant activation of the pathway (Yoon et al., 2009).

SHH medulloblastomas most commonly affect infants as well as adults (Juraschka & Taylor, 2019). Desmoplastic tumours are only presented in the SHH medulloblastoma subgroup (Fig. 1). The SHH medulloblastoma subgroup is further separated into 4 subtypes: SHH α , SHH β , SHH γ and SHH δ (Fig. 2). SHH β presents the worst prognosis with a 5 year-survival prediction of 65-70% when compared with the other SHH subtypes having survival prognosis of 70%+ (Fig. 3). SHH α medulloblastoma can have mutations in the *TP53* gene (Fig. 3) and amplification of the gene *MYCN* (Garcia-Lopez, Kumar, Smith and Northcott, 2021). Individuals possessing a germline mutation in the patched (PTCH) receptor (a receptor of the SHH pathway) have a predisposition to the childhood cancer medulloblastoma (Kijima & Kanemura, 2016).

1.5.3 Group 3 subgroup

Group 3 medulloblastoma is the most aggressive subgroup leaving patients with the poorest prognosis of the four subgroups of medulloblastoma (Kuzan-Fischer, Juraschka & Taylor, 2018). Males are more likely to be diagnosed with group 3 medulloblastoma than females at a ratio of 2:1 (Fig. 1). Metastasis occurs in approximately half of medulloblastoma group 3 patients (Kijima & Kanemura, 2016). 5-year survival probabilities of group 3 medulloblastoma drop to 45-60%, from a typical prognosis of 75%+ in all other medulloblastoma subgroups (Menyhárt, Giangaspero & Győrffy, 2019). Around 25% of all medulloblastomas are classified as group 3 tumours which most typically affect infants and children (Fig. 1). The high risk medulloblastoma subgroup, group 3, is associated with a high level of morbidity (Kijima & Kanemura, 2016). Upregulation of myelocytomatosis (*MYC*) is frequent in group 3 γ tumours while the loss of *MYC* expression is common in group 3 α (Tao et al., 2019). Over 70% of medulloblastoma patients experiencing amplified *MYC* expression do not survive the disease (Tao et al., 2019).

1.5.4 Group 4 subgroup

Group 4 medulloblastomas are the most common tumour affecting 35% of all medulloblastoma patients (Kijima & Kanemura, 2016; Cavalli et al., 2017) as shown in Fig. 1. Group 4 medulloblastoma has an intermediate survival prognosis and reoccurrence of the tumour typically occur late (Juraschka & Taylor, 2019). Males are 3 times more likely to be diagnosed with group 4 medulloblastoma than females (Fig. 1). Group 4 is further differentiated into 3 subtypes: group 4 α , group 4 β and group 4 γ (Fig. 2). Group 4 α and Group 4 γ tumours experience 8p chromosomal loss and 7q chromosomal gain (Doussouki, Gajjar & Chamdine, 2019).

1.6 Current treatments for medulloblastoma

Surgery, if possible, is the initial treatment for medulloblastoma patients to remove as much of the tumour as is feasible (National Cancer Institute, 2021). Once the tumour is removed analysis of the tissue can be undertaken to determine the subgroup category of the medulloblastoma tumour (National Cancer Institute, 2021). A number of factors affect the decisions made about further treatment after surgery including: the subgroup of the tumour, metastasis of the tumour and the age of the patient (Cancer Research UK, 2020). Craniospinal radiation is a common current treatment supplemented with boost radiotherapy to the tumour bed for medulloblastoma tumours in children over the age of 3 years (Juraschka & Taylor, 2019). Chemotherapy regimens chosen as treatment are predominantly determined by the child's age (Juraschka & Taylor, 2019). Children > 3 years old are treated with regimens including: vincristine, *N*-(2-chloroethyl)-*N'*-cyclo-hexyl-*N*-nitrosurea (CCNU) and cisplatin; vincristine, cisplatin, cyclophosphamide and etoposide, which have allowed for the survival rates of children living with medulloblastoma to increase as high as 85% (Packer & Vezina, 2008). Chemotherapy is usually a focused treatment in infants < 3 years of age rather than craniospinal radiotherapy due to the neurocognitive damage caused as a result of craniospinal radiotherapy (Packer & Vezina, 2008). Chemoresistance characteristics that medulloblastoma tumours can possess such as upregulation of anti-apoptotic/pro-survival signalling pathways can play a role in treatment failure (Huang et al., 2016). Subgroup targeted chemotherapies lack exploration and

research, yet personalising therapy based on individual characteristics of each subgroup may allow for better treatment (Doussouki, Gajjar & Chamdine, 2019). Aberrant mesenchymal epithelial transition factor (c-Met) signalling can promote tumorigenesis and is found to be upregulated in several cancers as such c-Met targeted chemotherapy may improve current treatment in hepatocyte growth factor - mesenchymal epithelial transition factor (HGF-Met) dependent medulloblastoma tumours (Faria, Smith & Rutk, 2011).

1.7 The role of the HGF-Met signalling pathway in cancer

Studies have identified overexpression of the mesenchymal epithelial transition receptor in a multitude of tumours (Birchmeier, et al., 2003). Cancer development has been associated with mutations in the receptor tyrosine kinase (RTK) c-Met (Matsumoto, et al., 2017; Garajova, Giovannetti, Biasco & Peters, 2015). C-Met has been identified as an oncogene (Organ & Tsao, 2011). Upregulated c-Met, by either *Met* amplification or c-Met overactivation, has been observed in various primary tumours including: medulloblastomas, colon carcinoma, thyroid carcinomas, ovarian cancer, pancreatic tumours, lung tumours and breast cancer (Organ & Tsao, 2011). Amplified c-Met activation, with hepatocyte growth factor (HGF), enables metastasis initiation, cell growth and cell survival (Viticchiè & Muller, 2015). The receptor tyrosine kinase c-Met is spontaneously unregulated in approximately 2% to 3% of cancers (Cruickshanks et al., 2017). Overexpressed c-Met is linked to poor survival in cancer patients (Hack, Bruey & Koeppen, 2014). The HGF-Met signaling pathway plays a key role in development of the cerebellum (Faria, Smith & Rutk, 2011). In brain tumours HGF amplification, in human glioma cells, increased tumorigenicity and angiogenesis (Mulcahy, Colón & Abounader, 2020). Overactivation of the signalling pathway by increased HGF expression in medulloblastoma cells induced proliferation, anchorage-independent cell growth and chemoresistance (Faria, Smith & Rutk, 2011). Studies indicate that a key target for cancer therapy may be the HGF-Met signalling pathway (Garajova, Giovannetti, Biasco & Peters, 2015).

1.7.1 Hepatocyte growth factor and mesenchymal epithelial transition protein

Scatter factor, also known as the hepatocyte growth factor, is essential for migration, growth and the survival of epithelial and endothelial cells (Mungunsukh, McCart & Day, 2014). The receptor of the ligand HGF is c-Met (Zhang, Jain & Zhu, 2015).

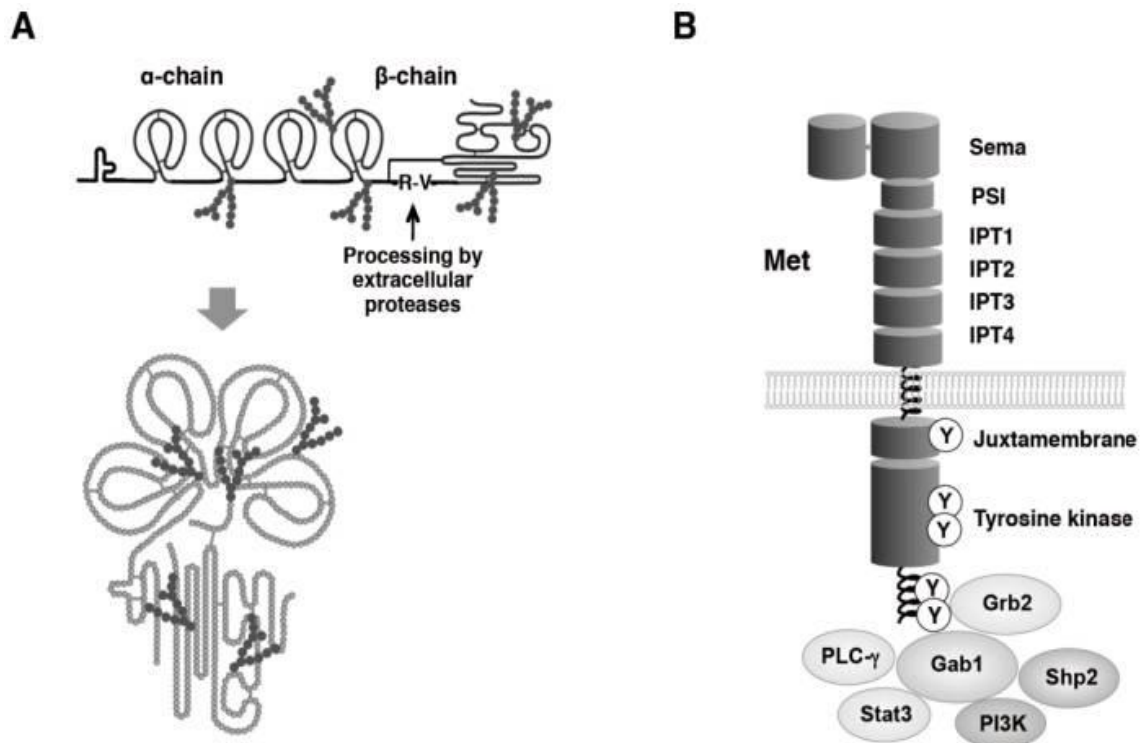


Fig. 4: Illustrative structures of HGF (a) and c-Met RTK (b). Mature hepatocyte growth factor is made up of an α and β chain which are linked via a disulfide bridge. Mature HGF is produced from proteolytically cleaved pro-HGF. The key extracellular domains of c-Met are the four Immunoglobulin-like plexins transcription (IPT) domains, a semaphorin (SEMA) domain and a Plexin, Semaphorin and Integrin cysteine-rich (PSI) domain. The SEMA domain is essential for the binding of the ligand to c-Met. The juxtamembrane and tyrosine kinase domains are located intracellularly (Matsumoto, et al., 2014).

The HGF structure is comprised of two subunits: a light α chain and a heavy β chain. These two chains are linked by a disulfide bridge (Matsumoto et al., 2017). There are four kringle domains that make up the α chain, whilst the β chain is composed of a serine-protease like

structure (Fig. 4) (Matsumoto et al., 2014). The N-terminal of HGF contains a hairpin loop domain. Pro-HGF is the raw form of HGF that is not yet biologically active and must be cleaved by extracellular proteases in order to form its mature state (Fig. 4) (Garajova, Giovannetti, Biasco & Peters, 2015). Pro-HGF is secreted as a biologically inert molecule by mesenchymal cells (Organ & Tsao, 2011). HGF is located on chromosome 7 and its subsequent receptor is c-Met (Nakamura & Mizuno, 2010).

The proto-oncogene mesenchymal epithelial transition (Appleman, et al., 2014) encodes for the c-Met protein which is a part of the receptor tyrosine kinase family (Kato, 2017). The glycoprotein heterodimer is made up of an α subunit, which is extracellular, and a β subunit, which is transmembrane (Garajova, Giovannetti, Biasco & Peters, 2015). These are linked through a disulphide bond (Organ & Tsao, 2011). The main domains of the c-Met heterodimer that are extracellular are: four Immunoglobulin-like plexins transcription (IPT) domains, a semaphorin (SEMA) domain and a Plexin, Semaphorin and Integrin cysteine-rich (PSI) domain (Garajova, Giovannetti, Biasco & Peters, 2015). Whereas the catalytic region, the juxtamembrane sequence (containing tyrosine kinases) and the C-terminal of c-Met, which contains a docking site, are all located intracellularly (Organ & Tsao, 2011). C-Met can be found on the cell surface of endothelial cells and epithelial cells (Garajova, Giovannetti, Biasco & Peters, 2015).

1.7.2 The hepatocyte growth factor-Met Kinase signalling pathway

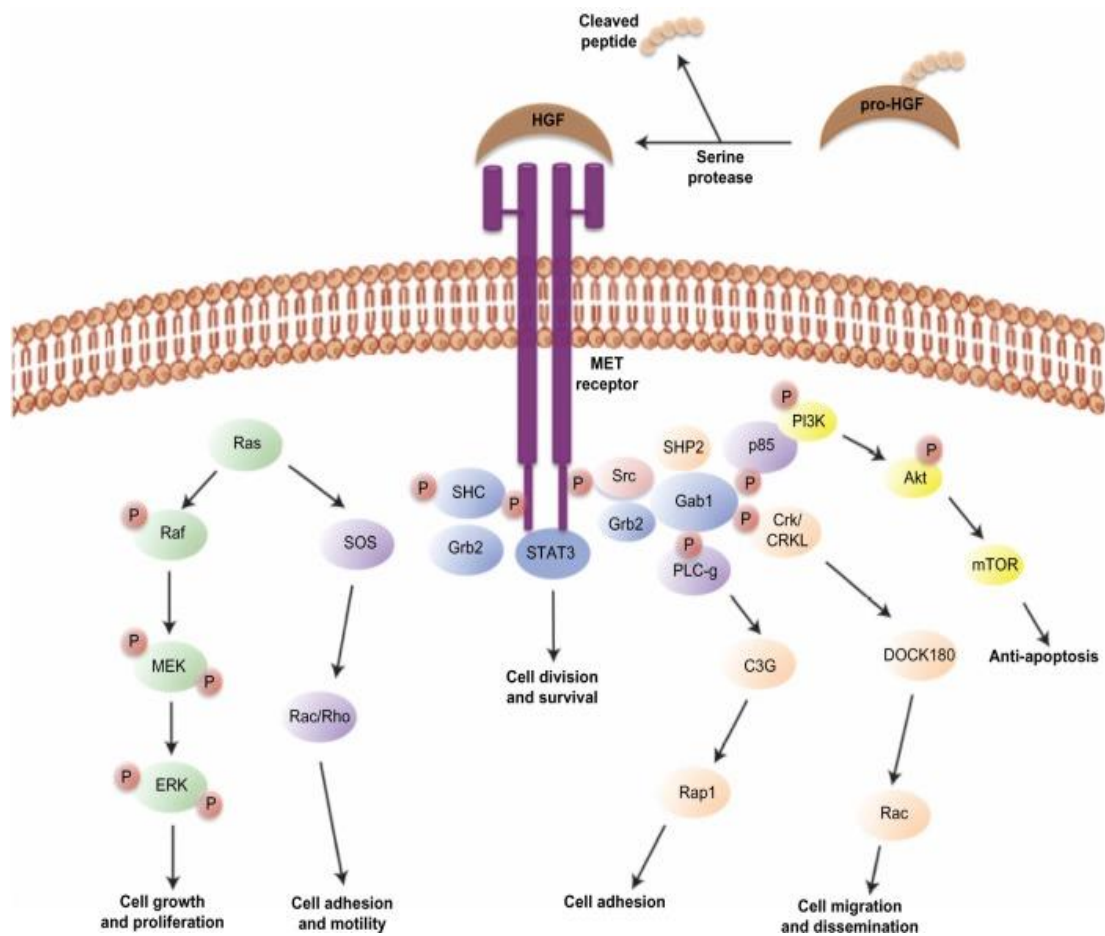


Fig. 5: The hepatocyte growth factor and mesenchymal epithelial transition receptor signalling pathway and its subsequent downstream signalling pathways (Appleman, et al., 2014).

HGF can bind to c-Met at two different sites, the first of which allows the N-terminal of HGF to bind to IPT3 and IPT4 domain of c-Met (Garajova, Giovannetti, Biasco & Peters, 2015). The second binding site is the domain containing the serine proteases homology will bind c-Met's extracellular SEMA domain (Garajova, Giovannetti, Biasco & Peters, 2015). The second binding site has a lower affinity for HGF than the first and will only bind mature HGF rather than the inactive form (Garajova, Giovannetti, Biasco & Peters, 2015). Once c-Met has bound HGF a resulting phosphorylation cascade occurs (Organ & Tsao, 2011). The phosphorylation of Y1234 and Y1235 initiates the phosphorylation of Y1349 and Y1356 which are docking tyrosine's that reside at the C-terminal (Organ & Tsao, 2011). This key

phosphorylation enables c-Met to bind to different Src homology-2 (SH2) domains containing proteins that each initiate their own phosphorylation cascade (Mulcahy, Colón & Abounader, 2020) allowing for different cellular functions to take place such as cell proliferation, the invasiveness of cells, the migration of cells and overall cell survival (Fig. 5) (Garajova, Giovannetti, Biasco & Peters, 2015). Somatic or germline mutations that are presented in either the c-Met receptor or the HGF ligand can lead to unregulated downstream signaling pathways of the HGF-Met signaling pathway (Maroun & Rowlands, 2014).

The downstream signalling pathways of HGF-Met contribute to many essential cellular processes. These biological mechanisms of action include cell proliferation, cell survival, angiogenesis, cell mobility, cell migration (Appleman, et al., 2014; Kato, 2017), cell adhesion and anti-apoptosis (Appleman, et al., 2014). Proteins involved in downstream signalling pathways include: Phosphoinositide 3-kinase (PI3K), Signal transducer and activator of transcription 3 (STAT3), Growth factor receptor bound protein 2 (GRB2) and GRB2 associated binding protein 1 (GAB1) (Mulcahy, Colón & Abounader, 2020). When these protein kinases are bound the phosphorylation cascade of multiple signalling pathways are activated (Organ & Tsao, 2011). GRB2 activates the rat sarcoma viral oncogene homolog (RAS)/ Rapidly accelerated fibrosarcoma (RAF)/ Mitogen-activated protein kinase (MEK)/ Extracellular signal-regulated kinase (ERK) pathway (Fig. 5). The scaffold protein GAB1 allows for the recruitment and resulting activation of PI3K/ protein kinase B (AKT) signalling (Mulcahy, Colón & Abounader, 2020). Negative regulation of c-Met is essential for the control of mechanisms activated by c-Met signalling (Organ & Tsao, 2011). This can be achieved by the Y1003 negative regulatory site or the binding of protein tyrosine phosphatases (PTPs) to c-Met (Organ & Tsao, 2011). When a cell is placed under stress a caspase-3-mediated mechanism cleaves c-Met (Boissinot, Vilaine & Hermouet, 2014). This produces a fragment, 40 kDa in size, that is critical for the initiation of apoptosis (Boissinot, Vilaine & Hermouet, 2014).

1.7.3 Inhibitors of the HGF-Met signalling pathway

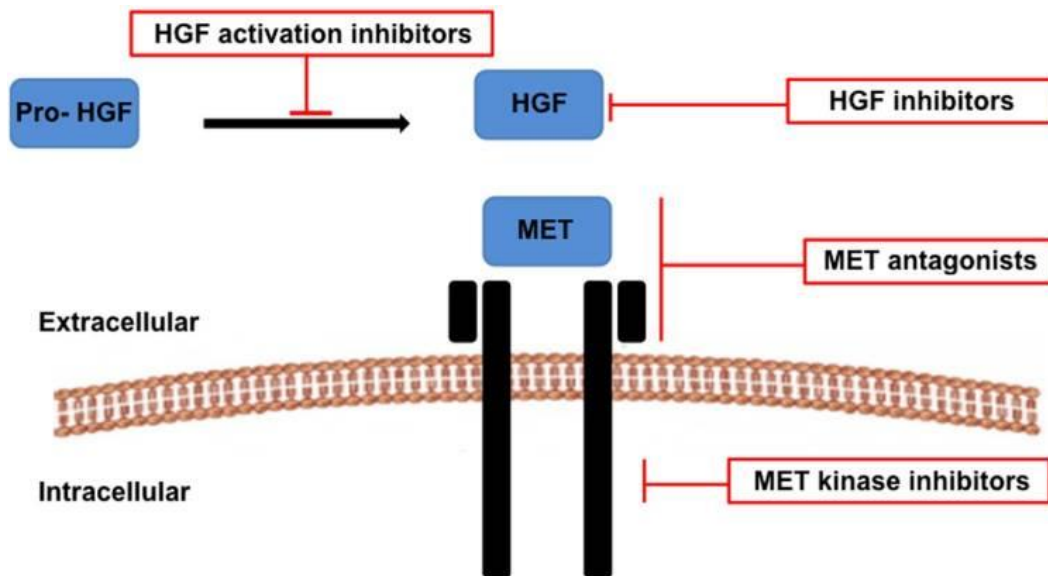


Fig. 6: Diagram of the location that potential inhibitors will inactivate the HGF-Met signaling pathway (Garajova, Giovannetti, Biasco & Peters, 2015).

There are many different inhibitors of the signaling pathway that occur when HGF binds c-Met and as such these inhibitors are classified as either: HGF activation inhibitors, HGF inhibitors, c-Met tyrosine kinase inhibitors and c-Met antagonists (Fig. 6). These can then be further classified as either small molecules or monoclonal antibodies (mAb). (Garajova, Giovannetti, Biasco & Peters, 2015). C-Met tyrosine kinase inhibitors (TKIs) can cause inhibition in both HGF-independent and HGF-dependent c-Met signalling pathways as both signals are dependent on c-Met kinase activity (Bouattour et al., 2018). TKIs can be either selective or nonselective. TKIs are usually defined as being selective when the only kinase inhibited by the TKI is c-Met (Bouattour et al., 2018). However, TKIs that have only c-Met as a known target in vitro could be nonselective against untested targets (Bouattour et al., 2018).

Table 1: List of clinically notable inhibitors of the HGF-Met signalling pathway (adapted from Bouattour et al., 2018; El Darsa, El Sayed & Abdel-Rahman, 2020; Hughes et al., 2016).

Drug Name	Type	Mechanics	Therapeutically relevant targets	Phase 2 indications
AMG337	Small-molecule TKI	ATP competitive	c-Met	-
Tivantinib	Nonselective TKI	Non-ATP competitive	c-Met, tubulin	Gastric, CRC, RCC, HNSCC, prostate, breast, pancreas, mesothelioma, myeloma, sarcoma
Tepotinib	Selective TKI	ATP competitive	c-Met	HCC, NSCLC
Foretinib	Nonselective TKI	ATP competitive	c-Met, KDR, TIE-2, RON, FLT-4, FLT-3	Gastric, SCCHN, pRCC, NSCLC, breast
Crizotinib	Nonselective TKI	ATP competitive	c-Met, ALK	NSCLC, Lymphoma, melanoma, gastric, urothelial cancer

Nonselective c-Met inhibitors may have heightened antitumor activity due to the inhibition of other targets (Bouattour et al., 2018). The small c-Met inhibiting molecule tivantinib is an Adenosine triphosphate (ATP) competitive inhibitor that is highly selective for binding its receptor c-Met (Lath et al., 2018). Tivantinib has been shown to inhibit the assembly of microtubules along with c-Met and has been shown to be cytotoxic with numerous cell lines (Bouattour et al., 2018). The chemotherapeutic drug is metabolised through cytochrome P450 2C19 and cytochrome P450 3A4 pathways (Pievsky & Pysopoulos, 2016). The elimination of the drug from the body is performed through the kidneys and the digestive tract (Pievsky & Pysopoulos, 2016). Tivantinib is metabolised by the protein cytochrome P450 family 2 subfamily C member 19 (CYP2C19) (Geller et al., 2017). De Mello et al., (2020) reports clinical trials performed by Scagliotti et al., (2015) and Scagliotti et al., (2017) using tivantinib which the study found there to be conflicting results for the adverse side effects

that may be caused by tivantinib. Remsing Rix et al., (2015) found glycogen synthase kinase-3 alpha ($GSK3\alpha$) to be a possible target of tivantinib. In this study the cell viability of KRAS mutant and wild type lung cancer cell lines when treated with 0.5 μ M and 2.5 μ M of tivantinib, crizotinib and cabozinib was tested (Remsing Rix et al., 2013). The study found tivantinib to be the most cytotoxic drug despite both crizotinib and cabozinib being more effective c-Met inhibitors (Remsing Rix et al., 2013). It was found that crizotinib and cabozinib has no significant cytotoxicity to the cells thus suggesting that the overall cytotoxicity of tivantinib on the lung cell lines was unrelated to the inhibition of c-Met (Remsing Rix et al., 2013). Therefore, suggesting that tivantinib may have another gene target (Remsing Rix et al., 2013). Further analysis of tivantinib and its interaction with a panel of kinases responsible for non-small cell lung cancer (NSCLC) were performed by applying a mass spectrometry-based strategy to categorise the profile of tivantinib's targets (Remsing Rix et al., 2013). It was deduced through use of in vitro kinase assays that glycogen synthase kinase-3 alpha and glycogen synthase kinase-3 beta ($GSK3\alpha$ and $GSK3\beta$) were inhibited by tivantinib which was supported by the increase in β -catenin which were found as this is consistent with the inhibition of glycogen synthase kinase 3 ($GSK3$) (Remsing Rix et al., 2013). Kuenzi et al., (2019) suggests that tivantinib is a potent $GSK3$ inhibitor. The study found treatment with tivantinib in HL60 cells decreased the phosphorylation of $GSK3\alpha$ and β at the autophosphorylation site Tyr279/216 which is directly correlated with the kinase activity of $GSK3$. Further suggesting that $GSK3\alpha$ and β are targets for the cytotoxic drug tivantinib (Kuenzi et al., 2019).

Tepotinib, otherwise known as MSC2156119J, is a highly selective c-Met inhibitor that is taken orally (Johne et al., 2020; Pudelko et al., 2020) This c-Met inhibitor has been approved in for treatment of patients in Japan (Pudelko et al., 2020). These patients are required to have advanced or recurrent non-small cell lung cancer with a skipping mutation located on c-Met exon 14 (Pudelko et al., 2020; Paik et al., 2020). Tepotinib and the products metabolised by the c-Met inhibitor are mostly excreted through faeces (Johne et al., 2020). Adverse side effects commonly experienced by individuals being treated with tepotinib include: nausea, diarrhoea, peripheral edema and blood creatinine increase (Takamori et al., 2021). U.S. food and drug administration (FDA) accelerated approval has been granted in

Feb 2021 for the treatment of individuals with metastatic NSCLC (U.S. Food and Drug Administration, 2021).

Foretinib is an inhibitor to multiple kinases, including RTKs (Chen, Tsai & Hung, 2015). Foretinib has been found to be an inhibitor of the HGF-Met signalling pathway resulting in the drugs ability to negatively affect key tumour functions (Zillhardt et al., 2011). Foretinib has been shown to reduce tumour growth and prevent tumorigenesis of ovarian cancer model systems (Zillhardt et al., 2011). Foretinib has been in phase II clinical trials for gastric cancer, Squamous cell cancer of the head and neck (SCCHN), Papillary renal cell carcinoma (pRCC), NSCLC and breast cancer as shown in Table 1 (Bouattour et al., 2018).

Crizotinib is an inhibitor that inhibits the kinases c-Met, Anaplastic lymphoma kinase (ALK) and ROS proto-oncogene 1 (ROS1). Most NSCLC are resistant to crizotinib (Ding et al, 2020). Crizotinib is a nonselective tyrosine kinase inhibitor that is ATP competitive (Bouattour et al., 2018). Crizotinib was approved by china FDA in 2013 to treat metastatic anaplastic lymphoma kinase (ALK⁺) NSCLC (Guo et al., 2021). Ding et al., 2020 found crizotinib to have increased sensitivity to NSCLC when administered in tandem with chidamine.

AMG337 is an inhibitor of c-Met signalling and is found to inhibit c-Met dependent cancer model cell lines (Hong et al., 2018). AMG337 is a potent molecule, administered orally, that is highly selective for c-Met (El Darsa, El Sayed & Abdel-Rahman, 2020). AMG337 has been found to be generally well tolerated with manageable toxicities (Hong et al., 2018).

1.7.3.1 GAG Mimics and JD compounds

Glycosaminoglycans (GAGs) are biomolecules typically attached to proteins, forming proteoglycans, and are ubiquitous to mammalian cells (Morla, 2019). The interaction between GAGs, growth factors and growth factor receptors are linked to cancer progression and metastasis (Morla, 2019). GAG/heparin mimetics are synthetic compounds that are analogues of GAGs (Mohamed & Coombe, 2017). New synthesised GAG mimetics have recently been identified for their use in therapeutics (Ferro, 2016). The JD compounds (JD-1, JD-2, JD-3, JD-4 and JD-5), see Table 2 for skeletal chemical structures, used in this study as novel putative c-Met inhibitors were designed to be GAG mimetics (supplied by Dr. James Wilkinson as a gift) to hopefully inhibit the HGF-Met signaling pathway and in turn hopefully act as a treatment in medulloblastoma cell lines.

1.7.4 HGF-Met signalling pathway's role in wound healing

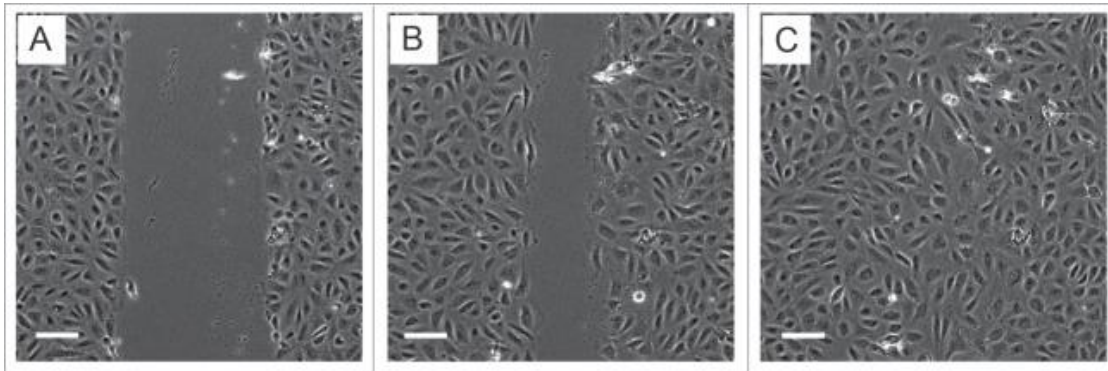


Fig. 7: Images produced from a scratch assay performed taken at different times in the experiments to show the migration of the cells to close the wound created. P20 pipette tip was used to create the initial wound shown in image **A** (Jonkman et al., 2014).

The HGF-Met signalling pathway controls cell growth and migration thus is essential for wound healing (Chmielowiec et al., 2007). As a downstream signalling pathway of HGF-Met signalling is linked to cell migration (Fig. 3), a wound/scratch assay can be utilised in the analysis of the hepatocyte growth factor and mesenchymal epithelial transition receptor signalling pathway (Owusu et al., 2016). Pipette tips are used to create the “wound” in a scratch assay (Jonkman et al., 2014). The creation of the “wound” creates a limitation in using a scratch assay as the depth and size of the wound creates different microenvironments in which the cells have to migrate (Riahi, Yang, Zhang & Wong, 2012).

1.8 Model systems for medulloblastoma

Table 2: A list of the model systems of medulloblastoma cell lines utilised in this study (Adapted from Ivanov, Coyle, Walker & Grabowska, 2016).

Cell line	Subtype	P53
DAOY	SHH	Mutated
UW228	SHH	Mutated
HD-MB03	Group 3	Wild type
ONS-76	SHH	Wild type

All group 3 medulloblastoma cell lines possess amplified MYC (Ivanov, Coyle, Walker & Grabowska, 2016). Daoy, UW228 and ONS-76 are model systems of SHH tumours however only Daoy and UW228 have mutated P53 (also known as tumour protein 53 or TP53) as shown in Table 2. SHH and Group tumours are widely available as model cell line systems whereas group 4 and WNT tumours are largely underrepresented (Ivanov, Coyle, Walker & Grabowska, 2016). UW228 cell lines have been described as less invasive and possess a slower rate of cell division than ONS76 cells (Zanini et al., 2013). UW228, Daoy and ONS76 are considered to represent primary medulloblastoma tumours and are widely used medulloblastoma cell lines (Zanini et al., 2013). HD-MB03 represents group 3 medulloblastoma tumours (Table. 2).

1.9 Current work being performed at The University of Salford on c-Met inhibition and Medulloblastoma.

Dr. James Wilkinson (lecturer) has designed a series of novel potential c-Met inhibitors named JD compounds (structures can be found in Table 3). These compounds have been designed to be GAG mimetics to prevent the binding of HGF to c-Met thus blocking the resulting phosphorylation cascade that activates other signalling pathways. As this pathway is prevalent in many cancers the inhibition of HGF-Met may be a key therapeutic tool to treat various cancers. Sonia Morlando (A PhD student at The University of Salford) has teamed up with Dr. James Wilkinson to test these novel putative c-Met inhibitors on model medulloblastoma cell lines to identify if the JD compounds can be utilised as potential treatments for group 3 medulloblastoma. Sonia Morlando's main objective is to treat group 3 medulloblastoma's with these compounds along with other known Met inhibitor's such as: tivantinib, crizotinib and foretinib. Sonia has a particular focus on group 3 medulloblastoma due to this subgroup having the poorest prognosis of the medulloblastoma subgroups. Sonia is performing cell migration assays, MTT assays, western blots and spheroid formation assays to test these potential treatments on.

Aims and Objectives

The HGF-Met activated signalling pathway is a significant pathway that contributes to the progress and survival of many tumours. Therefore, c-Met may prove to be a key target for the treatment of many cancers including the predominantly childhood brain tumour, medulloblastoma. Using model cell culture systems (ONS76, UW228, Daoy and HD-MB03), Thiazolyl Blue tetrazolium bromide (MTT) assays and the genomics database known as R2 this project aimed to identify if inhibition of c-Met could provide a treatment option for medulloblastoma patients which could allow improved treatment efficacy and/or help reduce late effects suffered by medulloblastoma patients. Both SHH and group 3 medulloblastoma tumours express the tyrosine kinase c-Met and cell lines selected belong to these two sub-groups. The initial aim of this project was to explore the efficacy of five novel putative c-Met inhibitors as potential chemotherapeutics for the treatment of medulloblastoma tumours. The novel potential c-Met inhibitors utilised were supplied by Dr. James Wilkinson and were named JD-1, JD-2, JD-3, JD-4 and JD-5 (skeletal chemical structures provided in table 2). Three known c-Met inhibitors (AMG337, tepotinib and tivantinib) were included in the screening process of the cytotoxicity of these drugs as a point of reference.

This project was originally designed as a package of assays to assess the capacity of these novel putative c-Met inhibitors to target the c-Met in the HGF-Met signalling pathways and, in addition to measuring the impact on cell viability, was intended to also include western blotting and cell migration assays to analyse any changes in activating phosphorylation status of proteins downstream of c-Met. Due to the unforeseen circumstances presented by the coronavirus pandemic this work was not completed. Subsequently, an investigation was performed to further investigate the suitability of the different subgroups of medulloblastoma for treatment by c-Met inhibitors using a genomics database known as R2.

This database was able to help us explore how the levels of expression of *Met* and other downstream genes of interest may affect the response of the medulloblastoma cell line to the treatments administered. Thus, improving the understanding of the effects of *Met*, and its inhibition, in the medulloblastoma subgroups SHH and group 3. The new line of research will help provide awareness on the need to potentially tailor treatment to different medulloblastoma cell lines therefore helping to improve treatment efficacy while hopefully

lessening the impact of late effects on those that suffer from medulloblastoma, as more research is undertaken.

The objectives of the project were:

- To use an MTT assay to determine the impact of a panel of eight novel and putative c-Met inhibitors on the cell viability of three SHH model cell lines UW228, ONS76 and Daoy cells.
- To use an MTT assay to determine the impact of a panel of eight novel and putative c-Met inhibitors on the cell viability of a group 3 model cell line HD-MB03.
- To use the Cavalli dataset within the R2 database to determine the expression levels of *Met* in the sub-groups and sub-types of medulloblastoma.
- To use the Cavalli dataset within the R2 database to determine the survival probability of each medulloblastoma subgroup and establish how it correlates to *Met* expression levels.
- To use the Cavalli dataset within the R2 database to determine the expression levels of *Met* in relation to the patient characteristics of age, gender and tumour histology.
- To use the Cavalli dataset within the R2 database to determine the expression levels in the SHH and G3 medulloblastoma subgroups of key downstream genes in the HGF-Met signalling pathway, namely *GSK3 α* , *GSK3 β* , *STAT3*, Mechanistic target of rapamycin (*MTOR*), Deducator of cytokinesis 1 (*DOCK1*), *RAP1A*, AKT serine/threonine kinase 1 (*AKT1*) and (mitogen-activated protein kinase 1) *MAPK1*.

Methods

2.1 Media Preparation

The medulloblastoma cell lines used for this study were ONS76, UW228 (both a gift from Dr. Gianpiero Di Leva of Keele University), DAOY (purchased from ATCC) and HD-MB03 (a gift from Dr. Till Milde of the German Cancer Research Center).

To prepare complete media, foetal bovine serum (FBS (Fisher Scientific)) was added to Roswell Park Memorial Institute 1640 (RPMI 1640) media (Labtech) in the ratio 1:10. Then 5 mL p/s 5000 U/mL (Labtech) was added to the solution.

2.2 Cell Thawing

Cryovials containing the frozen cells were removed from the -80 °C or liquid nitrogen storage and immediately placed into 37 °C water bath. The cells were quickly thawed in under a minute by swirling the cryovial, containing the cells, slowly and gently in the water bath until there was a minimal amount of ice left in the vial. The thawed cells were then added dropwise into a tube containing a desired amount of complete media. Cells were then centrifuged at 10000 rpm for 5 minutes. The resulting supernatant was removed without disturbing the pellet. The pellet of cells was then gently resuspended in complete growth medium. The resuspended cells were added to a T75 flask containing fresh complete media (RMPI 1640 (Labtech) and FBS (Fisher scientific)) in the ratio 1:10 (resuspended cells: complete media). The T75 flask containing the cells was then incubated at 37.5 °C in a humidified environment.

2.3 Cell culture

Pre-prepared media was warmed to 37 °C in the water bath. Cells were then viewed through a microscope to ensure that they were at least 70% confluent. If the cells were 70%-80% confluent they were ready to be split. Under the cell culture hood the media on the cells was discarded. Five mL of phosphate buffered saline (PBS (Labtech)) was used to wash the cells and discarded. This was repeated twice. 1.5 mL Trypsin (Fisher Scientific),

warmed to body temperature, was added to the washed cells, ensuring that the cell monolayer was covered when the flask was flat. The flask was incubated at 37.5 °C for 3-5 minutes (long enough to detach the cells). Once the cells were detached 8 mL of complete growth media was added to the cells. This was mixed by gently aspirating and dispensing the solution and then transferred to a 15 mL tube to be centrifuged at 1500 rpm for 5 minutes. The supernatant was removed. The pellet of cells was then flicked to break up the cells. 10 mL of media was added to resuspend the cells. Cell solution was added to complete media in a new flask in the ratio 1:10. The newly made flask was then incubated at 37.5 °C until splitting or treatment was required.

If the cells were less than 70% confluent, they were not ready to be split and therefore were 'fed' more complete media instead. The old media was discarded from the cells. The cells were washed with 5 mL of PBS (Labtech) twice which was then discarded. 10 mL of fresh complete media was added to the cells and the cells were returned to the incubator to incubate at 37 °C until splitting or treatment was required.

2.4 Cell counting using a haemocytometer

Adherent cells that were counted were detached from flask using 1.5 mL trypsin (Fisher scientific) after being washed with 5 mL PBS (Labtech) twice. The cells were then placed in an incubator at 37.5 °C. The cells were then checked after 3-5 minutes to ensure trypsinization had occurred and the cells were in suspension. 5 mL of complete media was then added to the flask to prevent any further enzyme activity from the trypsin (Fisher Scientific) The solution containing the cells were then centrifuged at 12,000 rpm for 5 minutes. The supernatant was removed then pellet of cells were broken. 10 mL of complete media was then added to resuspend the cells. A 40 µL of a homogenous solution was prepared containing 50% of trypan blue (Sigma-Aldrich) and 50% of cell suspension. 10 µL of the solution, containing the cell suspension and trypan blue (Sigma-Aldrich), was placed on the haemocytometer to be counted. The concentration of the cell suspension was then calculated as number of cells per mL. Once this was calculated the cell concentration was then calculated using the formula $((\text{total cells counted} / \text{number squares counted}) * \text{dilution factor} * 10,000)$. Once the concentration of cells in the suspension this could then be used to

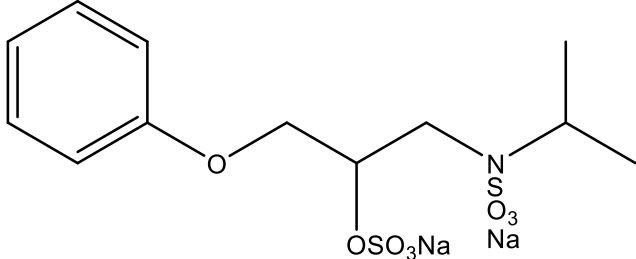
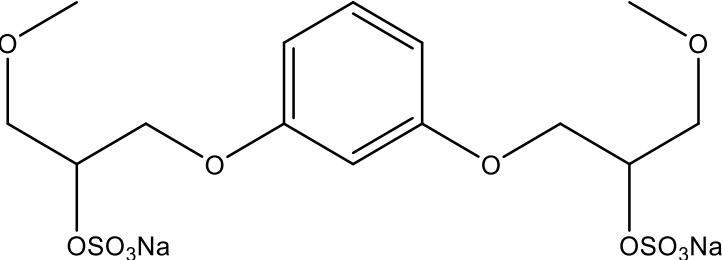
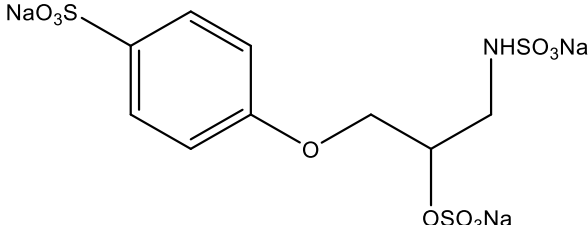
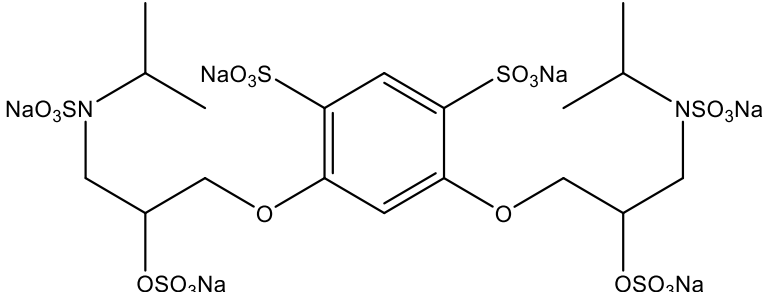
assist in plating a specific number of cells in each well in a multi-well plate. If plating a 96-well plate with 2000 cells/well 192,000 cells in total were needed. A volume of 100 μ L per well was required thus needing 9.6 mL of solution (cells + complete media). A calculation was then done to determine how much volume was required from the cell suspension for the final concentration of cells. The following formula was used (total cells to plate/original concentration of cells= mL of original cell suspension to plate). Therefore 192,000 cells/900,000 cells per mL = 0.213 mL. To conclude a new solution was prepared with 0.213 mL of the original cell suspension and 9.36 mL of new complete media to compose a final volume of 9.6 mL which were plated on the 96-well plate.

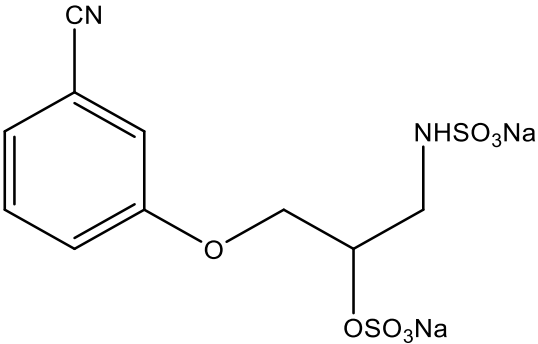
2.5 Plating a 96-well plate

The 96-well plate growing the desired cells was removed from the incubator (37 °C). Complete cell media was removed from the culture and the cells were washed with 5 mL PBS (Labtech) twice. The adherent cells were then detached using 1.5 mL trypsin (Fisher Scientific) which is enough to cover the monolayer of cells on a T75 flask. The plate was then incubated at 37 °C for 3-5 minutes to allow the cells to detach from the plate. Once cells were in suspension media was added in a ratio of 2:1 with trypsin (Fisher Scientific). The suspension was then centrifuged at 12,000 RPM, after the cells were transferred to a tube, for 5 minutes. The supernatant was then removed, being careful of the cell pellet. The pellet of cells was broken, and 10 mL of complete media was used to resuspend the cells. 40 μ L of the cell suspension solution and trypan blue (Sigma-Aldrich) was prepared in the ratio 1:1. 10 μ L of this solution was placed on a haemocytometer in order to count the cells. Once the cells were counted and the concentration of cells were calculated as number of cells per millilitre. 2000 cells per well of the 96-well plate were calculated for the cells, unless handling ONS76 cells as these cells proliferate faster and therefore only 1500 cells per well were required for ONS76 cells. The cells were resuspended in the cell solution before they were used to ensure the cells were the multichannel pipette was used to pipette 2000 cells/well in the 96-well plate. The plate was then incubated for later treatments.

2.6 JD Compounds

Table 3: The skeletal structures of the series of organic JD compounds used in the experiments performed on different medulloblastoma cell lines (Adapted from data provided by Sonia Morlando of The University of Salford).

Name	Skeletal Structure	Molecular Weight
JD-1		413.37
JD-2		490.40
JD-3		473.32
JD-4		952.70

JD-5		396.30
-------------	--	---------------

The JD compounds displayed in Table 3 (JD-1, JD-2, JD-3, JD-4 and JD-5) are the organic compounds (provided by Dr James Wilkinson) used as potential chemotherapeutic treatment in the MTT assay performed against various medulloblastoma cell lines. These compounds are used as possible inhibitors of the tyrosine kinase c-Met. Thus, if are proven to be successful at inhibiting c-Met activity they will prevent the HGF-Met signalling cascade that follows the activation of c-Met by its ligand HGF.

2.7 Serial dilution

An initial concentration of 100 μM was tested for the treatment being utilised. The range of treatments used in this study was: tivantinib (Stratech), tepotinib (Stratech), AMG337 (Adooq Bioscience) and the JD compounds (supplied by Dr. James Wilkinson). A stepwise dilution was then performed on the treatment with a dilution factor of 10^{-1} until a concentration of 1×10^{-4} μM was composed. Thus, resulting in seven varying concentrations of the treatment using a logarithmic scale.

2.8 MTT Assay

50 mL of MTT dye stock (Alfa-Aesar) was prepared by dissolving MTT powder (Alfa-Aesar) in PBS (Labtech) in the ratio 3mg:1mL. Once the MMT dye stock (Alfa-Aesar) was dissolved in PBS (Labtech) the solution was filtered using a 0.2 μm syringe filter. The filtered solution was aliquoted into bijoux's and stored in the freezer (at $-20\text{ }^{\circ}\text{C}$) for later use. A 96-well plate was plated with the required cells. Once the plate has been incubated for 24 hours, to allow for cell growth and adherence of the cells to the plate, treatment of the cells took place. The reagents used as treatment were one of the following: tivantinib (Stratech), tepotinib (Stratech), AMG337 (Adooq Bioscience) or JD compounds (supplied by Dr. James Wilkinson). The columns 1, 2, 11 and 12 of the wells were left untreated as a negative control. The columns used as a negative control only contained cells and media with no treatment added. In columns 3-10 treatment was added with a starting concentration of $100\text{ }\mu\text{M}$. This was done by performing a serial dilution from the highest concentration to the lowest concentration. $100\text{ }\mu\text{L}$ of each treatment concentration was added to their respective wells. The plate was then left in incubation for 72 hours. After incubation, $50\text{ }\mu\text{L}$ of MTT solution (comprised of MTT dye stock (Alfa-Aesar) and PBS (Labtech)) was added to each well using a multichannel pipette and the plate was incubated for a further 3 hours. All liquid in each well was removed using a multichannel pipette. $200\text{ }\mu\text{L}$ of Dimethyl sulfoxide (DMSO (Fisher Scientific)) was placed in each well again using a multichannel pipette and mixed. Absorbance at 540 nm (MTT absorbance) and 690 nm (background absorbance) in each well was measured using an Omega Fluo-star plate reader. Background absorbance was subtracted from MTT absorbance. Raw data from the plate reader was "normalised" into percentages to make the sets data more comparable to one another. The values from the raw data was processed into percentages by making use of the negative controls on the 96-well plate and producing a 100% cell viability from the average of the values given from the negative control. The subsequent values from the varying concentrations of treatment were then converted into a percentage of the average value of the negative controls. This gave the percentage of cell viability at each concentration of treatment. These values enabled the cell viability of different cell lines and treatments to be compared and analysed.

The number of technical repeats performed per MTT assay experiment is 4 with the exception of eight of the total MTT assay experiments carried out having only 3 technical repeats each. 32 technical repeats of the negative control were performed in each MTT assay that had 4 technical repeats however, in each of the MTT assays that had 3 technical repeats performed there were 24 subsequent technical repeats of the negative control was carried out.

Experimental repeats of the MTT assays performed varied from one experimental repeat to three experimental repeats per experiment. Four of the MTT assay experiments performed had 3 experimental repeats. Seven of the MTT assay experiments performed had 2 experimental repeats. Each of the remaining MTT assay experiments all had 1 experimental repeat.

2.9 R2 database

R2 genomics database (R2 Genomics Analysis and Visualization Platform [<http://r2.MC.NL>], 2021) is a genomics analysis database developed by Jan Koster (From department of oncogenomics in the Academic Medical Centre, Amsterdam). This database allows for the exploration into gene expression data. R2 was used to interrogate gene expression data from medulloblastoma patient biopsies. The Cavalli 2017 medulloblastoma expression dataset was selected due to the large number of patients in the cohort (763) and due to the classification of sub-types as well as sub-groups within the dataset. Kaplan-curve survival probability graphs and box plots displaying relative gene expression levels to show a clear indication of the differences in the different medulloblastoma subgroups/sub types.

Table 4: The gene symbol, name, gene ID and other known names of the genes utilised in the R2 database experiments (Adapted from information given in entrez gene, <https://www.ncbi.nlm.nih.gov/gene/>)

GENE SYMBOL	FULL NAME	ALSO KNOWN AS	GENE ID
<i>MET</i>	MET proto-oncogene, receptor tyrosine kinase	HGFR; AUTS9; RCCP2; c-Met; DFNB97	4233
<i>HGF</i>	hepatocyte growth factor	SF; HGFB; HPTA; F-TCF; DFNB39	3082
<i>GSK3a</i>	glycogen synthase kinase 3 alpha	-	2931
<i>GSK3B</i>	glycogen synthase kinase 3 beta	-	2932
<i>STAT3</i>	signal transducer and activator of transcription 3	APRF; HIES; ADMIO; ADMIO1	6774
<i>MTOR</i>	mechanistic target of rapamycin kinase	SKS; FRAP; FRAP1; FRAP2; RAFT1; RAPT1	2475
<i>DOCK1</i>	dedicator of cytokinesis 1	DOCK180, ced5	1793
<i>RAP1A</i>	RAP1A, member of RAS oncogene family	RAP1, C21KG, G-22K, KREV1, KREV-1, SMGP21	5906
<i>AKT1</i>	AKT serine/threonine kinase 1	RAC, AKT, PKB, PRKBA, PKB-ALPHA, RAC-ALPHA	207
<i>MAPK1</i>	mitogen-activated protein kinase 1	ERK; p38; p40; p41; ERK2; ERT1; NS13; ERK-2; MAPK2; PRKM1; PRKM2; P42MAPK; p41mapk; p42-MAPK	5594

2.10 Statistical analysis

Insufficient experimental repeats of the MTT assay experiments were produced to perform statistical analysis. A complete dataset of the MTT assays were not produced, as such very few of the MTT assays have 3 experimental repeats. Thus, no statistical analysis was performed on the MTT assays due to the lack of experimental repeats. The R2 database was the software used to produce statistical analysis for the experiments performed using the R2 database. A one-way anova test is the default statistical analysis performed by R2 database to compare two groups of data and determine the statistical significance using p-values (R2 Genomics Analysis and Visualization Platform [<http://r2.MC.NL>], 2021). However, when comparing multiple groups within the one-gene-view, a brute force t-test (R2 Genomics Analysis and Visualization Platform [<http://r2.MC.NL>], 2021) was performed to highlight which combinations of 2 groups tested against one another showed statistical significance ($P < 0.05$).

Results

3.1 Screening of potential Met inhibitors, in addition to known Met inhibitors, using MTT assays on different medulloblastoma cell lines.

To investigate the efficacy of five novel putative c-Met inhibitors as potential therapeutics for the treatment of medulloblastoma MTT assays were performed on four medulloblastoma cell lines (ONS76, UW228, Daoy and MB03). As a point of reference three known c-Met inhibitors were also included in the screening process of the cytotoxicity of the drugs. The known inhibitors used as references included: AMG337, tepotinib and tivantinib. The novel inhibitors were named JD-1, JD-2, JD-3, JD-4 and JD-5 (see Table 2 for chemical structures). As potential c-Met inhibitors the cytotoxic effects of the JD compounds were important to determine to help analyse whether the compounds are having effects on the cells lines and if these effects may be linked to c-Met inhibition. If the drugs were found to be cytotoxic it may suggest that more experiments would be required to determine if the compounds are inhibiting the activity of c-Met.

This work was originally designed as part of a package of assays to assess the capacity of these putative c-Met inhibitors to target the c-Met signalling pathways, and was intended to also include migration assays and western blotting to assess any changes in activating phosphorylation status of proteins downstream of c-Met. Due to the coronavirus pandemic this work was not completed and instead an investigation was performed to further investigate the suitability of the different subgroups of medulloblastoma for treatment by c-Met inhibitors using a genomics database known as R2.

3.2 Known c-Met inhibitors reduced the viability of ONS76 cells, whereas the novel JD compounds had less impact on cell viability

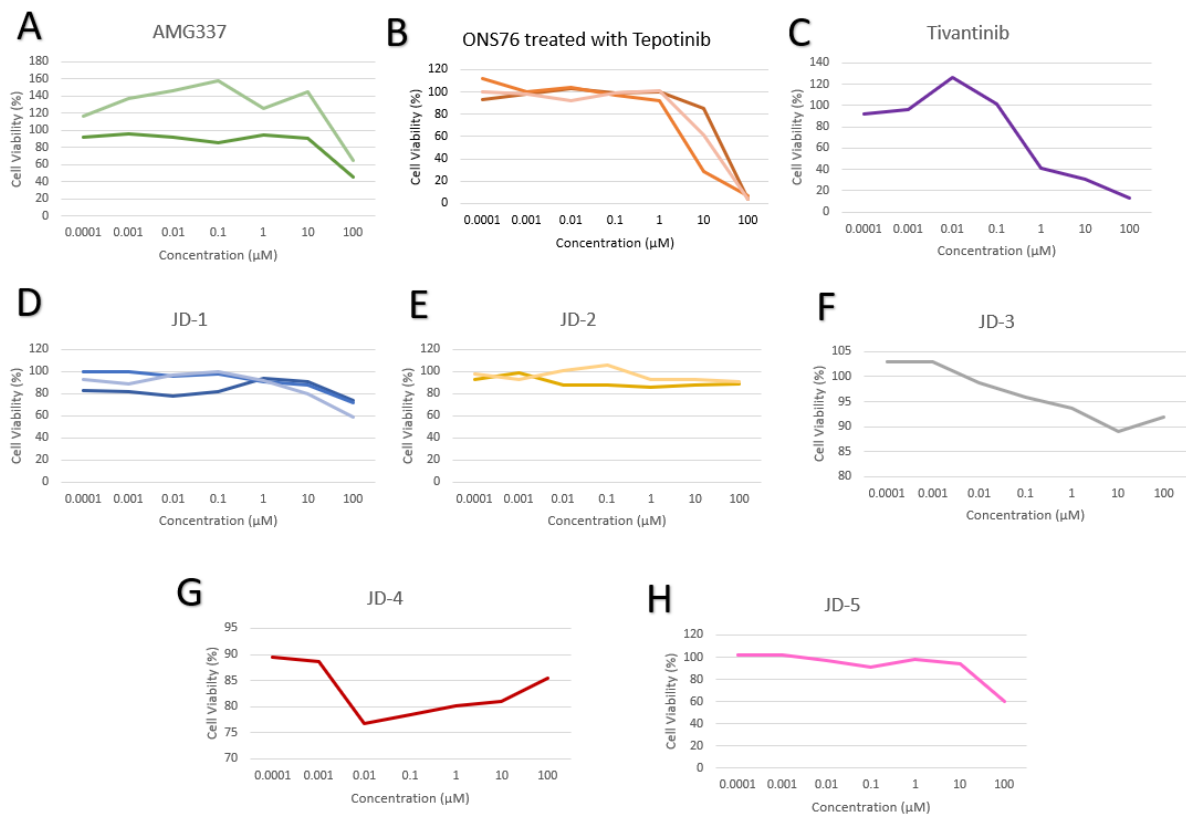


Fig. 8: MTT Assay results to show the cell viability of the cell line ONS76 when treated with different potential chemotherapeutic drugs. **A-C** Treatment with AMG337, tepotinib and tivantinib. **D-H** Treatment with JD-1, JD-2, JD-3, JD-4 and JD-5. Each line on each graph represents repeats of the experiment. Four technical repeats were performed on every experiment with the exception of the AMG337 experiment represented by the light green line (**A**) and the tivantinib experiment (**C**) which had 3 technical repeats performed on each experiment.

In order to explore if potential and/or known c-Met inhibitors had an impact on the cell viability of the ONS76 medulloblastoma cell line, the cells were exposed to the treatments (AMG337, tepotinib, tivantinib, JD-1, JD-2, JD-3, JD-4 and JD-5) and the absorbance was measured which was then used to calculate the cell viability of the treated cells. Figure 8A shows an overall decrease in cell viability when ONS76 is treated with AMG337 reaching the half maximal inhibitory concentration (IC_{50}) at approximately 100 μ M. The highest peak in cell viability was given at a concentration of 0.1 μ M at approximately 160% suggesting that AMG337 did not have a cytotoxic effect on the ONS76 cells at this concentration (Fig. 8A). However, the other repeat of the MTT assay using AMG337 at a concentration of 0.1 μ M gave a cell viability of approximately 85% which suggests that the drug has a slight cytotoxic effect (Fig. 8A). The MTT assay performed on the ONS76 cells treated with tepotinib showed a negative correlation in each repeat after a concentration of 1 μ M (Fig. 8B). This suggests that after 1 μ M the drug tepotinib had a strong cytotoxic effect on the ONS76 cells. Tepotinib was shown to have an IC_{50} at < 10 μ M on one repeat and an IC_{50} > 10 μ M on two of the tepotinib MTT assay repeats (Fig. 8B). Fig. 8C has the fastest decrease in cell viability of each drug with IC_{50} achieved at < 1 μ M when the cells are treated with tivantinib. When treating ONS76 with JD-1 there was a slight decreasing trend presented after a concentration of > 1 μ M with the cell viability dropping between 60%-70% at the highest concentration (Fig. 8D). The IC_{50} was not reached when treating with JD-1 in any instance, even at the highest concentration of 100 μ M (Fig. 8D). In Fig. 8E the cell viability, of ONS76 with the treatment of JD-2, plateaus with each repeat at approximately 90% therefore the IC_{50} is not reached. Figure 8F shows a decrease in cell viability to 90% at 10 μ M when treating ONS76 with JD-3 before an increase is presented as the concentration of JD-3 is increased to 100 μ M thus the IC_{50} is not reached. Fig. 8G shows a decrease in cell viability to < 80% at 0.01 μ M when treating ONS76 with JD-4 before the trend shows an increase in cell viability as the concentration is increased above 0.1 μ M. Again, the IC_{50} is not reached when treating ONS76 with JD-4 (Fig. 8G). In Fig. 8H the cell viability shows a decrease to 60% at 100 μ M with the IC_{50} unreached when the ONS76 cells are treated with JD-5.

3.3 Known c-Met inhibitors reduced the viability of UW228 cells, whereas the novel JD compounds had less impact on cell viability

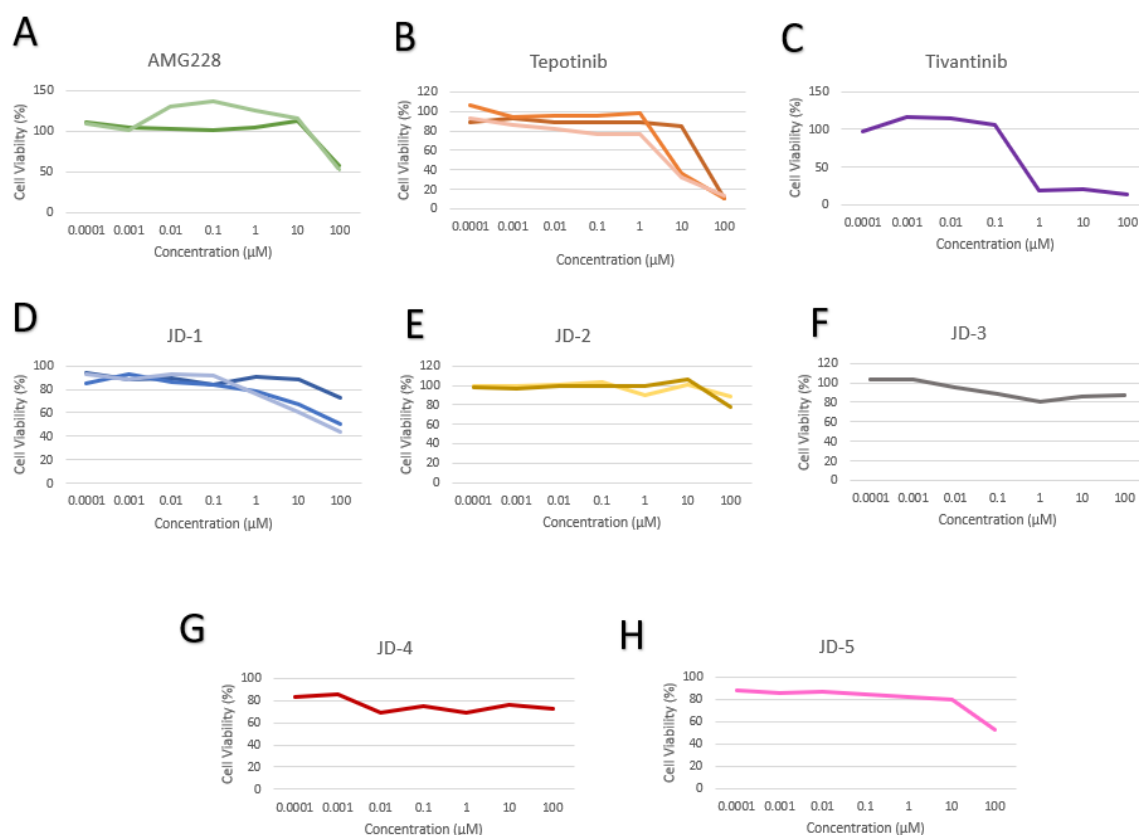


Fig. 9: MTT Assay to show the cell viability of the cell line UW228 when treated with different potential chemotherapeutic drugs. **A-C** Treatment with AMG337, tepotinib and tivantinib. **D-H** Treatment with JD-1, JD-2, JD-3, JD-4 and JD-5. Each line on each graph represents repeats of the experiment. Four technical repeats were performed on every experiment with the exception of the AMG337 experiment represented by the light green line (**A**) and the tivantinib experiment (**C**) which had 3 technical repeats performed on each experiment.

In order to explore if potential and/or known c-Met inhibitors had an impact on the cell viability of the UW228 medulloblastoma cell line, the cells were exposed to the treatments (AMG337, tepotinib, tivantinib, JD-1, JD-2, JD-3, JD-4 and JD-5) and the absorbance was measured which was then used to calculate the cell viability of the treated cells. The data collected from the MTT assay performed on UW228 cells with the treatment of AMG337 (Fig. 9A) suggested that cell proliferation happens between 0.001 μ M and 0.1 μ M on one of the experimental repeats with the cell viability reaching as high as 137%. The other experimental repeat has a cell viability close to 100% between 0.001 μ M and 0.1 μ M (Fig. 9A) which suggests that while the cells are not dying, they are also not thriving. Both repeats show some cytotoxicity after a drug concentration of > 10 μ M (Fig. 9A). The IC₅₀ was almost reached at a concentration of 100 μ M when treating UW228 cells with AMG337. Fig. 9B presents a steeper decrease when treating with tepotinib (1 μ M > IC₅₀ < 100 μ M) on each repeat. The cell viability of UW228 when treated with tivantinib showed an increase at lower concentrations (Fig. 9C). The cell viability decreased after a drug concentration of 0.1 μ M and higher (Fig. 9). At 0.1 μ M the cell viability of UW228 was 105.92% (Fig. 9C). This decreased to 18.88% when the concentration increased to 1 μ M (Fig. 9C) thus the IC₅₀ was reached before 1 μ M. Tivantinib had the highest cytotoxic effects on the cells at the lowest concentration when compared with the other treatments utilised in the MTT assays shown in Fig. 9. JD-1 was shown to have some cytotoxic effect after a concentration of >0.1 μ M (Fig. 9D). The IC₅₀ was reached on only one repeat of the MTT assays performed using JD-1 as the treatment as shown in Fig. 9D. The MTT assay performed using the compound JD-2 as treatment (Fig. 9E) showed no significant change in the cell viability from the drug concentration 0.0001 μ M to 1 μ M after which the cell viability increases and decreases. The lowest cell viability reached by the potential c-Met inhibitor JD-3 was 81.15% at a concentration of 1 μ M (Fig. 9F). As the concentration of JD-3 was increased further the cell viability increased (Fig. 9F). Treatment with JD-4 showed the cell viability did not follow a set pattern as the concentration of the drug was increased (Fig. 9G). JD-5 showed cytotoxicity from the lowest concentration (0.0001 μ M) to the highest concentration (100 μ M) in the MTT assay performed on UW228 cells (Fig. 9H). The IC₅₀ was not reached at any concentration when UW228 was treated with JD-5 (Fig. 9H).

3.4 Known c-Met inhibitors reduced the viability of Daoy cells, whereas the novel JD compounds had less impact on cell viability

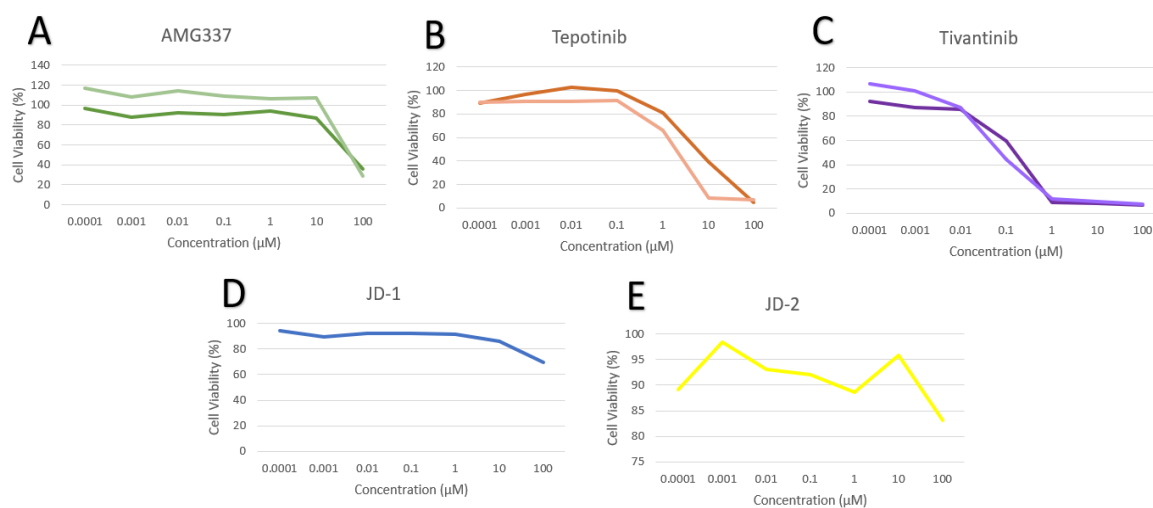


Fig. 10: MTT Assay to show the cell viability of the cell line Daoy when treated with different potential chemotherapeutic drugs. **A-C** Treatment with AMG337, tepotinib and tivantinib. **D-E** Treatment with JD-1 and JD-2. Each line on each graph represents repeats of the experiment. Four technical repeats were performed on every experiment with the exception of the AMG337 experiment represented by the light green line (**A**) and tivantinib experiment represented by the light purple line (**C**) which both had 3 technical repeats performed on each experiment.

In order to explore if potential and/or known c-Met inhibitors had an impact on the cell viability of the Daoy medulloblastoma cell line, the cells were exposed to the treatments (AMG337, tepotinib, tivantinib, JD-1 and JD-2) and the absorbance was measured which was then used to calculate the cell viability of the treated cells. When treating the medulloblastoma cell line Daoy with the c-Met inhibitor AMG337 (Fig. 10A) clear cytotoxicity was shown after the drug concentration reached 10 μM. The IC₅₀ was reached in both repeat experiments carried out as shown in Fig. 10A. At lower concentrations of AMG337 there was no clear cytotoxic effect as the cell viability does not drop significantly

until 10 μM (Fig. 10A). Initially tepotinib presented an increase in the cell viability of the Daoy cells between the drug concentrations 0.0001 μM to 0.01 μM (Fig. 10B) on one of the experimental repeats performed. At drug concentrations higher than 0.01 μM the cell viability starts to decrease as the drug concentration increases (Fig. 10B). In both repeats of the experiment shown in Fig. 10B the IC_{50} was reached by 10 μM . However, at 10 μM one of the repeats had a cell viability of 39.0% whereas the other repeat performed had a cell viability of 8.3% at 10 μM (Fig. 10B). This suggests that in one of the MTT assays performed tepotinib was a more potent cytotoxic drug than it was in the other MTT assay performed. Although at a concentration of 100 μM the cell viability was >7% in both repeats of the MTT assay shown in Fig. 10B. The graph presenting the treatment of Daoy with the c-Met inhibitor tivantinib showed a negative correlation between the cell viability and the concentration of the drug (Fig. 10C). The line graph measuring cell viability starts to plateau after the concentration increases above 1 μM (Fig. 10C). Both repeats have a cell viability of >12% after 1 μM (Fig. 10C) therefore the IC_{50} was reached in both MTT assays performed on Daoy cells treated with tivantinib. The similarities shown in both repeats of the experiment using tivantinib as the potential chemotherapeutic drug (Fig. 10C) suggests that the data may be reliable however a third repeat will have to be performed to confirm this. JD-1 showed some cytotoxicity on the Daoy cells after the concentration was increased above 1 μM (Fig. 10D). The lowest cell viability reached by the MTT assay performed using JD-1 as a treatment was 69.4% (Fig. 10D). In Fig. 9E the peaks and troughs are present throughout with the lowest cell viability presented as 83% at 100 μM thus the IC_{50} was not reached in any instance.

3.5 Known c-Met inhibitors reduced the viability of HD-MB03 cells.

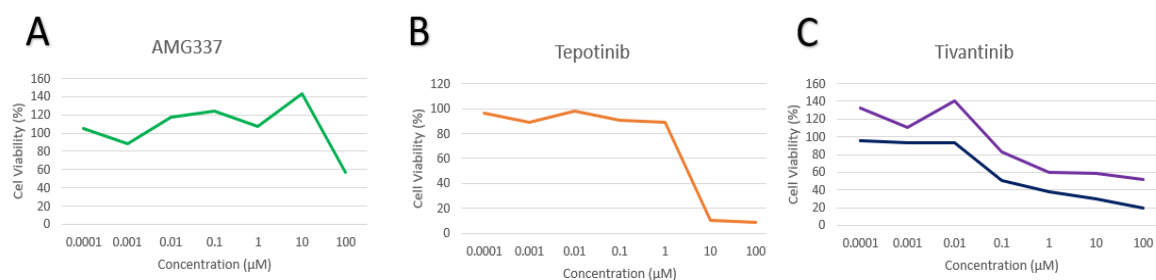


Fig. 11: MTT Assay to showcase the cell viability of the cell line HD-MB03 when treated with different potential chemotherapeutic drugs. **A-C** Treatment with AMG337, tepotinib and tivantinib. Each line on each graph represents repeats of the experiment. Four technical repeats were performed on every experiment with the exception of the AMG337 experiment (**A**) and the tivantinib experiment represented by the light purple line (**C**) which both had 3 technical repeats performed in the experiments.

In order to explore if known c-Met inhibitors had an impact on the cell viability of the HD-MB03 medulloblastoma cell line, the cells were exposed to the treatments (AMG337, tepotinib and tivantinib) and the absorbance was measured which was then used to calculate the cell viability of the treated cells. HD-MB03 treated with AMG337 showed the highest peak of cell viability was 143.8% presented at a drug concentration of 10 μM however the lowest cell viability produced was 57.6% at a drug concentration of 100 μM (Fig. 11A). These results suggest that there is no relationship between the cell viability of HD-MB03 cells and AMG337. After a drug concentration of 1 μM tepotinib was shown to have a negative effect on the cell viability of HD-MB03 (Fig. 11B). The steep decrease in cell viability from 89.2% to 10.3% when the concentration was increased from 1 μM to 10 μM (Fig. 11B) suggests that tepotinib has a cytotoxic effect on the medulloblastoma cell line HD-MB03. The negative correlation presented in Fig. 11 C in both experimental repeats, after the concentration is higher than 0.01 μM , suggests that tivantinib has a cytotoxic effect on the HD-MB03 medulloblastoma cell line. The increase in cell viability from 0.001 μM to 0.01 μM in one of the repeats (Fig. 11C) may be significant or may be an error as the literature shows that tivantinib is cytotoxic against several cell lines. The IC_{50} was reached before 1 μM in one of the repeats performed but was not reached in the other repeat (Fig. 11C).

3.6 Tivantinib treatment had the most potent effect on cell viability in all cell lines (HD-MB03, Daoy, ONS76, UW228).

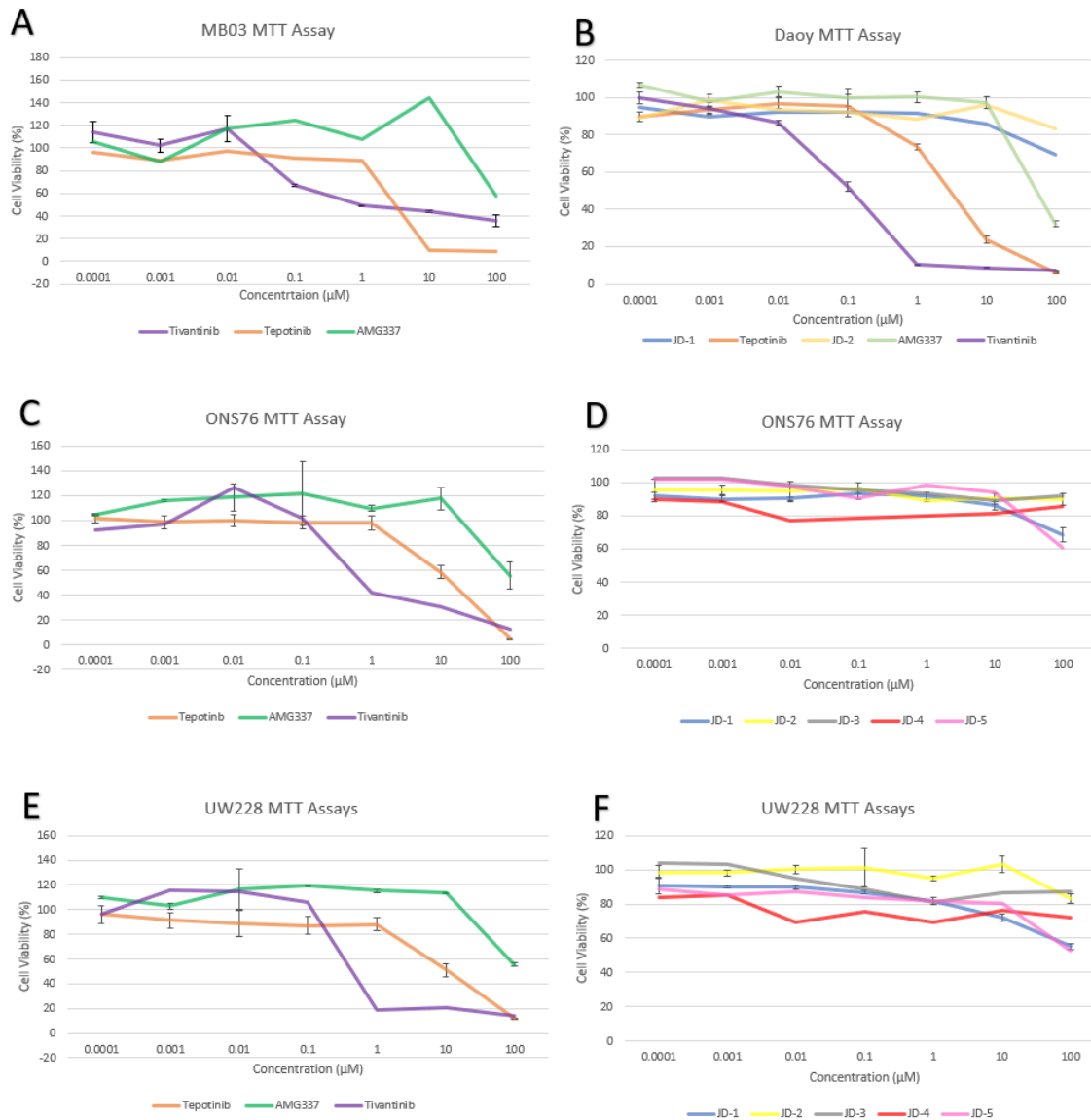


Fig. 12: MTT Assays to show the cell viability of each potential chemotherapeutic treatment in each medulloblastoma cell line. **A** MB03 cell line. Tivantinib (n=2). AMG337 and tepotinib (n=1). **B** Daoy cell line. AMG337, tepotinib and tivantinib (n=2). JD-1 and JD-2 (n=1). **C-D** ONS76 cell line. JD-1 and tepotinib (n=3), JD-2 and AMG337 (n=2), tivantinib, JD-3, JD-4 and JD-5 (n=1). **E-F** UW228 cell line. JD-1 and tepotinib (n=3), JD-2 and AMG337 (n=2), tivantinib, JD-3, JD-4 and JD-5 (n=1).

In order to explore if potential and/or known c-Met inhibitors had an impact on the cell viability of the each medulloblastoma cell line (HD-MB03, Daoy, UW228 and ONS76), the

cells were exposed to the treatments (AMG337, tepotinib, tivantinib, JD-1, JD-2, JD-3, JD-4 and JD-5) and the absorbance was measured which was then used to calculate the cell viability of the treated cells. Each experimental repeat was averaged and then grouped into the cell lines that were treated. This allowed for the analysis of which treatment was the most cytotoxic on each cell line. Fig. 12A shows tivantinib as reaching the IC₅₀ at the lowest concentration of any other drug which is presented at 1 μM. Although treatment with tepotinib on HD-MB03 (Fig. 12A) shows a lower cell viability than tivantinib after a concentration of 5 μM with the final cell viability of tepotinib showing 8% at 100 μM and tivantinib showing 35% at 100 μM. While AMG337 did show some cytotoxic effects on the group 3 medulloblastoma cell line HD-MB03 it did not reach the IC₅₀. These results suggest that tivantinib has more cytotoxic effects at lower concentrations while tepotinib causes lower cell viability of HD-MB03 at concentrations above 10 μM when compared with the other cytotoxic drugs used as treatment of HD-MB03. The error bars shown on the tivantinib MTT assay (Fig. 12A) were relatively small at each concentration suggesting the results are reliable. Fig. 12B presents tivantinib as having the lowest IC₅₀ concentration of 0.1 μM. With tepotinib reaching the IC₅₀ at < 10 μM and AMG337 having an IC₅₀ of < 100 μM. In Fig. 12C and 12D the potential chemotherapeutic drugs JD-1 to JD-5 do not reach their IC₅₀ but mostly have an overall decrease in the cell viability as the concentration of each drug is increased. Tivantinib however shows the best IC₅₀ of < 1 μM with tepotinib having the second lowest IC₅₀ of < 10 μM. AMG337 had a cell viability of 55% at a concentration of 100 μM and therefore did not reach the IC₅₀ of the drug. An error bar produced at a concentration of 0.1 μM on the AMG337 results shown in Fig. 12C is large showing that there were significant variations in the results produced from each repeat for this experiment. Fig. 12E and 12F showcase the drugs JD-1 to JD-5 have a general decreasing trend across the graph but do not reach their IC₅₀. Tivantinib once again presents the best IC₅₀ at < 1 μM with tepotinib as a close second with an IC₅₀ of approximately 10 μM. AMG337 had a cell viability of 55% at the highest concentration and as a result has not reached the IC₅₀. Most of the error bars produced in the graphs showcased in Fig. 12 were relatively small therefore suggesting the results produced in these experiments are relatively reliable.

3.7 The novel c-Met inhibitors displayed lower efficacy than the known c-Met inhibitors.

Table 5: Cytotoxicity of various treatment on four medulloblastoma cell lines (ONS76, UW228, DAOY and MB03) as determined by MTT assays. (✓) indicates cytotoxic drug, (X) indicates no cytotoxic effect, (ND) indicates cytotoxic effects were not determined due to erratic data or insufficient replicates and (-) indicates not tested.

	ONS76	UW228	DAOY	HD-MB03
AMG337	✓	✓	✓	ND
Tepotinib	✓	✓	✓	✓
Tivaninib	✓	✓	✓	✓
JD-1	✓	✓	ND	-
JD-2	X	X	ND	-
JD-3	ND	X	-	-
JD-4	ND	X	-	-
JD-5	✓	✓	-	-

Table 5 highlights which treatments showed some level of cytotoxicity on the tested medulloblastoma cell lines within the MTT assay experiments. Tepotinib and tivantinib have cytotoxic effects in all the medulloblastoma cell lines tested. AMG337 has cytotoxic effects on ONS76, UW228 and DAOY. The drug's effects on HD-MB03 were not determined. The potential c-Met inhibitor JD-1 only showed cytotoxic effects on the UW228 cell line and its effects on DAOY were not determined due to insufficient replications. However, the general trend of Daoy treated with JD-1 did suggest that the drug may have some cytotoxicity towards the cell line (Fig. 12B). The testing of JD-2 indicated no cytotoxic effects on both ONS76 and UW228 with the cytotoxicity on DAOY not determined. JD-3 showed cytotoxic effects on ONS76 while showing no cytotoxic effect on UW228. The results for JD-4 suggest the compound has no cytotoxic effect on ONS76 and UW228. The potential inhibitor JD-5 had cytotoxic effects on both ONS76 and UW228. The JD compounds were not tested on HD-MB03 and therefore the cytotoxicity of these potential therapeutic drugs on the medulloblastoma cell line HD-MB03 is unknown.

3.8 High *Met* expression correlates with increased survival probability in patients with SHH tumours and decreased survival probability in patients with group 3 tumours

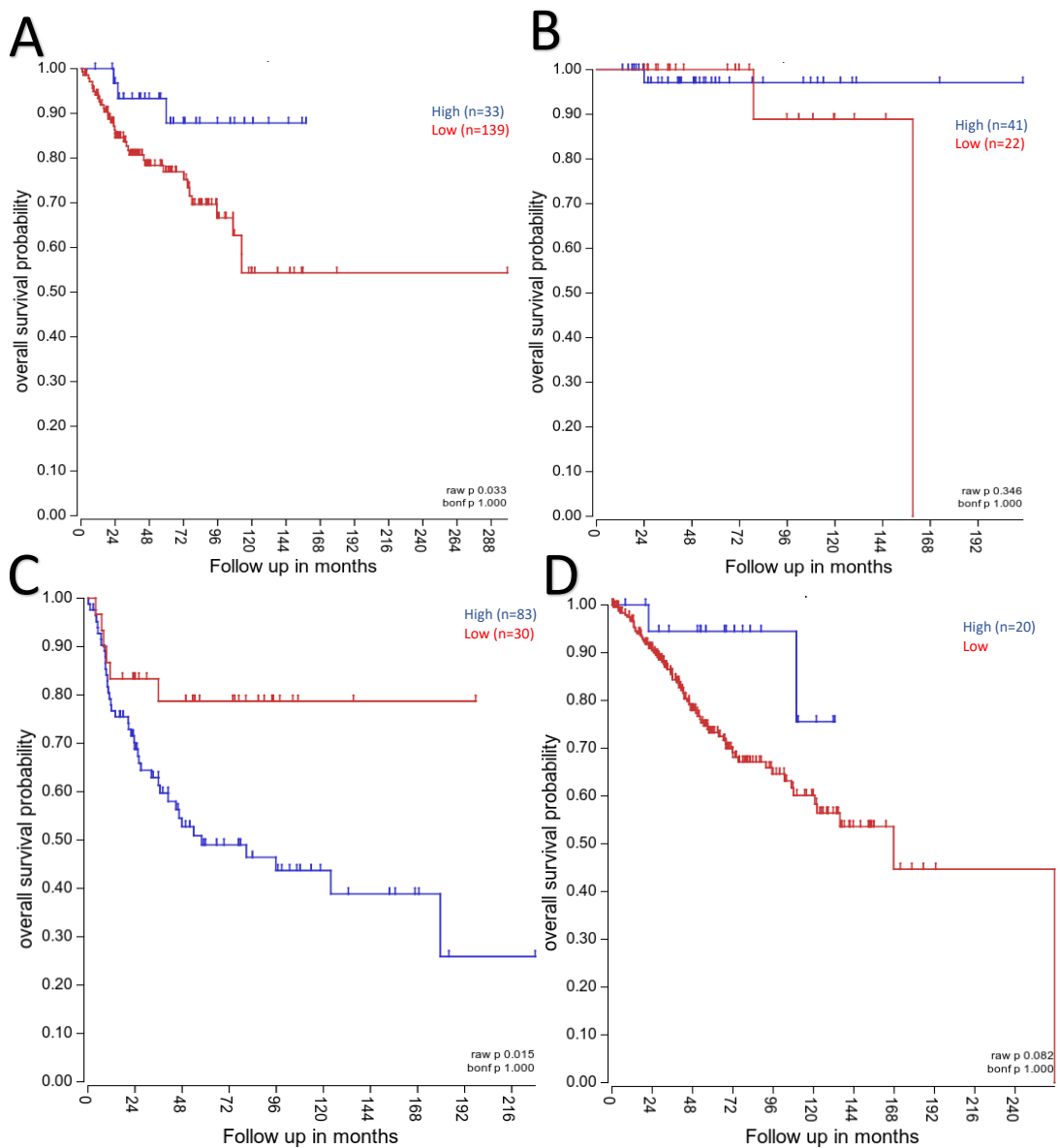


Fig 13. Kaplan curve using Cavalli medulloblastoma dataset showing survival of patients with high and low *Met* gene expression in **A** SHH medulloblastoma **B** WNT medulloblastoma **C** Group 3 and **D** Group 4.

In order to explore if the *Met* expression had an effect on the survival probability of each medulloblastoma subgroup the R2 database was used to measure the survival probability with high *Met* expression and low *Met* expression. This would help determine the suitability of each medulloblastoma subgroup being treated with c-Met inhibitors. The survival probability of SHH medulloblastoma (Fig. 13A) cancer patients is shown to be lower when low *Met* expression is present. With patients having a survival probability of less than 0.60 when *Met* expression is low yet having a survival probability of over 0.85 when *Met* expression is high. The Kaplan curve produced for SHH medulloblastoma has a P value of 0.033 which is statistically significant as $P < 0.05$ (Fig. 13A). This P value suggests that the *Met* expression levels correlates to the survival probability in SHH medulloblastoma. High *Met* expression in SHH medulloblastoma links to a higher survival probability when compared to that of SHH patients with low *Met* expression. The probability of WNT medulloblastoma cancer patient survival (Fig. 13B) suggests that after 72 months low levels of *Met* expression in WNT medulloblastoma has a worse survival prognosis. However, Figure 13B has a P value of 0.346 thus the results of this Kaplan curve are not statistically significant. This P value shows that in the case of WNT medulloblastoma the levels of *Met* expression does not have any correlation with the survival probability of a patient with WNT medulloblastoma. Group 3 medulloblastoma has a worse survival prognosis in tumours with a high *Met* expression (Fig. 13C). With the survival probability dropping to under 0.30 before 192 months as opposed to low *Met* expression tumour patients having a survival probability of over 0.75 at 192 months as shown in Figure 13C. The P value for Figure 13C is 0.015 which is statistically significant. This indicates there is a correlation between the levels of *Met* expression and the survival rate of a group 3 medulloblastoma patient. Group 3 medulloblastomas with high levels of *Met* expression have a lower survival probability. The Kaplan curve showcasing the survival probability of group 4 medulloblastoma (Fig. 13D) suggest low expression of the tyrosine kinase *Met* has the worst survival prognosis after 0 months. $P = 0.082$ in Figure 13D therefore the results in the graph produced is not statistically significant as the P value is not below 0.05. This suggests that in the case of group 4 medulloblastoma there is no correlation between the expression levels of *Met* and the survival probability of a patient.

3.9 Expression of *MET* is found to be highest in SHH medulloblastoma tumours

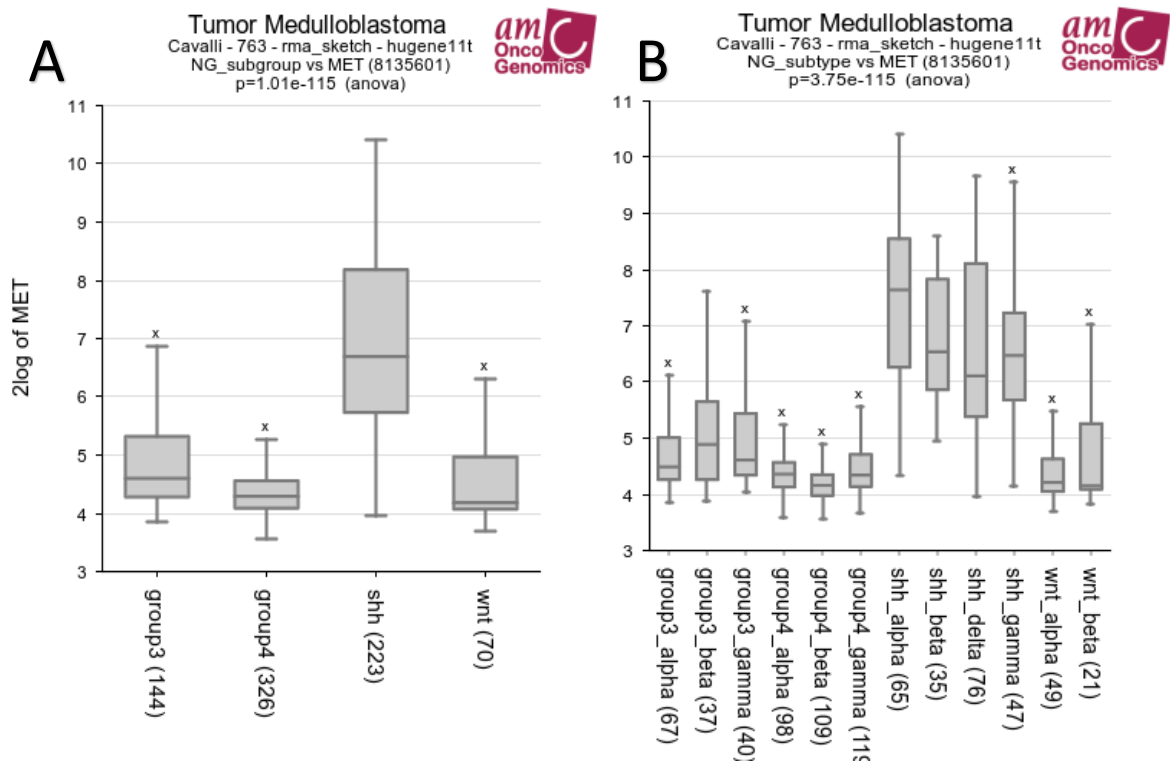


Fig. 14: **A** Expression of *Met* in the four main subgroups of medulloblastoma. **B** Expression of *Met* in each sub type of medulloblastoma (Generated using R2 database and Cavalli, 2018 Medulloblastoma dataset).

Table 6: P values created in correspondence with Fig. 14 (Data adapted from R2 database).

Fig. 14B Table presents intra subgroup p values. Coloured text is used to differentiate between P values that are statistically significant ($P < 0.05$, Red) and P values that are not statistically significant ($P > 0.05$, Black).

Fig. 14A	
Tested Combination	P Value
Group 3 Vs Group 4	1.67×10^{-8}
Group 3 Vs. SHH	9.94×10^{-35}
Group 3 Vs. WNT	1.98×10^{-3}
Group 4 Vs. SHH	1.55×10^{-66}
Group 4 Vs. WNT	0.147
SHH Vs. WNT	3.38×10^{39}

Fig. 14B	
Tested Combination	P Value
Group 3 α Vs. Group 3 β	0.312
Group 3 α Vs. Group 3 γ	0.386
Group 3 β Vs. Group 3 γ	0.974
Group 4 α Vs. Group 4 β	1.43×10^{-4}
Group 4 α Vs. Group 4 γ	0.030
Group 4 β Vs. Group 4 γ	7.81×10^{-7}
SHH α Vs. SHH β	0.011
SHH α Vs. SHH δ	1.35×10^{-3}
SHH α Vs. SHH γ	0.010
SHH β Vs. SHH δ	0.560
SHH β Vs. SHH γ	0.853
SHH δ Vs. SHH γ	0.725
WNT α Vs. WNT β	0.263

In order to explore if the *Met* expression was different in each medulloblastoma subgroup the R2 database was used to measure the *Met* expression in both medulloblastoma subgroups and sub-types. This would help determine the suitability of each medulloblastoma subgroup being treated with c-Met inhibitors. Figure 14A shows the highest average expression of *Met* in SHH medulloblastoma tumours while the lowest average expression of *Met* was shown to be in WNT medulloblastoma. Figure 14B shows all SHH medulloblastoma sub-types to have the highest average expression of *Met*. The sub-types group 4 beta and WNT alpha are shown to express the lowest levels of *Met*. The lowest average expressions of *Met* were shown to be in the WNT sub-group with WNT beta

showing the lowest average *Met* expression overall. The statistically significant P-values in Table 6 $P < 0.05$ (shown in Red) indicates that the expression of *Met* in the tested combinations is significantly different. The P values shows that SHH medulloblastoma has the highest level of expression while group 4 and WNT have the lowest level of expression as the P-value was not found to be statistically significant between the levels of *Met* expression in WNT and group 4 medulloblastoma. This experiment along with the P values suggest that group 3 and SHH medulloblastoma may be particularly susceptible to c-Met inhibitors when compared with WNT and group 4.

3.10 The average expression of *MET* was found to be highest in SHH medulloblastoma in both males and females.

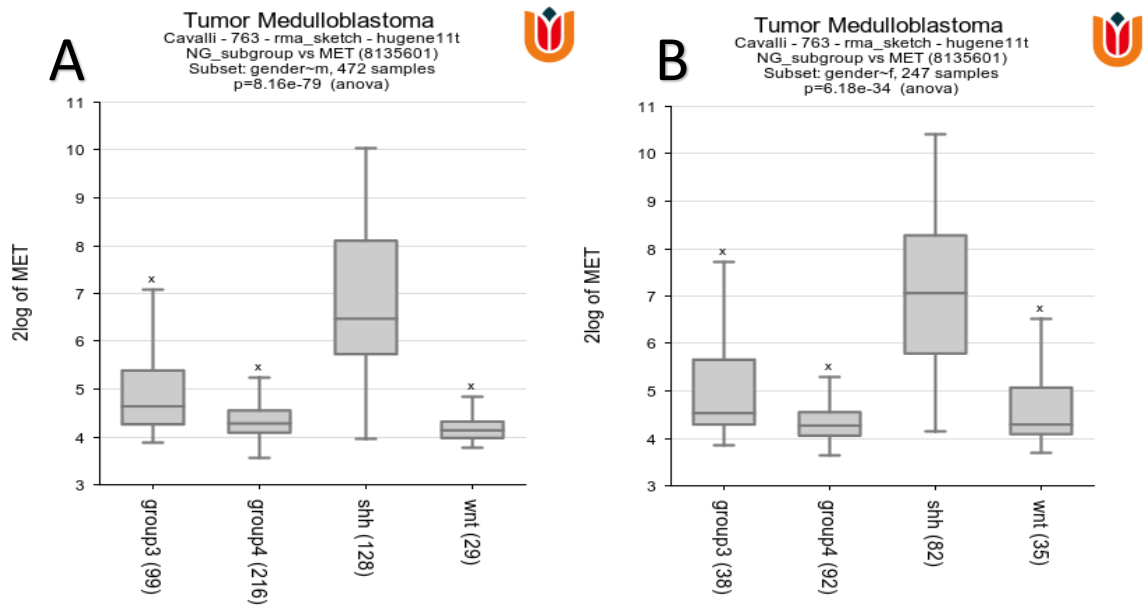


Fig. 15: A Expression of *Met* in males in each subgroup of medulloblastoma. **B** Expression of *Met* in females in each subgroup of medulloblastoma (Generated using R2 database)

Table 7: P values created in correspondence with Fig. 15 (Data adapted from R2 database). Coloured text is used to differentiate between P values that are statistically significant ($P < 0.05$, Red) and P values that are not statistically significant ($P > 0.05$, Black).

Fig. 15A		Fig. 15B	
Tested Combination	P Value	Tested Combination	P Value
Group 3 Vs Group 4	4.49×10^{-7}	Group 3 Vs Group 4	8.37×10^{-9}
Group 3 Vs. SHH	5.69×10^{-24}	Group 3 Vs. SHH	2.94×10^{-32}
Group 3 Vs. WNT	1.26×10^{-6}	Group 3 Vs. WNT	3.83×10^{-4}
Group 4 Vs. SHH	6.56×10^{-40}	Group 4 Vs. SHH	4.87×10^{-63}
Group 4 Vs. WNT	0.248	Group 4 Vs. WNT	0.259
SHH Vs. WNT	1.07×10^{-37}	SHH Vs. WNT	1.13×10^{-39}

In order to explore if the gender had any influence on the expression of *Met* the R2 database was used to measure the *Met* expression in each medulloblastoma subgroups for males and females. This would help determine whether gender characteristics may influence the treatment of medulloblastoma with c-Met inhibitors. The expression of *Met* is highest in the SHH medulloblastoma subgroup in both males and females as shown in Fig. 15. The expression of *Met* in group 4 and WNT medulloblastoma is also shown to be the lowest among females (Fig. 15A and 15B). Males also express the lowest *Met* expression in both the group 4 and WNT medulloblastoma subgroups (Fig. 15A and 15B). The P value for all tested combinations with the exception of group 4 vs WNT showed values of < 0.05 thus statistical significance is shown in each tested combination apart from group 4 vs. WNT. Group 3 medulloblastoma has a lower level of *Met* expression than SHH in both males and females (Fig. 15A and 15B). P value shown for group 3 vs. SHH is less than 0.05 indicating statistical significance in each graph when comparing the two medulloblastoma subgroups SHH and group 3 (Fig 15A and 15B). The P Values shown in Table 7 – Fig. 15A and B both show no statistical significance between group 4 and WNT whilst for every other tested combination the P-value is < 0.05 thus statistically significant. This, combined with the similar trend shown in both Figure 15A and 15B suggests that the gender of a medulloblastoma patient does not seem to be a characteristic that affects the *Met* expression of the patient.

3.11 The age group 4-17 year olds express the highest average level of *MET* expression when compared with other age groups.

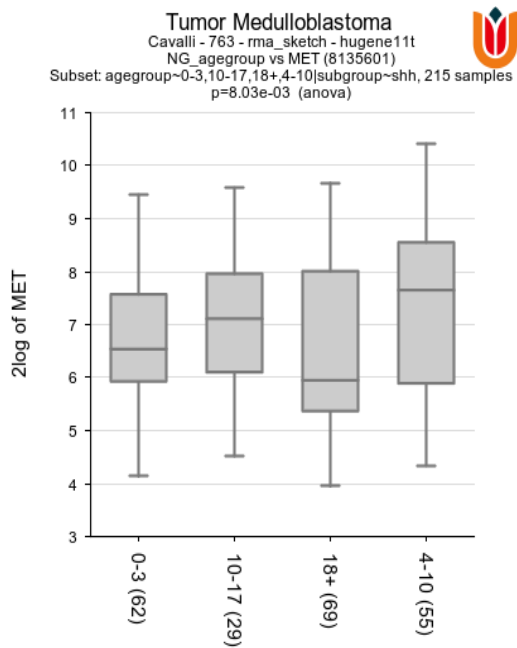


Fig. 16: Expression of *Met* in differing age groups of medulloblastoma patients (Generated using R2 database).

Table 8: P values created in correspondence with Fig. 16 (Data adapted from R2 database).

Coloured text is used to differentiate between P values that are statistically significant ($P < 0.05$, Red) and P values that are not statistically significant ($P > 0.05$, Black).

Fig. 16A	
Tested Combination	P Value
0-3 Vs 4-10	3.01×10^{-7}
0-3 Vs. 10-17	2.89×10^{-7}
0-3 Vs. 18+	0.723
4-10 Vs. 10-17	0.656
4-10 Vs. 18+	2.35×10^{-6}
10-17 Vs. 18+	2.09×10^{-6}

In order to explore if age had any influence on the expression of *Met* the R2 database was used to measure the *Met* expression in each medulloblastoma subgroups for different age groups. This would help determine whether age may influence the medulloblastoma cells susceptibility to treatment with c-Met inhibitors. In Fig. 16 the 4 to 10 year old and the 10 - 17 year old age group shows the largest expression of *Met*. Whilst 0 to 3 years and 18+ show the lowest expression of *Met* in medulloblastoma tumours. The P value of < 0.05 in the tested combinations of: 0-3 vs 10-17, 0-3 vs 4-10, 10-17 vs 18+ and 18+ vs 4-10 shows a statistical significance in these results. While there is no statistical significance shown in the tested combinations: 4-10 vs.10-17 and 0-3 vs. 18+. These P values suggest that the age of a patient is a contributing factor to the levels of *Met* expression found in the tumour. Those within the age range of 4-17 observe a higher level of *Met* expression than those outside this age range.

3.12 Expression of Met is higher in desmoplastic medulloblastoma tumours than in classic and LCA tumours

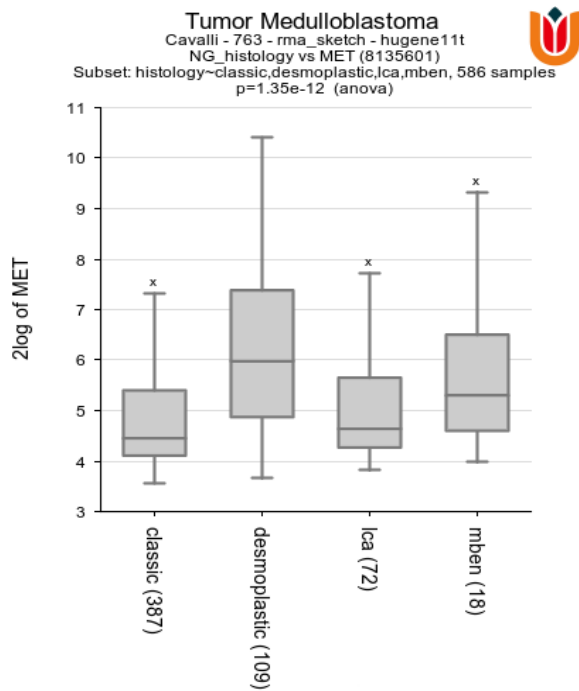


Fig. 17: *Met* expression in medulloblastoma tumours of different histology (Generated using R2 database).

Table 9: P values in correspondence with Fig. 17 (Data adapted from R2 database). Coloured text is used to differentiate between P values that are statistically significant ($P < 0.05$, Red) and P values that are not statistically significant ($P > 0.05$, Black).

Fig. 17A	
Tested Combination	P Value
Classic Vs Desmoplastic	6.08×10^{-11}
Classic Vs. LCA	0.384
Classic Vs. MBEN	0.093
Desmoplastic Vs. LCA	6.16×10^{-6}
Desmoplastic Vs. MBEN	0.089
LCA Vs. MBEN	0.247

In order to explore if histology had any influence on the expression of *Met* the R2 database was used to measure the *Met* expression in classic, desmoplastic, LCA and MBEN. This would help determine whether histology may influence the medulloblastoma cells susceptibility to treatment with c-Met inhibitors. The medulloblastoma tumour presenting desmoplastic histology shows the largest *Met* expression in Fig. 17. While LCA and classic medulloblastoma tumours show the lowest expression of the *Met* gene. Although there is not statistical significance between desmoplastic and MBEN tumours. The P values of the tested combinations: classic vs desmoplastic and desmoplastic vs LCA was less than 0.05 thus this result shows statistical significance. Whilst no statistical significance was found in any other tested combinations. These P values show that the level of *Met* expression found in desmoplastic medulloblastoma is higher than the levels of *Met* expression found in classic or LCA medulloblastoma. This suggests desmoplastic medulloblastoma, and possibly MBEN medulloblastoma, may be more susceptible to c-Met inhibitors than classic and LCA.

3.13 Expression of *GSK3α* and *GSK3β* in medulloblastoma subtypes

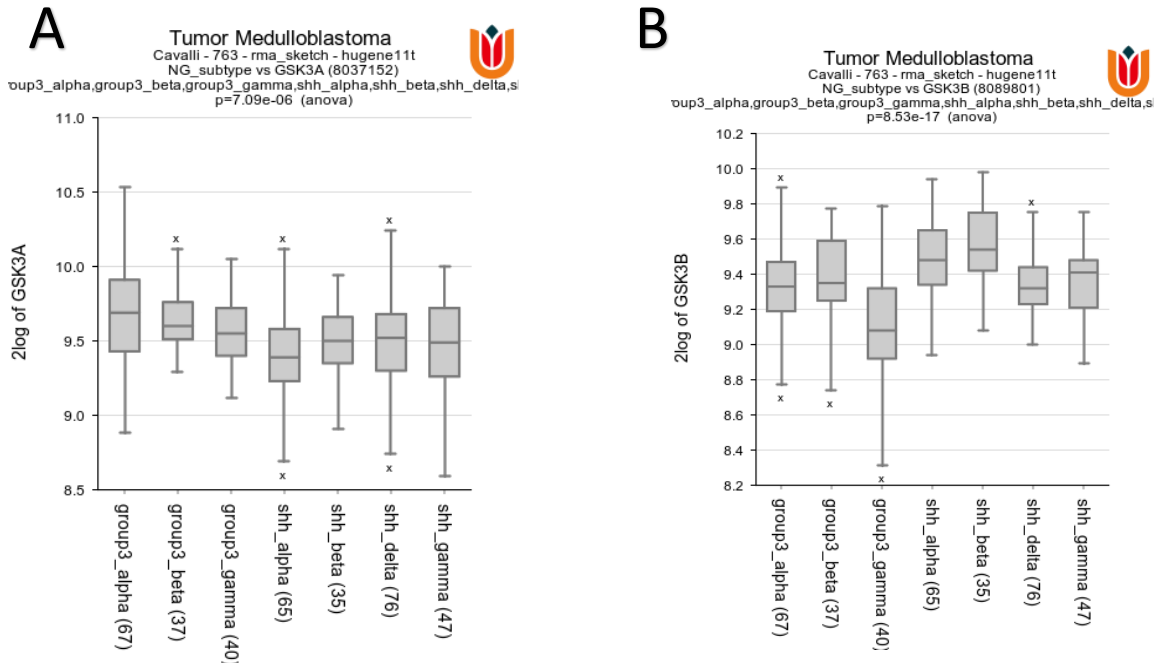


Fig. 18: The expression of *GSK3 alpha* (A) and *GSK3 beta* (B) in the different medulloblastoma sub types of the subgroups SHH and Group 3 medulloblastoma tumours (Generated using R2 database).

Table 10: P Value in correspondence with Fig. 18 (Data adapted from R2 database).

Coloured text is used to differentiate between P values that are statistically significant (P<0.05, Red) and P values that are not statistically significant (P>0.05, Black).

Fig. 18A	
Tested Combination	P Value
Group 3α Vs Group 3β	0.797
Group 3α Vs. Group 3γ	0.274
Group 3α Vs. SHHα	2.47 x 10⁻⁵
Group 3α Vs. SHHβ	0.016
Group 3α Vs. SHHγ	8.37 x 10⁻³
Group 3α Vs. SHHδ	7.17 x 10⁻³
Group 3β Vs. Group 3γ	0.136
Group 3β Vs. SHHα	1.60 x 10⁻⁶
Group 3β Vs. SHHβ	4.45 x 10⁻³
Group 3β Vs. SHHγ	1.84 x 10⁻³
Group 3β Vs. SHHδ	1.29 x 10⁻³
Group 3γ Vs. SHHα	4.89 x 10⁻⁴
Group 3γ Vs. SHHβ	0.123
Group 3γ Vs. SHHγ	0.079
Group 3γ Vs. SHHδ	0.076
SHHα Vs. SHHβ	0.082
SHHα Vs. SHHγ	0.096
SHHα Vs. SHHδ	0.069
SHHβ Vs. SHHγ	0.887
SHHβ Vs. SHHδ	0.935
SHHγ Vs. SHHδ	0.945

Fig. 18B	
Tested Combination	P Value
Group 3α Vs Group 3β	0.231
Group 3α Vs. Group 3γ	4.38 x 10⁻⁴
Group 3α Vs. SHHα	2.44 x 10⁻⁵
Group 3α Vs. SHHβ	9.55 x 10⁻⁷
Group 3α Vs. SHHγ	0.175
Group 3α Vs. SHHδ	0.140
Group 3β Vs. Group 3γ	4.60 x 10⁻⁵
Group 3β Vs. SHHα	0.020
Group 3β Vs. SHHβ	7.62 x 10⁻⁴
Group 3β Vs. SHHγ	0.909
Group 3β Vs. SHHδ	0.963
Group 3γ Vs. SHHα	1.63 x 10⁻⁹
Group 3γ Vs. SHHβ	6.74 x 10⁻¹¹
Group 3γ Vs. SHHγ	9.00 x 10⁻⁶
Group 3γ Vs. SHHδ	5.77 x 10⁻⁶
SHHα Vs. SHHβ	0.087
SHHα Vs. SHHγ	1.63 x 10⁻³
SHHα Vs. SHHδ	1.49 x 10⁻³
SHHβ Vs. SHHγ	4.44 x 10⁻⁵
SHHβ Vs. SHHδ	4.14 x 10⁻⁵
SHHγ Vs. SHHδ	0.927

In order to explore if the expression of GSK3 alpha and beta may have had any influence on the medulloblastoma cells susceptibility to treatment with c-Met inhibitors (tivantinib in particular) the R2 database was used to measure GSK3 alpha and beta expression in each medulloblastoma subtype. GSK3 was selected as tivantinib has been shown to be a potent inhibitor of GSK3 (Kuenzi et al., 2019). Analysis of the expression of *GSK3* in SHH and Group 3 medulloblastoma may present a deeper understanding into why tivantinib is consistently a more potent drug in each medulloblastoma cell line tested. *GSK3 α* shows the highest level of expression in group 3 α medulloblastoma and SHH gamma medulloblastoma (Fig. 18A) as there is no statistical significance shown in the P-value of this tested combination. *GSK3 β* shows higher levels of expression in SHH α and SHH β medulloblastoma tumours (Fig. 18B). There is no statistical significance found between the tested combination SHH α vs. SHH β as $P > 0.05$. The higher prevalence of *GSK3 α* expression in medulloblastoma group 3 α and SHH γ and the *GSK3 β* expression in SHH α and SHH β may influence these medulloblastomas susceptibility to the drug tivantinib in particular as tivantinib is not a c-Met specific inhibitor.

3.14 Expression of genes of interest in Group 3 and SHH medulloblastoma.

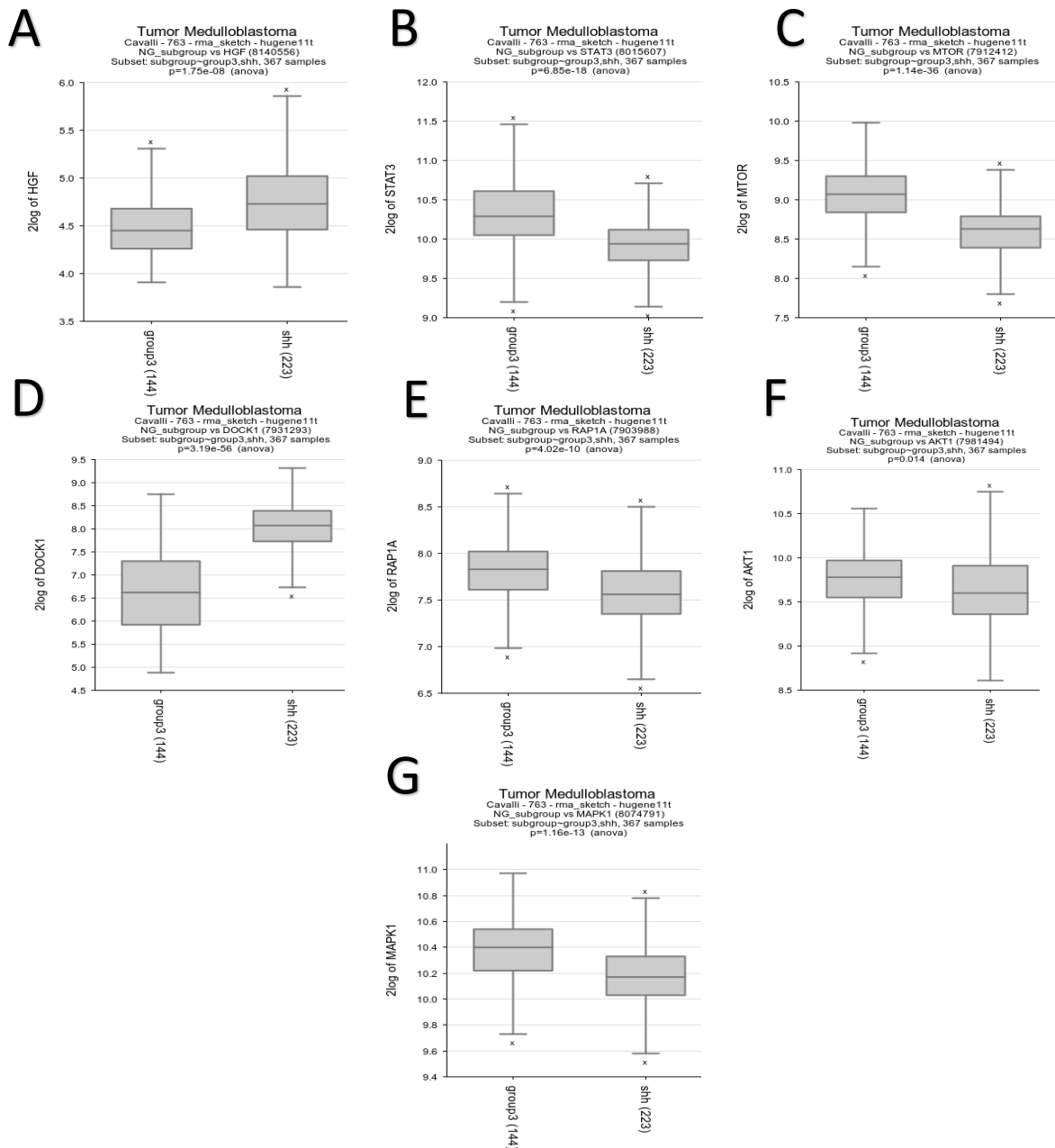


Fig. 19: Boxplot showing the expression levels of key genes that are important in the HGF-*Met* signalling pathway (Genes of interest: *HGF*, *STAT3*, *MTOR*, *DOCK1*, *RAP1A*, *AKT1* and *MAPK1*).

Table 11: P values of the R2 database box plot graphs produced in Fig. 19. Coloured text is used to differentiate between P values that are statistically significant (P<0.05, Red) and P values that are not statistically significant (P>0.05, Black).

GENE SYMBOL	TESTED COMBINATION	P value
<i>HGF</i>	Group 3 Vs. SHH	1.14 x 10 ⁻⁹
<i>STAT3</i>	Group 3 Vs. SHH	8.81 x 10 ⁻¹⁷
<i>MTOR</i>	Group 3 Vs. SHH	7.61 x 10 ⁻³⁶
<i>DOCK1</i>	Group 3 Vs. SHH	8.91 x 10 ⁻⁴³
<i>RAP1A</i>	Group 3 Vs. SHH	3.22x10 ⁻¹⁰
<i>AKT1</i>	Group 3 Vs. SHH	1.00 x 10 ⁻²
<i>MAPK1</i>	Group 3 Vs. SHH	4.71 x 10 ⁻¹⁴

In order to explore if different genes downstream of the HGF-Met signalling pathway had any influence on the expression of *Met* the R2 database was used to measure the *HGF*, *STAT3*, *MTOR*, *DOCK1*, *RAP1A*, *AKT1* and *MAPK1* expression in Group 3 and SHH medulloblastoma. This will help determine whether the expression of these genes may influence SHH and group 3 medulloblastoma cell lines susceptibility to treatment with c-Met inhibitors. The genes of interest chosen for analysis are each of the genes are present downstream of the HGF-Met signalling pathway this will enable the exploration of whether the expression of these genes correlate with the expression of *Met* in SHH or Group 3 medulloblastoma. The expression of the hepatocyte growth factor in SHH medulloblastomas is on average higher than the expression presented in group 3 medulloblastoma (Fig. 19A). The P value for this tested combination of levels of *HGF* expression was less than 0.05 (Table) thus the data in Fig. 19A was found to be statistically significant. *STAT3* has a higher average level of expression in group 3 medulloblastoma than in SHH (Fig. 18B). P was found to be less than 0.05 (Table 11) in the graph produced in Fig. 19B meaning the difference in the averages between the tested combination Group 3 and SHH were found to be statistically significant. The gene *MTOR* has a has a higher mean level of expression in group 3 than in SHH (Fig. 18C). P<0.05 in the tested combination Group 3

Vs. SHH (Table **11**) of the expression levels of MTOR in the two medulloblastoma subgroups therefore the data produced is statistically significant. *DOCK1* has a higher level of expression in sonic hedgehog medulloblastoma when compared with Group 3 medulloblastoma (Fig. **18D**). Upon statistical analysis the P value is found to be less than 0.05 for the graph produced in Fig. **18D** as shown in Table **11** therefore this result is statistically significant. The expression levels of *RAP1A* were found to be higher on average in Group 3 medulloblastoma (Fig. **18E**). The statistical analysis of the graph produced for the expression levels of *RAP1A* showed P to have a value less than 0.05 (Table **11**) thus the data is statistically significant meaning Group 3 medulloblastoma does express a higher level of *RAP1A* than SHH medulloblastoma (Fig. **18E**). Upon the initial analysis of the expression of *AKT1* in group 3 and SHH medulloblastoma the highest average level of expression looks to be in group 3 medulloblastoma (Fig. **18F**). However, when the P value was produced for the expression of *AKT1* in group 3 Vs. SHH (Table **11**) P was found to be > 0.05 therefore there is no statistical significance in the difference in averages of gene expression of *AKT1* between the medulloblastoma subgroups Group 3 and SHH. The box plot produced in Fig. **18G** suggests Group 3 medulloblastoma has the highest average level of expression of *MAPK1* when compared with the expression of the gene in SHH medulloblastoma. The P value produced in Table **11** for the graph showcasing the expression of *MAPK1* in group 3 and SHH (Fig. **18G**) was found to be < 0.05 thus the graph produced is statistically significant and SHH has a higher average level of expression of *MAPK1* than Group 3 medulloblastoma. The P-values shown in Table **11** highlight that *STAT3*, *MTOR*, *RAP1A* and *MAPK1* have a higher level of expression in group 3 medulloblastoma while *HGF* and *DOCK1* have a higher level of expression in SHH medulloblastoma. This suggests that group 3 medulloblastoma may be more susceptible to c-Met inhibitors as more genes of interest were found in a higher level of expression in group 3 medulloblastoma than in SHH medulloblastoma.

4. Discussion

4.1 Aims and Objectives of this project

The HGF-Met activated signalling pathway is a significant pathway that contributes to the progress and survival of many tumours. Therefore, *Met* may prove to be a key target for the treatment of many cancers including the predominantly childhood brain tumour, medulloblastoma. Using model cell culture systems (ONS76, UW228, Daoy and HD-MB03), MTT assays and the genomics database known as R2 this project aimed to identify if inhibition of c-Met could provide a treatment option for medulloblastoma patients which could allow improved treatment efficacy and/or help reduce late effects suffered by medulloblastoma patients.

4.2 The medulloblastoma cell lines utilised in this study (ONS76, UW228, DAOY and HD-MB03)

The initial objective of this study was to explore whether the potential c-Met inhibiting drugs were cytotoxic to medulloblastoma cell lines. To achieve this a screening process was designed consisting of MTT assays, cell migration assays and western blotting to determine the impact of treatment on the activation of c-Met targets in various medulloblastoma cell lines. Due to the pandemic, this work was limited and only the MTT assays were performed. The dataset is not complete but does provide an indication as to the potential utility of these compounds.

The subgroup, and subtype, of a medulloblastoma cell line is an important factor in the cell lines used as each subgroup has different genetic characteristics that may affect the efficacy of a drug. DAOY expresses a mutant tumour protein 53 (TP53) gene and is a member of the SHH subgroup (Bonfim-Silva et al., 2019) thus this cell line can be identified as SHH α (Fig. 3). UW228 is another SHH medulloblastoma cell line that expresses a mutant TP53 gene (Tantravedi et al., 2019) therefore this cell line is categorised as the medulloblastoma subtype SHH α (Fig. 3). ONS76 is also categorised as a SHH medulloblastoma however this cell line expresses the wild type TP53 gene (Bonfim-Silva et al., 2019) therefore this cell line

is not SHH α but rather another SHH subtype, no data yet exists to further characterise this cell line as to which sub-type it belongs to (Fig. 2).

HD-MB03 is a group 3 medulloblastoma cell line that presents MYC amplification (Milde et al., 2012; Chaturvedi et al., 2019) suggesting that the subtype of this cell line is group 3 γ (Fig. 2). It is important to keep in mind that the subgroup and subtype of each of the cell lines analysed in this study may influence how they ultimately respond to the potentially chemotherapeutic reagent they are treated with.

4.3 Tivantinib, tepotinib, AMG337 JD-1 and JD-5 had cytotoxic effects on the SHH medulloblastoma cell line ONS76

The data presented for the treatment of the medulloblastoma cell line ONS76 with AMG337 (Fig. 8A) showed the drug has some cytotoxicity towards the cell line. Although AMG337 did not show cytotoxic effects on the cell line until higher concentrations were reached. This suggests that AMG337 is not as potent as tivantinib or tepotinib. However, the significant difference given in both repeats of the MTT assays shown in Fig. 8A, indicates the experiment would need to be repeated before the data can be reliably interpreted. Thus, no firm conclusions can be made about the effects of AMG337 on the medulloblastoma cell line ONS76. Tepotinib had a cytotoxic effect on the ONS76 cell line (Fig. 8B). However, as the IC₅₀ was reached at higher concentrations on average than other drugs, tepotinib may not be a viable option for treatment of patients with a SHH medulloblastoma subgroup (Fig. 8B). The high concentration required of this drug on ONS76 cells may ultimately cause adverse side effects. Shitara et al., 2020 found tepotinib to be a generally well tolerated drug among the 12 patients treated using a maximum dose of 500 mg once daily which was the recommended dose for phases II testing of the drug. Tivantinib was found to be highly cytotoxic to the ONS76 cell line (Fig. 8C) although the MTT assay only has one repeat thus no firm conclusions can be drawn from this data. The initial increase in cell viability of the ONS76 cells at concentrations < 0.01 μ M (Fig. 8C) may suggest that tivantinib at minute concentrations does not have a cytotoxic effect although the literature surrounding the drug tivantinib and its cytotoxicity shows it to be a highly cytotoxic drug. Geller et al., 2017 found the average half-life of tivantinib to be 2.7 hrs across all doses analysed (170 mg/m²,

200 mg/m² and 240 mg/m²) in the 29 patients (of a possible 35 patients) the half-life was able to be evaluated in. However, a considerable amount of inter-patient variability was identified in the pharmacokinetics of the drug (Geller et al., 2017). Kudo et al., 2020 conducted a phase III study placebo controlled double-blind study on HCC patients age \geq 20 years. 120 mg dose of tivantinib was taken twice daily as a starting dose which is in line with the recommended dose proposed by a previous phase 1 study involving HCC patients from Japan (Kudo et al., 2020). Adverse events occurring most frequently in the tivantinib group were found to be 8.3% anaemia, 18.8% leukopenia and 33.8% neutropenia (Kudo et al., 2020). One patient in this study suffered from neutropenia and consequently died of sepsis which was reported as a drug related death in the tivantinib group of the study (Kudo et al., 2020). JD-1 did not present any significant correlations across all three repeats when an MTT assay was performed on ONS76 cells treated with the compound (Fig. 8D). The data produced was too erratic, increasing and decreasing in cell viability across all three repeats at various concentrations of the potential drug (Fig. 8D). Human error may have been the cause of the erratic data produced in Fig. 8D. It can be determined that JD-1 does have some cytotoxic effect on ONS76 cells at higher concentrations of the drug. The potential c-Met inhibitor JD-2 did not show any notable cytotoxicity in the treated ONS76 cells (Fig. 8E). The IC₅₀ was not reached in this experiment, as shown in Fig. 8E, thus JD-2 may not be a viable option for the treatment of SHH medulloblastoma. Another repeat of this experiment would have to be performed to draw any firm conclusions about the JD compound JD-2. ONS76 cells treated with JD-3 does have a slight negative correlation between the cell viability and increasing concentration of the drug (Fig. 8F). However, the IC₅₀ was not reached which suggests that JD-3 does not have a significant cytotoxicity towards ONS76 cells. As only one repeat was performed (Fig. 8F) no firm conclusions can be given for JD-3, more repeats would be required. The data produced by the MTT assay performed on the ONS76 cell line treated with JD-4 was too erratic to determine whether the compound had a cytotoxic effect on the cells (Fig. 8G). More experimental repeats of ONS76 cells treated with JD-4 would need to be performed to determine whether JD-4 actually has a cytotoxic effect however, the initial results would suggest that JD-4 does not have a high cytotoxicity towards the SHH medulloblastoma cell line. The overall negative trend, between cell viability and increasing drug concentration, produced by JD-5 suggests that the potential c-Met inhibitor has a cytotoxic effect on the ONS76 cell line (Fig. 8H). While JD-5 was found to

be cytotoxic the known c-Met inhibitors (tivantinib, tepotinib and AMG337) had more potency when treating the medulloblastoma cell line ONS76. More repeats of the JD-5 MTT assay would have to be produced to give any firm indications of whether JD-5 is a cytotoxic drug.

4.4 Tivantinib was the most cytotoxic drug against the SHH α cell line UW228

The MTT assays performed on the medulloblastoma cell line UW228 (Fig. 9) showed AMG337, tepotinib, tivantinib, JD-1 and JD-5 to have some level of cytotoxicity towards the cells. While JD-2, JD-3 and JD-4 did not show an overall cytotoxic effect on the UW228 cell line (Fig. 9E-G). AMG337 was found to be cytotoxic against the SHH α medulloblastoma cell line ONS76 (Fig. 9A). However, it was the least potent drug of the other known c-Met inhibitors (tivantinib and tepotinib). This suggests that AMG337 may be the most favourable option for the treatment of SHH medulloblastoma cells due to the high concentration of the drug that would be required for the drug to be potent. More repeats of the MTT assay produced in Fig. 9A would need to be performed to make a reliable conclusion about the cytotoxicity AMG337 has on the SHH α medulloblastoma cell line UW228. In a phase I human trial AMG337, taken at a 300 mg daily oral dose, was found to have an overall response rate (ORR) of 9% of 111 patients with solid tumours with varying Met-amplification status (El Darsa, El Sayed and Abdel-Rahman, 2020). AMG337 showed an increased ORR of 29.6% in the patients with amplified c-Met expression (El Darsa, El Sayed and Abdel-Rahman, 2020). The side effects of AMG337 in this study were found to be nausea, vomiting, headache and fatigue (El Darsa, El Sayed and Abdel-Rahman, 2020). Tepotinib demonstrated cytotoxicity against the cell line UW228 (Fig. 9B). Each of the tepotinib MTT assay repeats performed reached the IC₅₀ in Fig. 9B, showcasing the potency of tepotinib on the UW228 cells. Johne et al., 2020 found tepotinib to have a high level of bioavailability (72%) and low sensitivity to factors, such as interactions with other drugs, that may increase inter-patient variability. Tepotinib was found to have a long half-life of 30 hours (Johne et al., 2020). Most aftereffects experienced by patients were mild showing the 500mg dose given to patients in the study was well tolerated on the whole (Johne et al., 2020). Tivantinib proved to be the most potent drug of all the drugs used as treatment on

UW228 (Fig. 9C). However, the data presented in Fig. 9C was too erratic to make any firm conclusions about the drugs overall effects on the cell line. More repeats will have to be performed before reliable conclusions can be made regarding the treatment of UW228 with tivantinib. A phase II clinical trial showed promising results for the non-ATP competitive c-Met inhibitor tivantinib where the drug had a longer average tumour progression time than was given from results of the placebo in patients with advanced hepatocellular carcinoma (Shao et al., 2020). JD-1 was shown have a cytotoxic effect on UW228 (Fig. 8D) however the concentration of the compound that would be required for the treatment of a patient may be too high to consider it a viable option for treatment. JD-2 was shown to have no cytotoxic effect on the medulloblastoma cell line UW228 (Fig. 9E). JD-3 has no cytotoxic effect on the UW228 cell line (Fig. 9F) however more repeats will be required to make this conclusion. The novel potential c-Met inhibitor JD-4 had no significant cytotoxic effect on the UW228 medulloblastoma cell line. As the data produced for the MTT assay using JD-4 as treatment was too erratic (Fig. 9G) no conclusions can be drawn. More repeats will be required to determine if any correlation between the cell viability and the drug concentration of JD-4 will emerge. JD-5 showed cytotoxic effects on the cell line UW228 at higher concentrations of the drug suggesting that the concentration that would be required of JD-5 may be high. This may mean it is not feasible to administer this to patients as a chemotherapeutic drug however more repeats of the MTT assay and further investigation would be required to determine this.

4.5 The known Met inhibitors all had cytotoxic effects on the SHH α cell line Daoy while the effects of the JD compounds were not determined

AMG337 has cytotoxic effects on the DAOY cell line at higher concentrations of the drug (Fig. 10A). However, another repeat would be required to make a firm conclusion based on this study. Phase I and II clinical trials involving AMG337 have revealed the drug has antitumour activity in esophageal cancer with upregulated c-Met (Yang et al., 2020). Literature showcasing the effects of AMG337 on other cancers are promising as these antitumorogenic properties may present themselves in medulloblastoma tumours when further research is undertaken. The results collected suggest tepotinib has cytotoxic effects on the Daoy cell line at higher concentrations of the drug (Fig 10B). More repeats of the MTT assay treating Daoy cells with tepotinib will need to be performed to make a conclusion about the cytotoxic effects of tepotinib on Daoy. Tepotinib is highly selective for the tyrosine kinase c-Met and was found to have an IC₅₀ of 1.7nM in another study (Shao et al., 2020). Tivantinib was shown to be cytotoxic to Daoy in this experiment (Fig. 10C) however three repeats of the experiment are needed before any firm conclusions are drawn. Tivantinib was found to inhibit the PI3K/AKT/mechanistic target of rapamycin (mTOR) signalling pathway (Wu, Li, Zhang & Liu, 2019), which is a downstream pathway of the HGF-Met signalling pathway (as shown in Fig. 5), and prevented the proliferation of glioblastoma cells (Wu, Li, Zhang & Liu, 2019). While JD-1 did show slight cytotoxicity towards Daoy cells, the IC₅₀ was not reached (Fig. 10D) therefore the concentration required for significant cell death may be too high to be viable for patient treatment. It cannot be determined whether JD-1 had true cytotoxicity towards the Daoy cells or if the results were reliable and more repeats of the experiment (Fig. 10D) would be necessary to determine the effect JD-1 has on the cell viability of the medulloblastoma cell line Daoy. The graph derived from the MTT assay performed on Daoy cells using JD-2 as the treatment (Fig. 10E) showed no clear correlation between the cell viability and the concentration of the drug. The data was too erratic (Fig. 10E) to form any conclusion about whether the concentration of JD-2 influenced the cell viability of the Daoy cells. The erratic results may be due to human error in the biological techniques performed in the MTT assays. Thus, three repeats would be required to make a conclusion about the presence of a relationship between JD-2 and the cell viability of the Daoy cells.

4.6 Tivantinib, tepotinib, AMG337 all showed cytotoxicity toward the group 3 medulloblastoma cell line HD-MB03

The data expressed in the MTT assay performed on HD-MB03 cells treated with AMG337 (Fig. 11A) was too erratic to determine if the c-Met inhibitor had any significant effect on the HD-MB03 cells. Repeat experiments of the MTT assay, in which HD-MB03 is treated with AMG337, will need to be performed to determine if there is any correlation between the cell viability of HD-MB03 and its treatment with AMG337. A study found antitumorigenic activity when gastric/gastroesophageal junction/esophageal adenocarcinoma with amplified c-Met expression was treated with AMG337 however when non-small cell lung cancer was treated with AMG337 it was not found to have antitumour activity (Van Cutsem et al., 2018). Tepotinib was shown to have cytotoxicity against HD-MB03 (Fig. 11B). However, three repeats of the experiment will need to be performed before any firm conclusions can be made regarding tepotinib and the drug's effects on the cell viability of HD-MB03. A study involving patients with a Met exon 14 skipping mutation in advanced NSCLC showed treatment with the drug tepotinib was linked was a partial response to the drug in roughly 50% of the patients (Paik et al., 2020). Tivantinib was shown to have the most cytotoxic effects on HD-MB03 (Fig. 11C) when compared with the other known c-Met inhibitors used as treatment on HD-MB03 (Fig. 11). A third repeat will need to be carried out to determine the reliability, repeatability, and the overall cytotoxic effect tivantinib has on HD-MB03. In the trial performed by Scagliotti et al., 2015 there was 142 treatment related deaths 14.8% of which were found to be related to the drug tivantinib (Zhang et al., 2017). This suggests that when choosing tivantinib as a drug for treatment of a patient the high potency of the drug needs to be carefully considered.

4.7 Tivantinib was the most potent against all medulloblastoma cell lines followed by tepotinib, with AMG337 having the least cytotoxic effects

Tepotinib, tivantinib and AMG337 were all found to have some degree of cytotoxic effects on HD-MB03 cells (Fig. 12A). Tivantinib was found to be the most potent at the lowest concentrations of the drug (Fig. 12A). More repeats of the experiment showcased in Fig. 12A are required to make a firm conclusion of the appropriate concentrations of each drug required to reach the IC_{50} . Tivantinib was shown to have the most cytotoxic effects on the medulloblastoma cell line Daoy (Fig. 12B). Tepotinib and AMG337 also caused the Daoy cells to reach the IC_{50} thus these drugs are shown to have strong cytotoxic effects on the cells (Fig. 12B). More repeat experiments need to be performed on the Daoy cells with each of the drugs (AMG337, tepotinib, tivantinib, JD-1 and JD-2) to form a conclusion on which drug produces the lowest cell viability or if the drugs have any effect on the Daoy cell line. AMG337, tepotinib and tivantinib were shown to have cytotoxic effects on the ONS76 medulloblastoma cell line (Fig. 12C). A large error bar shown in Fig. 12C for AMG337 treatment of ONS76. Thus, suggesting the results in one of the experiments may have been produced in error. This may have been due to human error in areas such as: pipetting, mixing, or other techniques used to plate the cells and treat them. In any case, tivantinib was shown to be the most cytotoxic when compared with AMG337 and tepotinib as the IC_{50} was reached at the lowest drug concentration when the cells were treated with tivantinib (Fig. 12C). However, at the highest concentrations of the drugs (100 μ M) tivantinib had the most cytotoxic effects on ONS76 (Fig. 12C), as was also the case in the HD-MB03 cell line (Fig. 12A), suggesting at higher concentrations tepotinib may be a more effective chemotherapeutic drug than tivantinib. However, at these high concentrations tepotinib may not be suitable for use *in vivo* as a chemotherapeutic drug due to its potential side effects at these concentrations. More repeats will need to be performed for both the tivantinib and AMG337 experiments to ensure the results produced are accurate, reliable, and repeatable. A number of studies/ reviews have been performed on the effects of tepotinib in NSCLC. A study reported tepotinib to be effective in patients with metastasised NSCLC and a Met exon 14 skipping mutation having an 35% ORR in 41 of the patients (Guo et al., 2019). JD-1 and JD-5 were shown to have cytotoxic effects on the medulloblastoma cell line ONS76 while JD-2, JD-3 and JD-4 were not (Fig. 12D). More repeats need to be performed of the

MTT assays using the drugs JD-2, JD-3, JD-4 and JD-5 as treatment to make any firm conclusions about these drugs and their effects on the ONS76 cell line. However, the data thus far suggests JD-2, JD-3 and JD-4 do not have cytotoxic effects on ONS76 as they do not make any significant change to the cell viability of the ONS76 cells (Fig. 12D). Tivantinib was shown to have the greatest chemotherapeutic effects on UW228 cells at the lowest concentrations of the drug when compared with AMG337 and tepotinib (Fig. 12E). Although AMG337, tepotinib and tivantinib were all shown to have cytotoxic effects on the cell line UW228 (Fig. 12E). More repeats would have to be performed on the experiments using AMG337 and tivantinib as treatment to make firm conclusions about these treatments on the Daoy cell line. JD-1 and JD-5 were shown to have cytotoxic effects on the cell line UW228 (Fig. 12F). The error bars produced for the MTT assay performed using JD-1 as the treatment were small suggesting this data is reliable and accurate (Fig. 12F). JD-2, JD-3 and JD-4 were not shown to have any significant effect on UW228 cells (Fig. 12F). More MTT assay repeats would need to be performed using the treatments JD-2, JD-3, JD-4 and JD-5 to make conclusions about these treatments and the effect they have on UW228 cells. Overall tivantinib was shown to have the most cytotoxicity against all the medulloblastoma cell lines (HD-MB03, Daoy, ONS76 and UW228). Zhang et al., 2017 found tivantinib was more successful at prolonging progression-free survival (PFS) of cancer patients when compared with other drugs. After effects of tivantinib of grade 3 and above included neutropenia and anaemia but tivantinib seemed to be well tolerated by individuals who participated in the study (Zhang et al., 2017) which is in line with other studies.

4.8 Tepotinib and tivantinib showed some level of cytotoxicity against all of the medulloblastoma cell lines (ONS76, UW228, Daoy and HD-MB03)

AMG337 was found to have cytotoxic effects in three of the tested cell lines (ONS76, UW228 and Daoy.) as shown in Table 5. It was not determined whether AMG337 had any cytotoxic effects on HD-MB03 due to the erratic results produced when the MTT assay was performed (Fig. 11A). This may have arisen due to human error in areas such as plating the cells, counting the cells, and pipetting accurate volumes. Tepotinib and tivantinib were found to be cytotoxic against each of the medulloblastoma cell lines (ONS76, UW228, Daoy and HD-MB03) treated with these compounds (Table 5). JD-1 was found to be cytotoxic against ONS76 and UW228 (Table 5). The effects of JD-1 on the Daoy cell line were not determined (Table 5) due to the lack of repeats of the MTT assay performed using JD-1 as treatment on this cell line. JD-2 was found to have no cytotoxic effects on the medulloblastoma cell lines ONS76 and UW228 however the drug's effects on Daoy were not determined (Table 5). This was due to the erratic results produced from the MTT assay (Fig. 10E). The erratic results may have been produced by a human error that may have occurred during the experiment. JD-3 and JD-4 were found to have no cytotoxic effects on UW228 cells although the drug's effects on the ONS76 cell line were undetermined (Table 5). This is due to the irregular results and lack of repeats performed (Fig. 8F & 8G). The irregular results may be accredited to human error during the experiment. JD-5 was found to be cytotoxic in both medulloblastoma cell lines it was tested against (Table 5). The cytotoxicity of JD-1 and JD-5 may extend itself to more medulloblastoma cell lines and therefore it is imperative to research these potential chemotherapeutic drugs further. Table 5 was a visual comparison of each of the treatments used from looking at graphs rather than a statistical analysis therefore some of these results may prove to be statistically insignificant however there were insufficient repeats performed to perform a T-test on the data to determine whether the results are significant.

4.9 Patients with high *Met* expression in HD-MB03 had a worse survival prognosis whereas patients with high *Met* expression in SHH had a better survival prognosis

The initial R2 database graph produced displayed the survival probability of each subgroup of medulloblastoma in high and low levels of *Met* expression (Fig. 13). This graph was generated to gain an understanding of the effect the tyrosine kinase *Met* had on each of the subgroups of medulloblastoma. The survival of WNT tumours and group 4 with different levels of *Met* expression showed no statistical significance (Fig. 13B and 13D) and therefore the survival prognosis of WNT medulloblastoma tumours and group 4 medulloblastoma tumours is not affected by the level of *Met* expression presented in the tumour. SHH medulloblastoma tumours (Fig. 13A) showed a lower survival probability in those with a low level of *Met* expression. Whereas group 3 medulloblastoma tumours had a lower survival probability in tumours expressing a high level of *Met* (Fig. 13C). The difference in the survival prognosis of the two subgroups of medulloblastoma having an opposite outcome when *Met* is expressed presents an interesting question as to the reasoning behind why high *Met* expression promotes a better survival probability in sonic hedgehog medulloblastomas yet high expression of *Met* in group 3 medulloblastoma presents a worse survival probability. To our knowledge this is the first report of the effects the levels of *Met* expression has on the survival of different medulloblastoma subgroups.

4.10 The levels of *Met* expression in each subgroup of medulloblastoma.

The results generated from R2 database showed the greatest expression of *Met* to be presented in the medulloblastoma subgroup sonic hedgehog (Fig 14A) with group 3 medulloblastoma having the second highest levels of expression of the *Met* gene. Wingless medulloblastoma is the subgroup that expresses the lowest average levels of the tyrosine kinase *Met* (Fig 14B). This suggests that the protein *Met* plays the largest role in both SHH medulloblastoma and group 3 medulloblastoma when compared with the other medulloblastoma subgroups. When exploring further into the subtypes of medulloblastoma using R2 database (Fig. 14B) it was shown that SHH beta and SHH gamma presented the lowest average expression of *Met* when compared with the other SHH medulloblastoma subtypes. The alpha subtype of the sonic hedgehog medulloblastoma subgroup expressed the highest average levels of *Met* (Fig. 14B). Group 3 beta medulloblastoma was shown to express the highest average levels of *Met* (Fig. 14B) when compared with group 3 gamma and group 3 alpha. These findings along with the analysis of the Kaplan curve, presenting overall survival probability with low and high levels of *Met* expression, suggests that *Met* is playing a role in the survival prognosis of both SHH and group 3 medulloblastoma. Although the role that *Met* has in the two subgroups may be different in each group which is supported by the opposite survival prognosis in both cases.

4.11 Gender has no apparent effect on the *Met* expression in the subgroups of medulloblastoma

Gender does not seem to be a factor affecting higher or lower levels of *Met* expression. This is shown using the boxplot created using R2 database presenting the Cavalli., 2017 medulloblastoma expression dataset. The P value given from group 4 vs. WNT is not <0.05 in both the Male and Female boxplot graph (Fig. 15A and 15B) therefore there is not statistical significance between the data produced for both group 4 and WNT medulloblastoma. However, $P < 0.05$ in all tested combinations against both WNT and group 4 (Fig. 15A and 15B). This shows that there is statistical significance shown in both males and females in the R2 database generated graph between both WNT against SHH and group 3 and group 4 against SHH and group 3. Indicating that both the WNT and group 3 subgroups have the lowest expression in both males and females when compared with other medulloblastoma subgroups. The P value displayed for group 3 vs. SHH in both genders shows statistical significance as the P value is less than 0.05 (Fig. 15A and 15B). This confirms that group 3 medulloblastoma expresses lower levels of *Met* than SHH medulloblastoma in both genders (Fig. 15A and 15B). From the data generated both genders follow similar patterns having SHH as the highest *Met* expression tumour subgroup with group 3 and WNT showing the lowest levels of *Met* expression (Fig. 15A and 15B). Thus, gender must not be factor in the overall levels of *Met* expression presented in each subgroup. Medulloblastoma more commonly affects males than females in a ratio of approximately 1:1.7 (Females:Males) in the age group 0-14 years (Bahmad and Poppiti, 2020). In a study involving 1226 patients (463 Female, 763 male), females were found to have a survival advantage over males only in children > 3 years of age (Curran et al., 2009). Overall, there was no significant difference found between the survival probability of a medulloblastoma patient and the gender of the patient (Curran et al., 2009).

4.12 The highest average levels of *Met* expression were presented in 4 to 17 year olds when compared with other age groups

Met expression on average is highest in children age 4 to 17-year-old (Fig. 16). 9.2% of paediatric brain tumours in children aged 0-14 years are medulloblastomas (Millard & De Braganca, 2016). Up to 30% of all medulloblastoma cases are reported in adults, most of which are below the age of 40 years (Millard & De Braganca, 2016). SHH α medulloblastoma occurs in children aged 4-17 years, SHH β and SHH γ medulloblastoma occurs in children aged <4 years and SHH δ medulloblastoma occurs in adults >7 years old (Yi & Wu, 2018).

Approximately 50% of SHH α medulloblastomas contain a TP53 mutation which results in these patients having the worst outcome of the other SHH medulloblastoma subtypes (Yi & Wu, 2018). The SHH α affecting children aged 4-17 years (Yi & Wu, 2018) and the low 5 year survival percentage of 70% in SHH α (Fig. 3) when compared with other SHH subtypes may be linked to the expression of *Met* in this age group (4-17 years). However further research will have to be performed to determine whether these are linked.

4.13 Desmoplastic tumours have the highest level of *Met* expression when compared with classic medulloblastoma tumours and LCA medulloblastoma tumours

Patients with LCA histology have the worst outcomes while patients with desmoplastic histology have the most favourable prognosis when compared other medulloblastoma histology (Bonfim-Silva et al., 2019). Classic medulloblastoma accounts for 72% of medulloblastomas and therefore is the most common medulloblastoma histological classification (Orr, 2020). LCA medulloblastoma patient survival was 67% compared with classic medulloblastoma tumours having an 81% survival percentage (Orr, 2020). The link between the LCA histology and a poor prognosis may relate to other factors such as MYC amplification as this occurs more frequently in LCA medulloblastoma (Orr, 2020). LCA medulloblastoma is also enhanced in group 3 medulloblastoma and SHH medulloblastoma with TP53 mutations both of which are associated with poor outcomes (Orr, 2020). Desmoplastic medulloblastoma tumours present a higher level of *Met* expression than classic and lca medulloblastoma tumours (Fig. 17) however there is no statistical significance in the average levels *Met* expression shown in desmoplastic vs. the average levels of *Met* expression shown in MBEN. Could there be a link between the level of *Met* expression presented in each histologic medulloblastoma subtype and the prognosis given to patients? The data presented in this study regarding a potential correlation between medulloblastoma histology, prognosis and *Met* expression cannot be concluded however this may be an area for further exploration.

4.14 *GSK3α* and *GSK3β* expression levels in SHH and group 3 medulloblastoma subtypes.

GSK3α and *GSK3β* have been identified as targets of the c-Met inhibitor tivantinib (Remsing Rix et al., 2013; Kuenzi et al., 2019). *GSK3α* and *GSK3β* are tumour suppressors that cause the inhibition of WNT signalling (Kuenzi et al., 2019). Despite this *GSK3* has been considered a therapeutic gene of interest in several disorders (Beurel, Grieco & Jope, 2015). *GSK3α* had no significant difference in expression in the group 3 medulloblastoma subtypes when compared to one another (Fig. 18A). However, Group 3α had a higher level of *GSK3α* expression than SHHα, SHHγ and SHHδ (Fig. 18A). Group 3β presented a higher average level of *Met* expression than in each of the SHH medulloblastoma cell lines (Fig. 18A). Group 3γ medulloblastoma showed a higher level of *GSK3α* than SHHα (Fig. 18A) although it had no statistically significant difference with any other SHH medulloblastoma subtype (Table 10). Each of the medulloblastoma SHH inter subtype tested combinations were found to have no statistical significance with one another as shown in table 10.

GSK3β was found to have a statistically significant higher level of expression in group 3α than in group 3γ but a lower level of expression than in SHHα and SHHβ however showed no statistical significance in results when tested with any other combination (Fig. 18B; Table 10). Group 3β showed a higher level of expression than group 3γ but a lower level of expression than SHHβ as these results were found to be statistically significant when a P value was produced (Table 10). The results produced for the *GSK3β* expression in group 3γ was found to be statistically significant from each of the other SHH and Group 3 subtypes (Table 10). Thus meaning group 3 gamma was found to have the lowest average expression of *GSK3β* when compared with all other group 3 and SHH subtypes (Fig. 18B). SHHα Vs. SHHβ and SHHγ Vs. SHHδ showed no statistical significance in the results presented in the R2 database graph generated for the expression of *GSK3β* (Table 10). All other inter SHH subtype tested combination showed statistical significance in the results. Meaning SHHα and SHHβ show the highest level of *GSK3β* expression of all of the SHH subgroups (Fig. 18B). The expression of *GSK3α* and *GSK3β* in all medulloblastomas may contribute to the effectiveness of the therapeutic drug tivantinib thus making it a more potent chemotherapeutic drug as is showcased throughout this study. Tivantinib may be more cytotoxic than tepotinib and AMG337 as it is not a c-Met specific inhibitor.

4.15 Genes of Interest and their level of expression in SHH and Group 3 medulloblastoma

HGF, the ligand for the protein c-Met, is associated with the metastasis and progression of various cancers (Wang et al., 2020). *HGF* was found to have a higher average level of expression in the SHH medulloblastoma subgroup than in group 3 medulloblastoma subgroup (Fig. 19A). This finding along with the higher average expression of *Met* found in SHH (Fig. 14A) suggests that the HGF-Met pathway has the potential to have more activity in SHH medulloblastoma than that found in group 3 medulloblastoma. Thus, the downstream signalling of the HGF-Met signalling pathway may also have more activity in SHH medulloblastoma than in group 3 medulloblastoma. Therefore, suggesting the overall cancer prognosis for SHH medulloblastoma patients should be worse than group 3 medulloblastoma patients due to the higher expression of *HGF* and *Met* found in SHH medulloblastoma. However, we know this is not the case.

STAT3 is a transcription factor protein that is a part of the STAT family of proteins (Qin, Yan, Zhang and Zhang, 2019). *STAT3* is the only member of the STAT transcription factor family whose ablation results in embryonic lethality (Johnson, O'Keefe and Grandis, 2018). The transcription factor, *STAT3*, is commonly associated with the progression and metastasis of cancer (Qin, Yan, Zhang and Zhang, 2019; Wang et al., 2018). Overactivation of *STAT3* correlates with a poor cancer prognosis (Johnson, O'Keefe and Grandis, 2018). *STAT3* was found to have a higher average level of expression in the group 3 medulloblastoma subgroup than in SHH medulloblastoma subgroup (Fig. 19B). The higher level of expression found in group 3 medulloblastoma may be a contribution factor to the poor prognosis given to patients diagnosed with group 3 medulloblastoma.

Overexpression of the protein mTOR can lead to cancer progression by promoting cell migration, proliferation, inhibition of autophagy and angiogenesis (Hua et al., 2019).

Hyperactivation of mTOR is common in many human cancers (Hua et al., 2019).

Upregulation of mTORC1 is estimated to be present in up to 70% of all human tumours (Conciatori et al., 2018). The gene *mTOR* was found to have a higher average level of expression in group 3 medulloblastoma subgroup than in SHH medulloblastoma (Fig. 19C).

The higher expression of the gene *mTOR* found in group 3 medulloblastoma may give rise to the poor patient outcome expected of group 3 medulloblastoma patients when compared with other medulloblastoma subgroups.

DOCK1 overexpression is associated with cell motility and proliferation (Lee et al., 2017). *DOCK1* was found to have a higher average level of expression in the SHH medulloblastoma subgroup than in group 3 medulloblastoma subgroup (Fig. 19D). The higher level of expression of *DOCK1* found in group 3 medulloblastoma may give rise to the poor patient prognosis given to group 3 patients when compared with other medulloblastoma subgroups.

RAP1A belongs to the RAS protein family that is associated with the promotion of metastasis in multiple tumours (Li et al., 2019). *RAP1A* is found to have a higher average level of expression in group 3 medulloblastoma subgroup than in SHH medulloblastoma subgroup (Fig. 19E). The higher level of expression of the gene *RAP1A* found in group 3 medulloblastoma may be a contributing factor to the poor patient prognosis given to group 3 patients when compared with other medulloblastoma subgroups.

AKT1 regulates the PI3K signalling pathway and which controls the growth and survival of human cells (Balasuriya et al., 2018). The AKT genes are found to be commonly upregulated in cancers (Balasuriya et al., 2018). *AKT1* was found to have no significant difference in the level of expression presented in SHH medulloblastoma and group 3 medulloblastoma (Fig. 19F) as is confirmed by the P value presented for *AKT1* in Table 11 being >0.05 thus having no statistical significance. As there was no significant difference in the levels of expression of *AKT1* in either medulloblastoma subgroup this suggests that *AKT1* expression is not a contributing factor to the poor patient prognosis seen in group 3 patients when compared with SHH patients.

MAPK1 is a member of the MAP kinase family, also known as ERKs (Chang et al., 2017). ERKs are involved in several important cellular processes including cellular proliferation (Chang et al., 2017). Studies have shown *MAPK1* was linked to the progression of some tumours which may suggest it could be a potential target of interest in cancer treatment (Chang et al., 2017). *MAPK1* was found to have a higher average level of expression in the group 3 medulloblastoma subgroup than in SHH medulloblastoma subgroup (Fig. 19G). The higher-level expression of the gene *MAPK1* found in group 3 medulloblastoma may be linked with the poor patient outcome expected of group 3 medulloblastoma patients when compared with SHH medulloblastoma patients.

Each of the genes of interest explored are key genes that are activated downstream of the HGF-Met signalling pathway (Fig. 5). The consequences of the overexpression of *HGF*, *STAT3*, *mTOR*, *DOCK1*, *RAP1A*, *AKT1* and *MAPK1* (Fig. 5) in cancers make c-Met a key target for inhibition in many human cancers.

Table 12: Summary of Fig. 19 showcasing the medulloblastoma subgroup (SHH or Group 3) that had the highest average levels of gene expression.

GENE SYMBOL	MB subgroup showing higher gene expression
HGF	SHH
STAT3	Group 3
MTOR	Group 3
DOCK1	SHH
RAP1A	Group 3
AKT1	No significant difference found
MAPK1	Group 3

While both Met and HGF were shown to have higher levels of expression in SHH medulloblastoma (Fig. 14 and Fig. 19A) other downstream genes of interest (*STAT3*, *mTOR*, *RAP1A* and *MAPK1*) were found to have higher levels of expression in group 3 medulloblastoma (Shown in Table 12). This may suggest that while SHH has more HGF and Met gene expression the HGF-Met signalling pathway may be more active in group 3 medulloblastoma thus producing higher levels of expression in certain downstream signalling genes. Potentially contributing to the poorer prognosis given to group 3 medulloblastoma patients.

Conclusion

The common consensus for all literature regarding the HGF-Met axis is that it is a therapeutic target that shows promise to the potential treatment of a wide variety of Met expressing cancers. As such it is imperative to thoroughly explore not only Met inhibitors but also HGF inhibitors along with inhibitors of downstream HGF-Met signalling genes to ultimately give the best possible drug efficacy with the least side effects and/or late effects. To conclude, the known met inhibitors in this project (AMG337, tepotinib and tivantinib) had the highest cytotoxic effects against the medulloblastoma (MB) cell lines explored (ONS76, UW228, HD-MB03 and Daoy) with tivantinib having the most potency. Of each of the 5 novel putative Met inhibitors, only JD-1 and JD-5 showed consistent cytotoxicity against the medulloblastoma cell lines treated with these compounds (Table 5) although these drugs were not as potent as the aforementioned confirmed Met inhibitors analysed (AMG337, tepotinib and tivantinib). The expression of *GSK3* in both SHH and group 3 medulloblastoma (Fig. 18) may contribute to the high level of potency tivantinib has against these cell lines as *GSK3* has previously been found to be a target of tivantinib. The non-specificity of tivantinib for Met may be linked with the drugs higher level of cytotoxic effects when compared with other, Met specific, inhibitors. High Met expression gave a better survival prognosis overall in SHH medulloblastoma patients yet gave a worse survival prognosis in group 3 medulloblastoma patients (Fig. 13). The highest average expression of Met was found in SHH medulloblastoma (Fig. 14). Gender had no effect on the Met expression, trends in Met expression were similar across medulloblastoma subgroups in both genders (Fig. 15) thus most likely gender will have no effect on the efficacy of any potential Met inhibiting chemotherapeutic drugs. 4-17-year olds showed the highest average expression of the gene Met (Fig. 16) this may be attributed to the prevalence of SHH α occurring most commonly in 4-17 year olds. Desmoplastic tumours have the highest level of Met expression when compared with other histologic variants. While Met and HGF are shown to have higher expression in SHH medulloblastoma (Fig. 14 and Fig. 19A) other downstream signalling genes (*STAT3*, *mTOR*, *RAP1A* and *MAPK1*) present a higher level of expression in group 3 medulloblastoma (Fig. 19). This may suggest that the HGF-Met signalling pathway is more active in group 3 medulloblastoma than in SHH medulloblastoma thus giving rise to the poorer prognosis associated with group 3 medulloblastoma patients.

Future testing

As high *Met* expression presents a worse survival prognosis in group 3 medulloblastoma future testing of Met inhibitors should be more focused towards group 3 model medulloblastoma cell lines as this is where a need is presented for a c-Met inhibitor. The MTT assay dataset will be completed as part of the future testing to enable statistical analysis to be performed on the MTT assay results. No statistical analysis was performed on the MTT assay results due to the incomplete dataset with each experiment having either 1, 2 or 3 experimental repeats. As such it was decided against performing statistical analysis at this time due to the insufficient data. Once the MTT assay dataset is completed a T-test will be performed to compare the data and to assess whether the results are statistically significant. For the future testing of the potential chemotherapeutic drugs a scratch assay will be performed on the drugs that have been proven to be cytotoxic thus far. Due to the cytotoxicity that AMG337, tepotinib, tivantinib, JD-1 and JD-5 have shown in the medulloblastoma cell lines these treatments will be taken forward into the next stage of analysis using the known c-Met inhibitors as a reference. A scratch assay will provide valuable knowledge into the mechanism of action of the drugs being analysed and whether they inhibit the action of the receptor tyrosine kinase Met. When performing a scratch assay, if 72 hours after treatment the “wound” created in the thin layer of cells plated is healed this shows that the HGF-Met signalling pathway is still active and therefore Met has not been inhibited successfully. In contrast if the “wound” created is not healed, the chemotherapeutic drugs have been successful in the inhibition of Met and the resulting inhibition of the HGF-Met downstream signalling pathway. JD-2, JD-3 and JD-4 compounds do not seem to have much of a cytotoxic effect on all of the model medulloblastoma cell lines tested but during another Salford University student’s analysis of these compounds they were found to have an effect on cell migration in a wound healing assay. Therefore, it is important to do further analysis of all of the JD-compounds via a scratch assay. Western blotting is another essential avenue of testing. A western blot would have been performed to explore the phosphorylation of other targets in the c-Met signalling pathway such as the list of genes shown in Table 10. Another consideration of this study is if the JD-compounds are found to inhibit c-Met these compounds can be tested against other tumour types with a higher Met-dependence than Medulloblastoma such as NSCLC. MYC overexpression

shown in group 3 tumours may present another key target for testing and analysis. A MYC inhibitor may prove to have a higher cytotoxicity towards group 3 medulloblastoma cell lines than c-Met inhibitors.

The impact of the Covid-19 pandemic on this thesis

Access to the laboratory was restricted meaning I was unable to enter the university or the laboratory from March 2020. This resulted in an inability to produce, analyse or collect any further novel results which would have otherwise been collected from March-September 2020. This thesis would have had complete MTT assays with at least three repeats on each medulloblastoma cell line treated with each drug available for testing. Cell migration assays would have been performed using the treatments that showed cytotoxic effects on the cell lines. Western blots would have also been performed using all of the drugs in each of the cell lines. As a result of the inability to create any further novel results R2 database was incorporated into this thesis. My thesis has been severely impacted as the majority of the results in my study has been produced remotely rather than as novel data in the laboratory. This has not only hindered my project but has had a huge impact on my ability to learn and/or carry out new techniques in the lab and it has also greatly affected my mental health. I have not felt connected to the university or my peers and feel like I have been forcibly distanced from my studies.

Bibliography

Adooq Bioscience, 2021. AMG 337. [online] Available at: <<https://www.adooq.com/amg-337.html>> [Accessed 25 August 2021].

Appleman, L., Parikh, R., Wang, P., Beumer, J., & Chu, E. (2014). The potential roles of hepatocyte growth factor (HGF)-MET pathway inhibitors in cancer treatment. *Oncotargets And Therapy*, 969. doi: 10.2147/ott.s40241

Bahmad, H., & Poppiti, R. (2020). Medulloblastoma cancer stem cells: molecular signatures and therapeutic targets. *Journal Of Clinical Pathology*, 73(5), 243-249. doi: 10.1136/jclinpath-2019-206246

Balasuriya, N., McKenna, M., Liu, X., Li, S. and O'Donoghue, P., 2018. Phosphorylation-Dependent Inhibition of Akt1. *Genes*, 9(9), p.450. doi: 10.3390/genes9090450

Bautista, F., Fioravanti, V., de Rojas, T., Carceller, F., Madero, L., Lassaletta, A., & Moreno, L. (2017). Medulloblastoma in children and adolescents: a systematic review of contemporary phase I and II clinical trials and biology update. *Cancer Medicine*, 6(11), 2606-2624. doi: 10.1002/cam4.1171

Beurel, E., Grieco, S., & Jope, R. (2015). Glycogen synthase kinase-3 (GSK3): Regulation, actions, and diseases. *Pharmacology & Therapeutics*, 148, 114-131. doi: 10.1016/j.pharmthera.2014.11.016

Bhakta, N., Liu, Q., Ness, K., Baassiri, M., Eissa, H., & Yeo, F. et al. (2017). The cumulative burden of surviving childhood cancer: an initial report from the St Jude Lifetime Cohort Study (SJLIFE). *The Lancet*, 390(10112), 2569-2582. doi: 10.1016/s0140-6736(17)31610-0

Boissinot, M., Vilaine, M., & Hermouet, S. (2014). The Hepatocyte Growth Factor (HGF)/Met Axis: A Neglected Target in the Treatment of Chronic Myeloproliferative Neoplasms?. *Cancers*, 6(3), 1631-1669. doi: 10.3390/cancers6031631

Bonfim-Silva, R., Salomão, K., Pimentel, T., Menezes, C., Palma, P. and Fontes, A., 2019. Biological characterization of the UW402, UW473, ONS-76 and DAOY pediatric

medulloblastoma cell lines. *Cytotechnology*, 71(5), pp.893-903. doi: 10.1007/s10616-019-00332-3

Bouattour, M., Raymond, E., Qin, S., Cheng, A., Stammberger, U., Locatelli, G., & Faivre, S. (2018). Recent developments of c-Met as a therapeutic target in hepatocellular carcinoma. *Hepatology*, 67(3), 1132-1149. doi: 10.1002/hep.29496

Birchmeier, C., Birchmeier, W., Gherardi, E., & Vande Woude, G. (2003). Met, metastasis, motility and more. *Nature Reviews Molecular Cell Biology*, 4(12), 915-925. doi: 10.1038/nrm1261

Cancer Research UK. 2018. Cancer Statistics For The UK. [online] Available at: <<https://www.cancerresearchuk.org/health-professional/cancer-statistics-for-the-uk#:~:text=There%20are%20around%20165%2C000%20cancer,88%2C900%20cancer%20deaths%20in%202017.>> [Accessed 19 November 2020].

Cancer research UK. 2020. Medulloblastoma | Children's Brain Tumours | Cancer Research UK. [online] Available at: <<https://www.cancerresearchuk.org/about-cancer/childrens-cancer/brain-tumours/types/medulloblastoma>> [Accessed 4 June 2020].

Carta, R., Del Baldo, G., Miele, E., Po, A., Besharat, Z., & Nazio, F. et al. (2020). Cancer Predisposition Syndromes and Medulloblastoma in the Molecular Era. *Frontiers In Oncology*, 10, 566822. doi: 10.3389/fonc.2020.566822

Cavalli, F., Remke, M., Rampasek, L., Peacock, J., Shih, D., & Luu, B. et al. (2017). Intertumoral Heterogeneity within Medulloblastoma Subgroups. *Cancer Cell*, 31(6), 737-754.e6. doi: 10.1016/j.ccell.2017.05.005

Chang, L., Zhang, D., Shi, H., Bian, Y. and Guo, R., 2017. MiR-143 inhibits endometrial cancer cell proliferation and metastasis by targeting MAPK1. *Oncotarget*, 8(48), pp.84384-84395. doi: 10.18632/oncotarget.21037

Chen, H., Tsai, C., & Hung, W. (2015). Foretinib inhibits angiogenesis, lymphangiogenesis and tumor growth of pancreatic cancer in vivo by decreasing VEGFR-2/3 and TIE-2 signaling. *Oncotarget*, 6(17), 14940-14952. doi: 10.18632/oncotarget.3613

Children with Cancer UK. 2019. *Childhood cancer facts and figures | Children with Cancer UK*. [online] Available at: <<https://www.childrenwithcancer.org.uk/childhood-cancer-info/understanding-cancer/childhood-cancer-facts-figures/>> [Accessed 27 March 2021].

Chmielowiec, J., Borowiak, M., Morkel, M., Stradal, T., Munz, B., & Werner, S. et al. (2007). c-Met is essential for wound healing in the skin. *Journal Of Cell Biology*, 177(1), 151-162. doi: 10.1083/jcb.200701086

Conciatori, F., Ciuffreda, L., Bazzichetto, C., Falcone, I., Pilotto, S., & Bria, E. et al. (2018). mTOR Cross-Talk in Cancer and Potential for Combination Therapy. *Cancers*, 10(1), 23. doi: 10.3390/cancers10010023

Curran, E., Sainani, K., Le, G., Propp, J., & Fisher, P. (2009). Gender affects survival for medulloblastoma only in older children and adults: A study from the surveillance epidemiology and end results registry. *Pediatric Blood & Cancer*, 52(1), 60-64. doi: 10.1002/psc.21832

Danilenko, M., Clifford, S., & Schwalbe, E. (2021). Inter and intra-tumoral heterogeneity as a platform for personalized therapies in medulloblastoma. *Pharmacology & Therapeutics*, 107828. doi: 10.1016/j.pharmthera.2021.107828

De Mello, R., Neves, N., Amaral, G., Lippo, E., Castelo-Branco, P., & Pozza, D. et al. (2020). The Role of MET Inhibitor Therapies in the Treatment of Advanced Non-Small Cell Lung Cancer. *Journal Of Clinical Medicine*, 9(6), 1918. doi: 10.3390/jcm9061918

Ding, N., You, A., Tian, W., Gu, L., & Deng, D. (2020). Chidamide increases the sensitivity of Non-small Cell Lung Cancer to Crizotinib by decreasing c-MET mRNA methylation. *International Journal Of Biological Sciences*, 16(14), 2595-2611. doi: 10.7150/ijbs.45886

Doussouki, M., Gajjar, A., & Chamdine, O. (2019). Molecular genetics of medulloblastoma in children: diagnostic, therapeutic and prognostic implications. *Future Neurology*, 14(1). doi: 10.2217/fnl-2018-0030

- El Darsa, H., El Sayed, R. and Abdel-Rahman, O., 2020. MET Inhibitors for the Treatment of Gastric Cancer: What's Their Potential?. *Journal of Experimental Pharmacology*, 12, pp.349-361. doi: 10.2147/jep.s242958
- Faria, C., Smith, C., & Rutk, J. (2011). The Role of HGF/c-Met Pathway Signaling in Human Medulloblastoma. *Molecular Targets Of CNS Tumors*, 1(1). doi: 10.5772/23296
- Ferro, V. (2016). Glycosaminoglycans and Their Mimetics. *Molecules*, 22(1), 20. doi: 10.3390/molecules22010020
- Frič, R., Due-Tønnessen, B., Lundar, T., Egge, A., Kronen Krossnes, B., & Due-Tønnessen, P. et al. (2020). Long-term outcome of posterior fossa medulloblastoma in patients surviving more than 20 years following primary treatment in childhood. *Scientific Reports*, 10(1), 9371. doi: 10.1038/s41598-020-66328-8
- Garajova, I., Giovannetti, E., Biasco, G., & Peters, G. (2015). c-Met as a Target for Personalized Therapy. *Translational Oncogenomics, Suppl. 1*(7), 13-31. doi: 10.4137/tog.s30534
- Garcia-Lopez, J., Kumar, R., Smith, K. and Northcott, P., 2021. Deconstructing Sonic Hedgehog Medulloblastoma: Molecular Subtypes, Drivers, and Beyond. *Trends in Genetics*, 37(3), pp.235-250. doi: 10.1016/j.tig.2020.11.001
- Geller, J., Perentesis, J., Liu, X., Minard, C., Kudgus, R., & Reid, J. et al. (2017). A phase 1 study of the c-Met inhibitor, tivantinib (ARQ197) in children with relapsed or refractory solid tumors: A Children's Oncology Group study phase 1 and pilot consortium trial (ADVL1111). *Pediatric Blood & Cancer*, 64(11), e26565. doi: 10.1002/pbc.26565
- Guo, L., Gong, H., Tang, T., Zhang, B., Zhang, L., & Yan, M. (2021). Crizotinib and Sunitinib Induce Hepatotoxicity and Mitochondrial Apoptosis in L02 Cells via ROS and Nrf2 Signaling Pathway. *Frontiers In Pharmacology*, 12, 620934. doi: 10.3389/fphar.2021.620934
- Guo, Y., Cao, R., Zhang, X., Huang, L., Sun, L., & Zhao, J. et al. (2019). Recent Progress in Rare Oncogenic Drivers and Targeted Therapy For Non-Small Cell Lung Cancer. *Oncotargets And Therapy*, Volume 12, 10343-10360. doi: 10.2147/ott.s230309

- Hack, S., Bruey, J., & Koeppen, H. (2014). HGF/MET-directed therapeutics in gastroesophageal cancer: a review of clinical and biomarker development. *Oncotarget*, 5(10). doi: 10.18632/oncotarget.2003
- Hong, D., LoRusso, P., Hamid, O., Janku, F., Kittaneh, M., & Catenacci, D. et al. (2018). Phase I Study of AMG 337, a Highly Selective Small-molecule MET Inhibitor, in Patients with Advanced Solid Tumors. *Clinical Cancer Research*, 25(8), 2403-2413. doi: 10.1158/1078-0432.ccr-18-1341
- Hua, H., Kong, Q., Zhang, H., Wang, J., Luo, T., & Jiang, Y. (2019). Targeting mTOR for cancer therapy. *Journal Of Hematology & Oncology*, 12(1), 71. doi: 10.1186/s13045-019-0754-1
- Huang, G., Xu, Q., Cui, Y., Li, N., Bian, X., & Lv, S. (2016). Medulloblastoma stem cells: Promising targets in medulloblastoma therapy. *Cancer Science*, 107(5), 583-589. doi: 10.1111/cas.12925
- Hughes, P., Rex, K., Caenepeel, S., Yang, Y., Zhang, Y., & Broome, M. et al. (2016). In Vitro and In Vivo Activity of AMG 337, a Potent and Selective MET Kinase Inhibitor, in MET-Dependent Cancer Models. *Molecular Cancer Therapeutics*, 15(7), 1568-1579. doi: 10.1158/1535-7163.mct-15-0871
- Ivanov, D., Coyle, B., Walker, D., & Grabowska, A. (2016). In vitro models of medulloblastoma: Choosing the right tool for the job. *Journal Of Biotechnology*, 236, 10-25. doi: 10.1016/j.jbiotec.2016.07.028
- Johne, A., Scheible, H., Becker, A., van Lier, J., Wolna, P., & Meyring, M. (2020). Open-label, single-center, phase I trial to investigate the mass balance and absolute bioavailability of the highly selective oral MET inhibitor tepotinib in healthy volunteers. *Investigational New Drugs*, 38(5), 1507-1519. doi: 10.1007/s10637-020-00926-1
- Johnson, D., O'Keefe, R., & Grandis, J. (2018). Targeting the IL-6/JAK/STAT3 signalling axis in cancer. *Nature Reviews Clinical Oncology*, 15(4), 234-248. doi: 10.1038/nrclinonc.2018.8

- Jonkman, J., Cathcart, J., Xu, F., Bartolini, M., Amon, J., Stevens, K., & Colarusso, P. (2014). An introduction to the wound healing assay using live-cell microscopy. *Cell Adhesion & Migration*, 8(5), 440-451. doi: 10.4161/cam.36224
- Juraschka, K., & Taylor, M. (2019). Medulloblastoma in the age of molecular subgroups: a review. *Journal Of Neurosurgery: Pediatrics*, 24(4), 353-363. doi: 10.3171/2019.5.peds18381
- Kato, T. (2017). Biological roles of hepatocyte growth factor-Met signaling from genetically modified animals (Review). *Biomedical Reports*, 7(6):495-503. doi: 10.3892/br.2017.1001
- Kahn, S., Wang, X., Nitta, R., Gholamin, S., Theruvath, J., & Hutter, G. et al. (2018). Notch1 regulates the initiation of metastasis and self-renewal of Group 3 medulloblastoma. *Nature Communications*, 9(1). doi: 10.1038/s41467-018-06564-9
- Kijima, N., & Kanemura, Y. (2016). Molecular Classification of Medulloblastoma. *Neurologia Medico-Chirurgica*, 56(11), 687-697. doi: 10.2176/nmc.ra.2016-0016
- Kudo, M., Morimoto, M., Moriguchi, M., Izumi, N., Takayama, T., & Yoshiji, H. et al. (2020). A randomized, double-blind, placebo-controlled, phase 3 study of tivantinib in Japanese patients with MET-high hepatocellular carcinoma. *Cancer Science*, 111(10), 3759-3769. doi: 10.1111/cas.14582
- Kuenzi, B., Remsing Rix, L., Kinose, F., Kroeger, J., Lancet, J., Padron, E., & Rix, U. (2019). Off-target based drug repurposing opportunities for tivantinib in acute myeloid leukemia. *Scientific Reports*, 9(1), 606. doi: 10.1038/s41598-018-37174-6
- Kuzan-Fischer, C., Juraschka, K., & Taylor, M. (2018). Medulloblastoma in the Molecular Era. *Journal Of Korean Neurosurgical Society*, 61(3), 292-301. doi: 10.3340/jkns.2018.0028
- Lath, D., Buckle, C., Evans, H., Fisher, M., Down, J., Lawson, M., & Chantry, A. (2018). ARQ-197, a small-molecule inhibitor of c-Met, reduces tumour burden and prevents myeloma-induced bone disease in vivo. *PLOS ONE*, 13(6), e0199517. doi: 10.1371/journal.pone.0199517

Lee, S., Chiu, Y., Li, Y., Lin, C., Hou, H., Chou, W., & Tien, H. (2017). High expression of dedicator of cytokinesis 1 (DOCK1) confers poor prognosis in acute myeloid leukemia. *Oncotarget*, *8*(42), 72250-72259. doi: 10.18632/oncotarget.19706

Li, Q., Xu, A., Chu, Y., Chen, T., Li, H., & Yao, L. et al. (2019). Rap1A promotes esophageal squamous cell carcinoma metastasis through the AKT signaling pathway. *Oncology Reports*, *45*(5), 1815-1824. doi: 10.3892/or.2019.7309

Luzzi, S., Giotta Lucifero, A., Brambilla, I., Semeria Mantelli, S., Mosconi, M., Foiadelli, T., & Savasta, S. (2020). Targeting the medulloblastoma: a molecular-based approach. *Acta bio-medica: Atenei Parmensis*, *91* (7), 79–100. <https://doi.org/10.23750/abm.v91i7-S.9958>

Macmillan Cancer Support. 2019. [online] Available at:

<https://www.macmillan.org.uk/_images/cancer-statistics-factsheet_tcm9-260514.pdf> [Accessed 27 March 2021].

Matsumoto, K., Umitsu, M., De Silva, D., Roy, A., & Bottaro, D. (2017). Hepatocyte growth factor/MET in cancer progression and biomarker discovery. *Cancer Science*, *108*(3), 296-307. doi: 10.1111/cas.13156

Matsumoto, K., Funakoshi, H., Takahashi, H., & Sakai, K. (2014). HGF–Met Pathway in Regeneration and Drug Discovery. *Biomedicines*, *2*(4), 275-300. doi: 10.3390/biomedicines2040275

Maroun, C., & Rowlands, T. (2014). The Met receptor tyrosine kinase: A key player in oncogenesis and drug resistance. *Pharmacology & Therapeutics*, *142*(3), 316-338. doi: 10.1016/j.pharmthera.2013.12.014

Menyhárt, O., Giangaspero, F., & Győrffy, B. (2019). Molecular markers and potential therapeutic targets in non-WNT/non-SHH (group 3 and group 4) medulloblastomas. *Journal Of Hematology & Oncology*, *12*(1), 29. doi: 10.1186/s13045-019-0712-y

Milde, T., Lodrini, M., Savelyeva, L., Korshunov, A., Kool, M., & Brueckner, L. et al. (2012). HD-MB03 is a novel Group 3 medulloblastoma model demonstrating sensitivity to histone

deacetylase inhibitor treatment. *Journal Of Neuro-Oncology*, 110(3), 335-348. doi: 10.1007/s11060-012-0978-1

Millard, N., & De Braganca, K. (2016). Medulloblastoma. *Journal Of Child Neurology*, 31(12), 1341-1353. doi: 10.1177/0883073815600866

Mohamed, S., & Coombe, D. (2017). Heparin Mimetics: Their Therapeutic Potential. *Pharmaceuticals*, 10(4), 78. doi: 10.3390/ph10040078

Morla, S. (2019). Glycosaminoglycans and Glycosaminoglycan Mimetics in Cancer and Inflammation. *International Journal Of Molecular Sciences*, 20(8), 1963. doi: 10.3390/ijms20081963

Mulcahy, E., Colón, R., & Abounader, R. (2020). HGF/MET Signaling in Malignant Brain Tumors. *International Journal Of Molecular Sciences*, 21(20), 7546. doi: 10.3390/ijms21207546

Mungunsukh, O., McCart, E., & Day, R. (2014). Hepatocyte Growth Factor Isoforms in Tissue Repair, Cancer, and Fibrotic Remodeling. *Biomedicines*, 2(4), 301-326. doi: 10.3390/biomedicines2040301

Nakamura, T., & Mizuno, S. (2010). The discovery of Hepatocyte Growth Factor (HGF) and its significance for cell biology, life sciences and clinical medicine. *Proceedings Of The Japan Academy, Series B*, 86(6), 588-610. doi: 10.2183/pjab.86.588

National Cancer Institute. 2020. *Late Effects Of Treatment For Childhood Cancer (PDQ®)– Health Professional Version*. [online] Available at: <<https://www.cancer.gov/types/childhood-cancers/late-effects-hp-pdq>> [Accessed 4 June 2020].

National Cancer Institute. 2021. *Medulloblastoma Diagnosis and Treatment*. [online] Available at: <<https://www.cancer.gov/rare-brain-spine-tumor/tumors/medulloblastoma>> [Accessed 29 March 2021].

Ncbi.nlm.nih.gov. 2021. *entrez gene*. [online] Available at: <<https://www.ncbi.nlm.nih.gov/gene/>> [Accessed 30 March 2021].

- Northcott, P., Dubuc, A., Pfister, S., & Taylor, M. (2012). Molecular subgroups of medulloblastoma. *Expert Review Of Neurotherapeutics*, 12(7), 871-884. doi: 10.1586/ern.12.66
- Organ, S., & Tsao, M. (2011). An overview of the c-MET signaling pathway. *Therapeutic Advances In Medical Oncology*, 3(1 Suppl), S7-S19. doi: 10.1177/1758834011422556
- Orr, B. (2020). Pathology, diagnostics, and classification of medulloblastoma. *Brain Pathology*, 30(3), 664-678. doi: 10.1111/bpa.12837
- Owusu, B., Bansal, N., Venukadasula, P., Ross, L., Messick, T., & Goel, S. et al. (2016). Inhibition of pro-HGF activation by SRI31215, a novel approach to block oncogenic HGF/MET signaling. *Oncotarget*, 7(20). doi: 10.18632/oncotarget.8785
- Packer, R., & Vezina, G. (2008). Management of and Prognosis With Medulloblastoma. *Archives Of Neurology*, 65(11), 1419. doi: 10.1001/archneur.65.11.1419
- Paik, P., Felip, E., Veillon, R., Sakai, H., Cortot, A., & Garassino, M. et al. (2020). Tepotinib in Non–Small-Cell Lung Cancer with MET Exon 14 Skipping Mutations. *New England Journal Of Medicine*, 383(10), 931-943. doi: 10.1056/nejmoa2004407
- Pievsky, D., & Pysopoulos, N. (2016). Profile of tivantinib and its potential in the treatment of hepatocellular carcinoma: the evidence to date. *Journal Of Hepatocellular Carcinoma*, 3, 69-76. doi: 10.2147/jhc.s106072
- Pudelko, L., Jaehrling, F., Reusch, C., Viteri, S., Stroh, C., & Linde, N. et al. (2020). SHP2 Inhibition Influences Therapeutic Response to Tepotinib in Tumors with MET Alterations. *Isience*, 23(12), 101832. doi: 10.1016/j.isci.2020.101832
- Qin, J., Yan, L., Zhang, J., & Zhang, W. (2019). STAT3 as a potential therapeutic target in triple negative breast cancer: a systematic review. *Journal Of Experimental & Clinical Cancer Research*, 38(1), 195. doi: 10.1186/s13046-019-1206-z
- R2 Genomics Analysis and Visualization Platform, 2021 [online] Available at: <<https://hgserver1.amc.nl/cgi-bin/r2/main.cgi>> [Accessed 30 March 2021].

Remsing Rix, L., Kuenzi, B., Luo, Y., Remily-Wood, E., Kinose, F., & Wright, G. et al. (2013). GSK3 Alpha and Beta Are New Functionally Relevant Targets of Tivantinib in Lung Cancer Cells. *ACS Chemical Biology*, 9(2), 353-358. doi: 10.1021/cb400660a

Riahi, R., Yang, Y., Zhang, D., & Wong, P. (2012). Advances in Wound-Healing Assays for Probing Collective Cell Migration. *Journal Of Laboratory Automation*, 17(1), 59-65. doi: 10.1177/2211068211426550

Scagliotti, G., von Pawel, J., Novello, S., Ramlau, R., Favaretto, A., & Barlesi, F. et al. (2015). Phase III Multinational, Randomized, Double-Blind, Placebo-Controlled Study of Tivantinib (ARQ 197) Plus Erlotinib Versus Erlotinib Alone in Previously Treated Patients With Locally Advanced or Metastatic Nonsquamous Non-Small-Cell Lung Cancer. *Journal Of Clinical Oncology*, 33(24), 2667-2674. doi: 10.1200/jco.2014.60.7317

Scagliotti, G., Shuster, D., Orlov, S., von Pawel, J., Shepherd, F., & Ross, J. et al. (2017). Tivantinib in Combination with Erlotinib versus Erlotinib Alone for EGFR-Mutant NSCLC: An Exploratory Analysis of the Phase 3 MARQUEE Study. *Journal Of Thoracic Oncology*, 13(6), 849-854. doi: 10.1016/j.jtho.2017.12.009

Selleckchem, 2021. *Tepotinib (EMD 1214063)*. [online] Available at: <<https://www.selleckchem.com/products/emd-1214063.html>> [Accessed 25 August 2021].

Selleckchem, 2021. *Tivantinib (ARQ 197)*. [online] Available at: <<https://www.selleckchem.com/products/arq-197.html>> [Accessed 25 August 2021].

Shitara, K., Yamazaki, K., Tsushima, T., Naito, T., Matsubara, N., & Watanabe, M. et al. (2020). Phase I trial of the MET inhibitor tepotinib in Japanese patients with solid tumors. *Japanese Journal Of Clinical Oncology*, 50(8), 859-866. doi: 10.1093/jjco/hyaa042

Shao, Z., Pan, H., Tu, S., Zhang, J., Yan, S., & Shao, A. (2020). HGF/c-Met Axis: The Advanced Development in Digestive System Cancer. *Frontiers In Cell And Developmental Biology*, 8, 801. doi: 10.3389/fcell.2020.00801

Susanto, E., Marin Navarro, A., Zhou, L., Sundström, A., van Bree, N., & Stantic, M. et al. (2020). Modeling SHH-driven medulloblastoma with patient iPS cell-derived neural stem

cells. *Proceedings Of The National Academy Of Sciences*, 117(33), 20127-20138. doi: 10.1073/pnas.1920521117

Tantravedi, S., Vesuna, F., Winnard, P., Martin, A., Lim, M., & Eberhart, C. et al. (2019). Targeting DDX3 in Medulloblastoma Using the Small Molecule Inhibitor RK-33. *Translational Oncology*, 12(1), 96-105. doi: 10.1016/j.tranon.2018.09.002

Takamori, S., Matsubara, T., Fujishita, T., Ito, K., Toyozawa, R., & Seto, T. et al. (2021). Dramatic intracranial response to tepotinib in a patient with lung adenocarcinoma harboring MET exon 14 skipping mutation. *Thoracic Cancer*, 12(6), 978-980. doi: 10.1111/1759-7714.13871

Tao, R., Murad, N., Xu, Z., Zhang, P., Okonechnikov, K., & Kool, M. et al. (2019). MYC Drives Group 3 Medulloblastoma through Transformation of Sox2+ Astrocyte Progenitor Cells. *Cancer Research*, 79(8), 1967-1980. doi: 10.1158/0008-5472.can-18-1787

Taylor, M., Northcott, P., Korshunov, A., Remke, M., Cho, Y., & Clifford, S. et al. (2011). Molecular subgroups of medulloblastoma: the current consensus. *Acta Neuropathologica*, 123(4), 465-472. doi: 10.1007/s00401-011-0922-z

Tidy, D., 2015. *Brain Tumours in Children*. [online] Patient. Available at: <<https://patient.info/doctor/brain-tumours-in-children>> [Accessed 27 March 2021].

Topham, C. H., Tighe, A. et al. (2016) *Cancer Cell* 28(1), 129-140

U.S. Food and Drug Administration, 2021. *FDA grants accelerated approval to tepotinib for metastatic non-small*. [online] Available at: <[https://www.fda.gov/drugs/drug-approvals-and-databases/fda-grants-accelerated-approval-tepotinib-metastatic-non-small-cell-lung-cancer#:~:text=Approvals%20and%20Databases-,FDA%20grants%20accelerated%20approval%20to%20tepotinib,non%2Dsmall%20cell%20lung%20cancer&text=On%20February%203%2C%202021%2C%20the,Tepmetko%2C%20EMD%20Serono%20Inc.\)&text=Patients%20received%20tepotinib%20450%20mg,disease%20progression%20or%20unacceptable%20toxicity.](https://www.fda.gov/drugs/drug-approvals-and-databases/fda-grants-accelerated-approval-tepotinib-metastatic-non-small-cell-lung-cancer#:~:text=Approvals%20and%20Databases-,FDA%20grants%20accelerated%20approval%20to%20tepotinib,non%2Dsmall%20cell%20lung%20cancer&text=On%20February%203%2C%202021%2C%20the,Tepmetko%2C%20EMD%20Serono%20Inc.)&text=Patients%20received%20tepotinib%20450%20mg,disease%20progression%20or%20unacceptable%20toxicity.)> [Accessed 29 March 2021].

Van Cutsem, E., Karaszewska, B., Kang, Y., Chung, H., Shankaran, V., & Siena, S. et al. (2018). A Multicenter Phase II Study of AMG 337 in Patients with MET-Amplified Gastric/Gastroesophageal Junction/Esophageal Adenocarcinoma and Other MET-Amplified Solid Tumors. *Clinical Cancer Research*, 25(8), 2414-2423. doi: 10.1158/1078-0432.ccr-18-1337

Viticchiè, G., & Muller, P. (2015). c-Met and Other Cell Surface Molecules: Interaction, Activation and Functional Consequences. *Biomedicines*, 3(1), 46-70. doi: 10.3390/biomedicines3010046

Wang, H., Rao, B., Lou, J., Li, J., Liu, Z., & Li, A. et al. (2020). The Function of the HGF/c-Met Axis in Hepatocellular Carcinoma. *Frontiers In Cell And Developmental Biology*, 8, 55. doi: 10.3389/fcell.2020.00055

Wang, Y., Shen, Y., Wang, S., Shen, Q., & Zhou, X. (2018). The role of STAT3 in leading the crosstalk between human cancers and the immune system. *Cancer Letters*, 415, 117-128. doi: 10.1016/j.canlet.2017.12.003

Waszak, S., Northcott, P., Buchhalter, I., Robinson, G., Sutter, C., & Groebner, S. et al. (2018). Spectrum and prevalence of genetic predisposition in medulloblastoma: a retrospective genetic study and prospective validation in a clinical trial cohort. *The Lancet Oncology*, 19(6), 785-798. doi: 10.1016/s1470-2045(18)30242-0

World Health Organisation. 2018. Cancer. [online] Available at: <<https://www.who.int/news-room/fact-sheets/detail/cancer>> [Accessed 19 November 2020].

Wu, Y., Li, Z., Zhang, L., & Liu, G. (2019). Tivantinib Hampers the Proliferation of Glioblastoma Cells via PI3K/Akt/Mammalian Target of Rapamycin (mTOR) Signaling. *Medical Science Monitor*, 25, 7383-7390. doi: 10.12659/msm.919319

Yang, Y., Hong, P., Xu, W., He, Q., & Li, B. (2020). Advances in targeted therapy for esophageal cancer. *Signal Transduction And Targeted Therapy*, 5(1), 229. doi: 10.1038/s41392-020-00323-3

Yi, J., & Wu, J. (2018). Epigenetic regulation in medulloblastoma. *Molecular And Cellular Neuroscience*, 87, 65-76. doi: 10.1016/j.mcn.2017.09.003

Yoon, J., Gilbertson, R., Iannaccone, S., Iannaccone, P., & Walterhouse, D. (2009). Defining a role for Sonic hedgehog pathway activation in desmoplastic medulloblastoma by identifying GLI1 target genes. *International Journal Of Cancer*, 124(1), 109-119. doi: 10.1002/ijc.23929

Zanini, C., Ercole, E., Mandili, G., Salaroli, R., Poli, A., & Renna, C. et al. (2013). Medullospheres from DAOY, UW228 and ONS-76 Cells: Increased Stem Cell Population and Proteomic Modifications. *Plos ONE*, 8(5), 63748. doi: 10.1371/journal.pone.0063748

Zhan, T., Rindtorff, N., & Boutros, M. (2016). Wnt signaling in cancer. *Oncogene*, 36(11), 1461-1473. doi: 10.1038/onc.2016.304

Zhang, Y., Jain, R., & Zhu, M. (2015). Recent Progress and Advances in HGF/MET-Targeted Therapeutic Agents for Cancer Treatment. *Biomedicines*, 3(1), 149-181. doi: 10.3390/biomedicines3010149

Zhang, H., Bao, Z., Liao, H., Li, W., Chen, Z., Shen, H., & Ying, S. (2017). The efficacy and safety of tivantinib in the treatment of solid tumors: a systematic review and meta-analysis. *Oncotarget*, 8(68), 113153-113162. doi: 10.18632/oncotarget.22615

Zillhardt, M., Park, S., Romero, I., Sawada, K., Montag, A., & Krausz, T. et al. (2011). Foretinib (GSK1363089), an Orally Available Multikinase Inhibitor of c-Met and VEGFR-2, Blocks Proliferation, Induces Anoikis, and Impairs Ovarian Cancer Metastasis. *Clinical Cancer Research*, 17(12), 4042-4051. doi: 10.1158/1078-0432.ccr-10-3387